Tracking at LHC

(Calibration and Alignment)

4th School on the Physics of LHC

Martignano (Le) Italy

Rino Castaldi

(rino.castaldi@pi.infn.it)

Lecture 1

Tracking at LHC

Outline

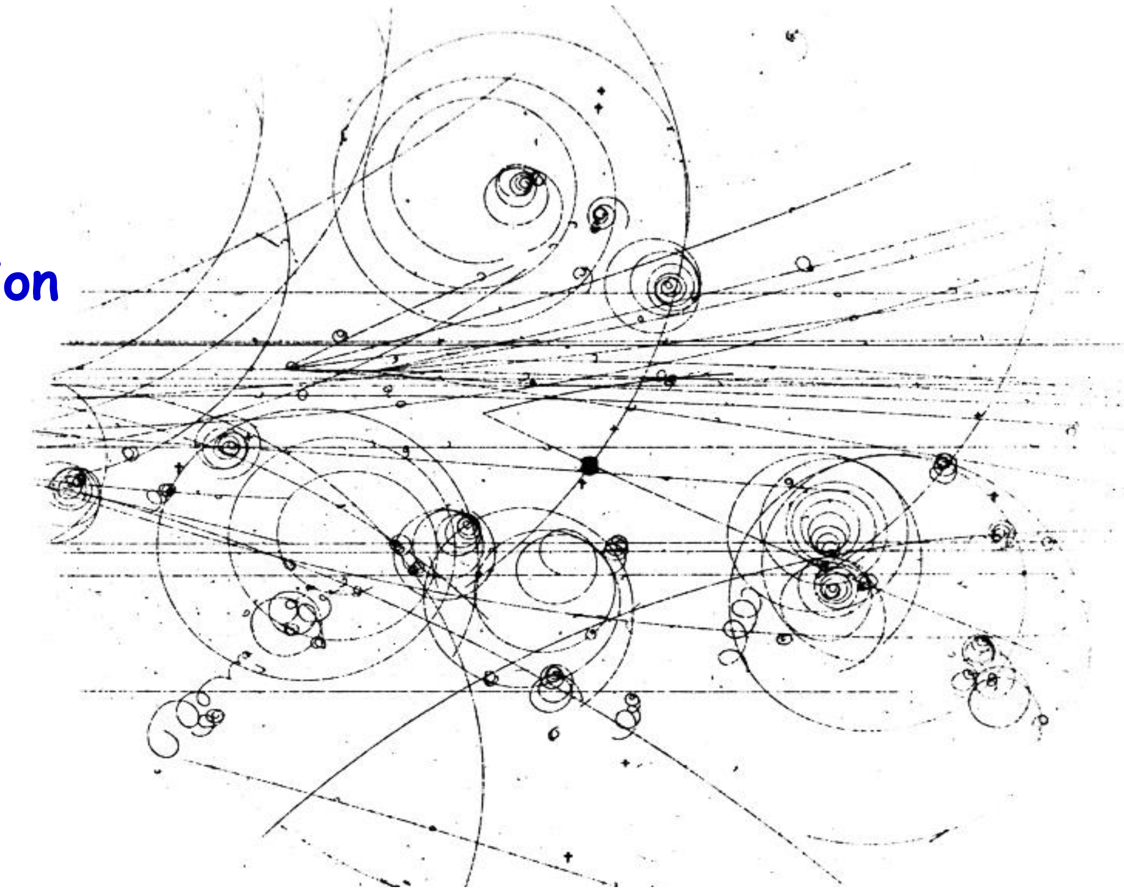

- ✓ Basic concepts* of detection
- ✓ The tracking detectors of the LHC experiments
- ✓ Commissioning and alignement with cosmics
- ✓ Commissioning and alignement with the first LHC data

*not much easy in 2 hours: add several backup slides

Tracking: why

At hadron colliders the challenging aim is the full reconstruction of the events produced in the interaction under study. Therefore primary goals are:

✓ reconstruct the trajectories ("tracking") of charged particles and measure their momenta

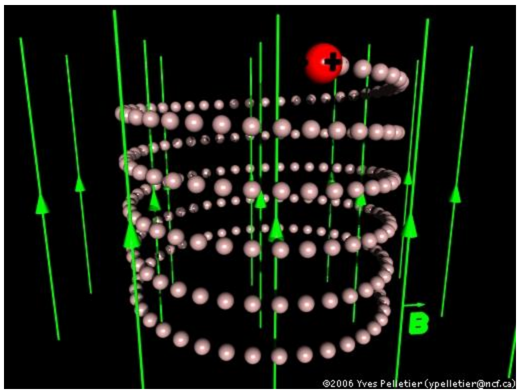

Most common case: in a solenoidal uniform magnetic filed the Lorentz force

$$\vec{F} = \frac{d\vec{p}}{dt} = q\vec{E} + q\left(\vec{v} \times \vec{B}\right)$$

induce charged particles to follow a helicoidal path:
- describe circles in the transverse plane
- move uniformly along the magnetic field direction

$$P_T(GeV) = 0.3\ B(T)\ R(m)$$

✓ identify the sign of the charge

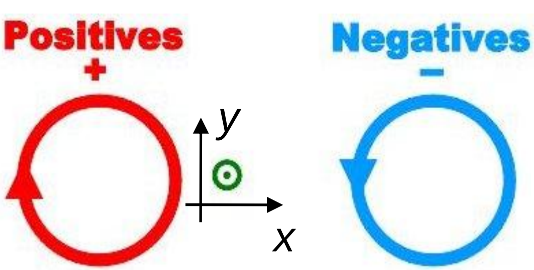

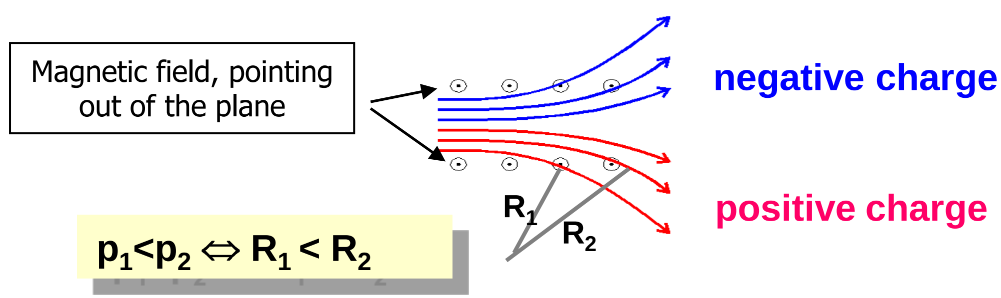

Tracking: why

✓reconstruct the primary and secondary vertices of the interaction (at LHC with large pile-up of events in the same bunch crossing !)

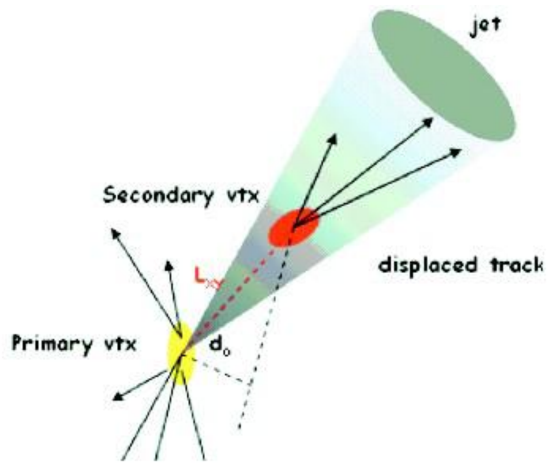

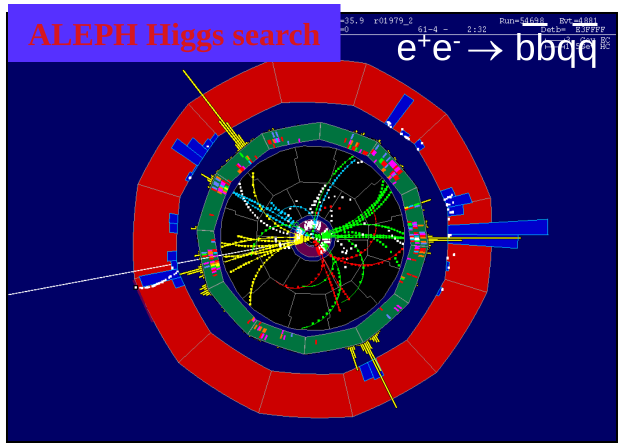

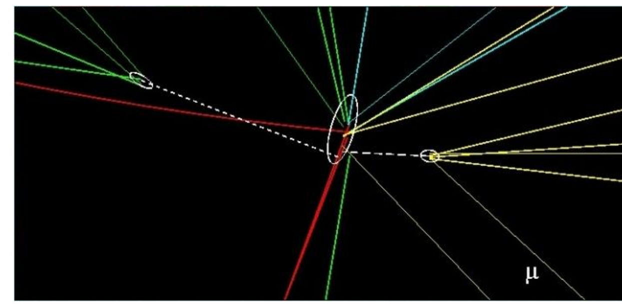

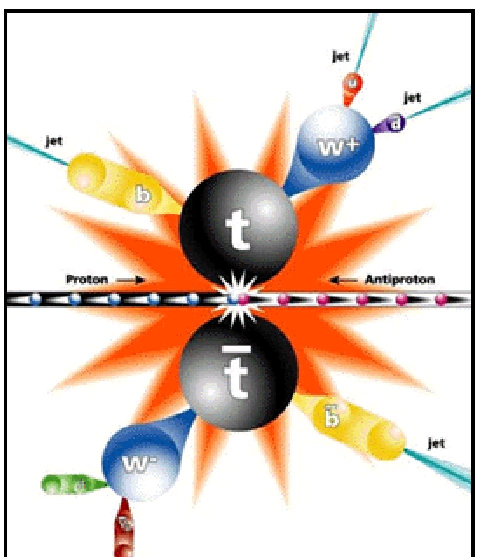

CDF Top Quark Event

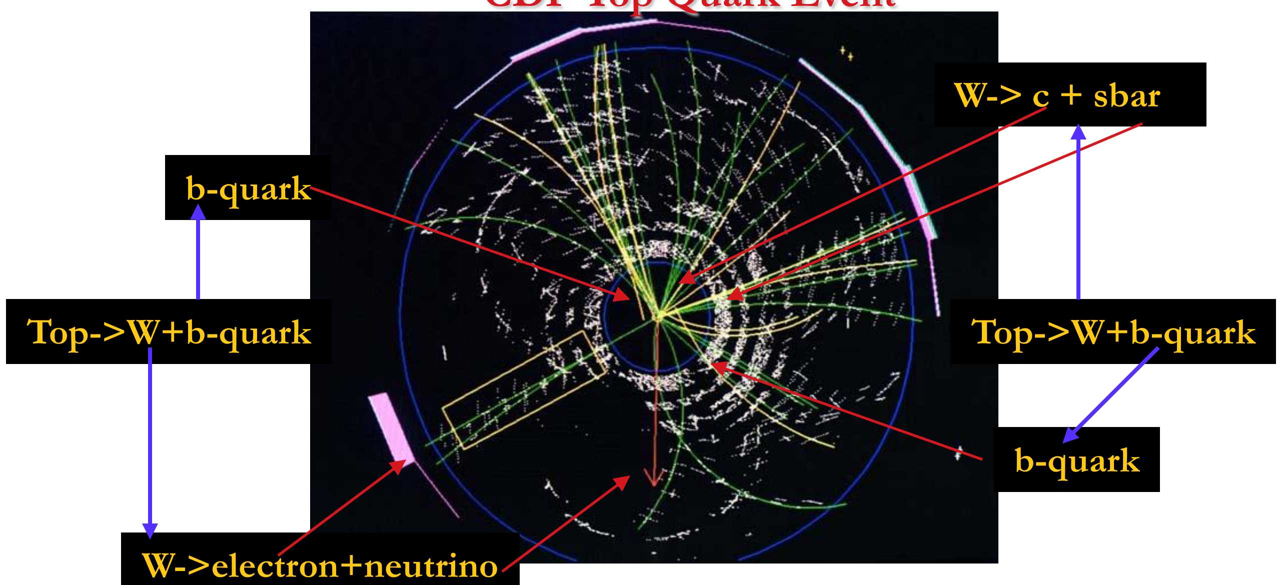

Tracking: a real challenge at LHC

- Tracking at LHC is a very complex procedure due to the high track density. It needs specific implementation adapted to the detector type and geometry

- Precise and efficient detector modules are required to measure where the particle crossed the module

- Fast and radiation hard detectors and electronics are needed

- Track reconstruction requires specific software implementation:
  - track finding (pattern recognition)
  - estimation of track parameters (fitting)

- Precise alignment of detector modules is a prerequisite for efficient tracking

Tracking: how

measureable signals occur via the interaction of particles with the detector material.

Dominant interaction is due to the coulomb interactions with the atomic *electrons* of the detector.

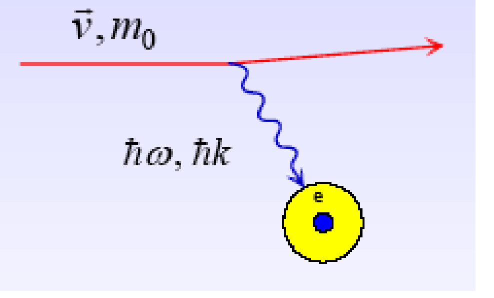

Depending on the $\hbar\omega$ value we may have:

- ionization   or   - excitation/scintillation

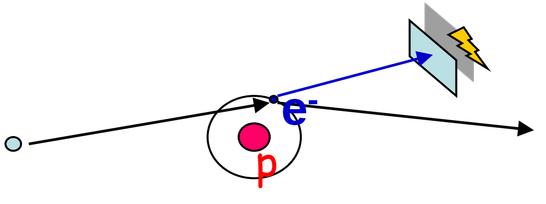

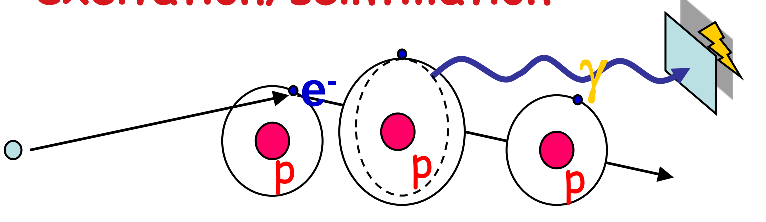

Ionization and excitation of atomic electrons in matter are the most common processes and allow to build precise tracking detectors .

Ionization: the Bethe-Bloch formula

$$\left\langle \frac{dE}{dx} \right\rangle = -4\pi N_A r_e^2 m_e c^2 z^2 \frac{Z}{A} \frac{1}{\beta^2} \left[\frac{1}{2} \ln \frac{2m_e c^2 \gamma^2 \beta^2}{I^2} T^{max} - \beta^2 - \frac{\delta}{2} \right]$$

$$T_{max} \approx 2m_e c^2 \beta^2 \gamma^2$$

$$\boxed{-\frac{dE}{dx} \approx Kq^2 \frac{Z}{A\beta^2} \left[\ln \frac{2m_e c^2 \beta^2 \gamma^2}{I^2} - \beta^2 \right]}$$

Charaterized by:

- a fall off at low energy $\sim 1/\beta^2$
- a relativistic rise $\sim \ln \beta\gamma$
- a minimum at $\beta\gamma \approx 3$
- depends only on $\beta\gamma$ not on m

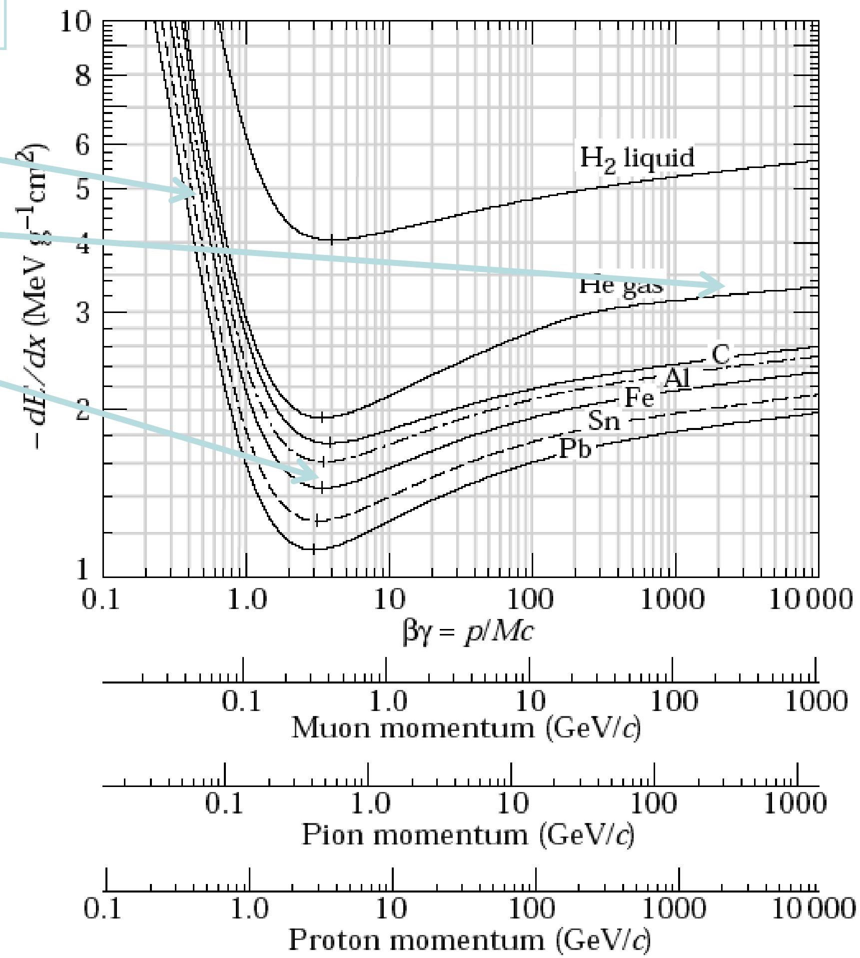

High energy charged particles lose energy slowly in material due to ionization leaving tracks as they pass (For $Z \approx 0.5A$ at $\beta\gamma \approx 3$ $1/\rho\ dE/dx \approx 1.4$ MeV cm^2/g)

➔ many kinds of tracking detectors can be done !

Tracking Detectors

Charged particles crossing a material loose energy by ionizing (and exciting) atoms and thus leaving along their path a trace of electron-ion pairs in gases and liquids and electron-hole pairs in solids.

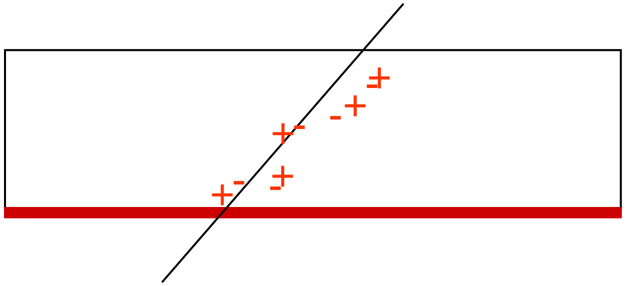

Measurable electronics signals can be induced by the charges produced in this way and can be read by dedicated electronics

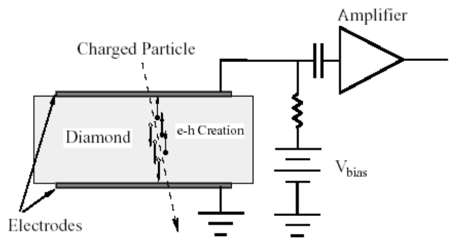

- In solid state detectors the charges produced by the ionization due to the incoming particle are sufficient to provide a measurable signal.

- Mean (most probable) energy loss: 116 (78) keV for 300μm Si thickness
- 3.6 eV to create an e-h pair
  - ⇒ 72 e-h/μm (most probable)
  - ⇒ 108 e-h/μm (mean)
- Most probable charge (300μm Si) ≈ 21600 e ≈ 3.5 fC

- In gas detectors the charges produced by the primary ionization due to the incoming particle need amplification in order to provide a measurable signal.

GAS)	Helium	Argon	Xenon	CH_4	DME
dE/ dx (keV/ cm)	0.32	2.4	6.7	1.5	3.9
<n>(ion-pair/ cm)	5.9	29	44	16	55

Wire Chamber: Electron Avalanche

- **Basic design:** ionization chamber with HV sense wire

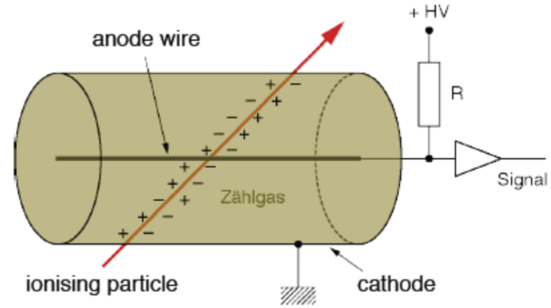

Typically a gas detector will have ~20 primary ions per cm created by a track: amplification needed in order to provide a measurable signal.

Consider a thin wire with radius a (10-25μm) at voltage V=0 in a tube of outer radius b (1-3cm) voltage V_0. The electric field inside the tube is given by:

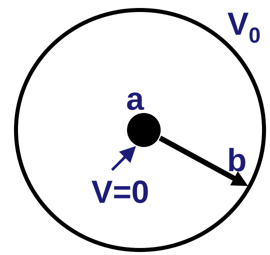

$$E = 2\lambda / r, \quad V_0 = 2\lambda \ln(b/a), \quad V(r) = V_0 \frac{\ln(r/a)}{\ln(b/a)}, \quad E(r) = \frac{V_0}{r \ln(b/a)}$$

Example: V_0=1000V, a=10μm, b=10mm, E(a)=150kV/cm

Electric field is sufficient to accelerate electrons to energies which are sufficient to produce secondary ionization → electron avalanche → signal.
(tipical amplification: 10^3-10^5)

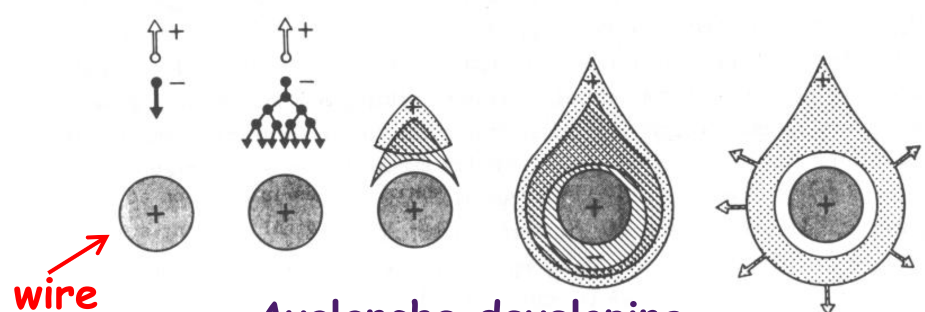

Avalanche developing

Multiwire Proportional Chambers

The MWPC was invented by Charpak at CERN 1992  Prize

Principle of proportional counter is extended to large areas. One plane of thin sense wires is placed between two parallel plates. Typical dimensions: wire distance 2-5mm, distance between cathode planes ~10mm.
Electrons ($v \approx 5cm/\mu s$) are collected within ≈ 100ns.
The movement of the charges induces a signal on the wire AND on the cathode. By segmentation of the cathode plane and charge interpolation, resolutions of 50μm can be achieved.
Stack several wire planes up in different direction to get position location.

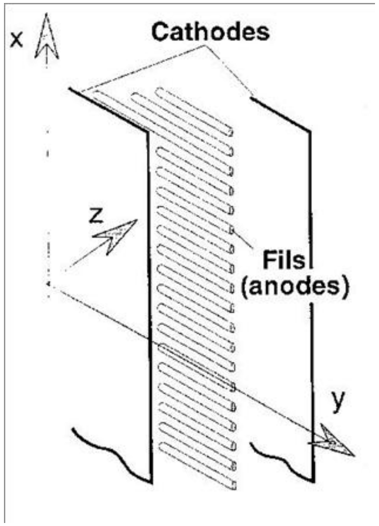

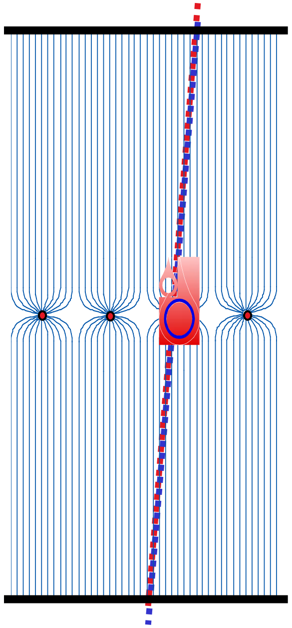

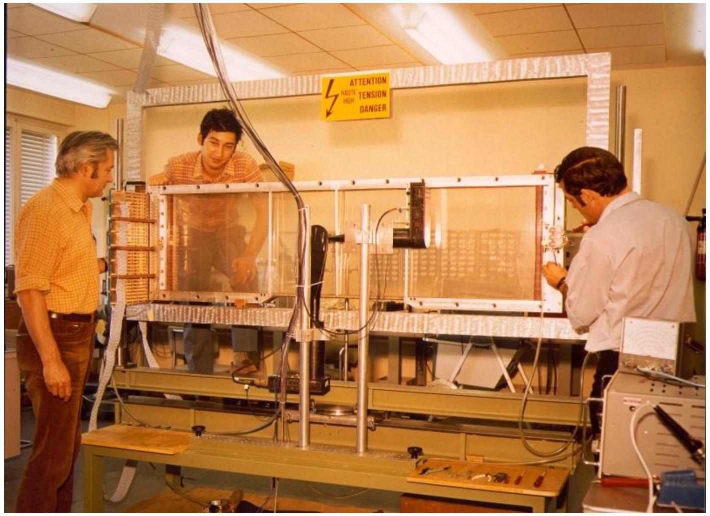

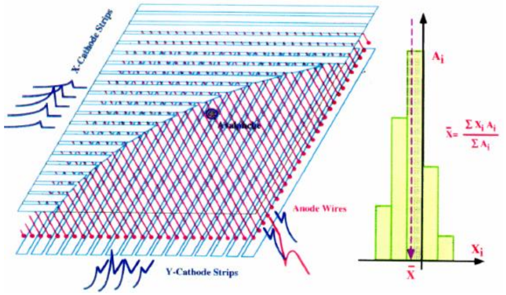

Drift Chamber (1971: H. Walenta)

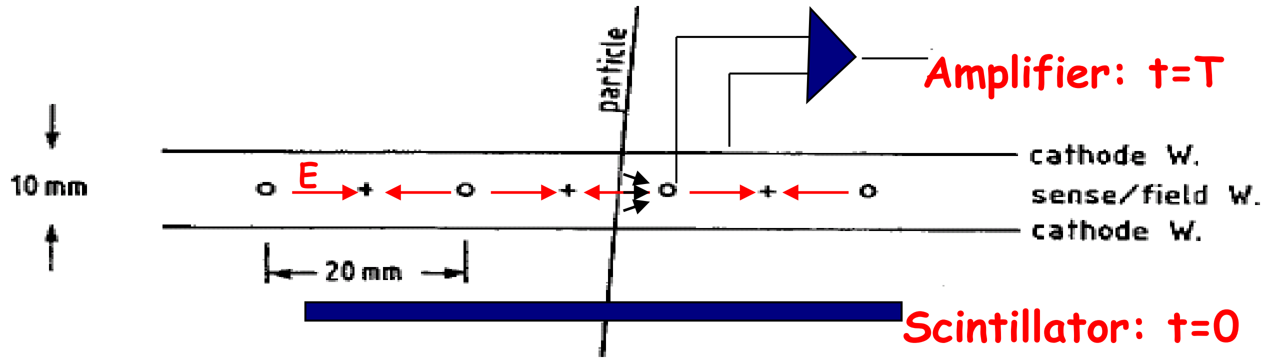

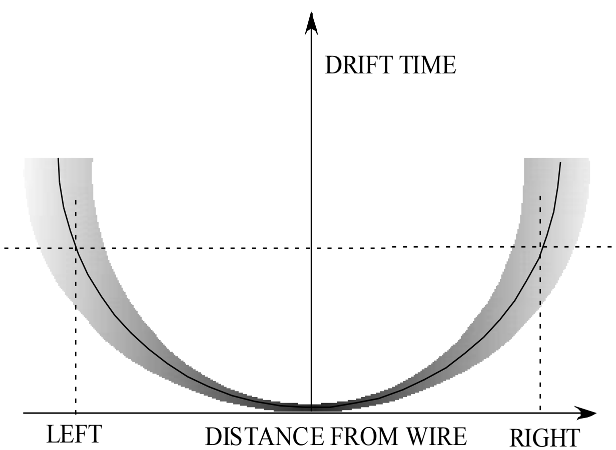

The electric field in an alternating sequence of sense and field wires at different potentials cause the electrons to drift toward the sense wire. The measurement of the drift time T between the passage of the particle and the arrival of the electrons at the sense wire is a measurement of the position of the particle (precision ~100μm)
The wire distance can be increased up to several centimeters (drift time ~μs; v≈5cm/μs) saving a lot of electronics channels with respect to the MWPC. however:

- ❑ Left-Right ambiguity
- ❑ Not a linear relation between drift time and distance from the wire

Time Projection Chamber (TPC)

1976: D. Nygren (LBL)

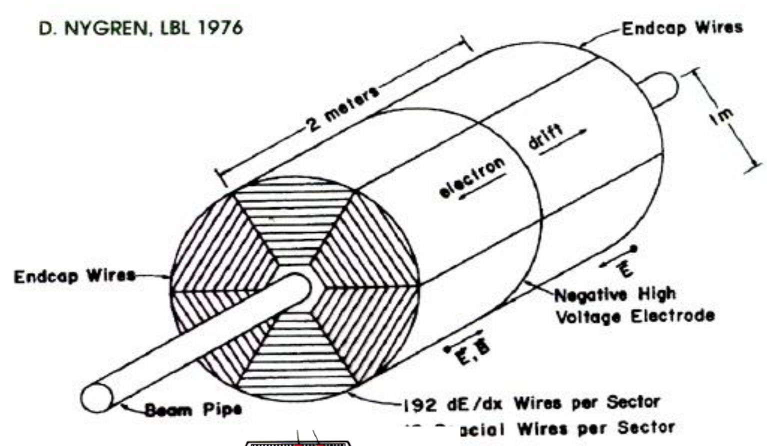

- ❑ E~100-300 V/cm. Drift times 10-100 μs
- ❑ B for momentum measurement
  (limit electron diffusion up to a factor 5)
- ❑ Wire chamber to detect projected tracks.
  Timing gives z measurement
- ❑ Long drift distances up to 2.5 m

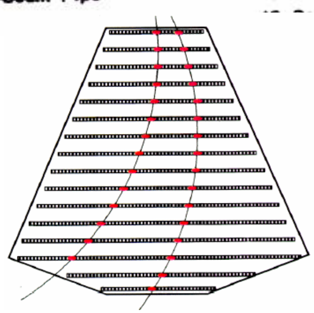

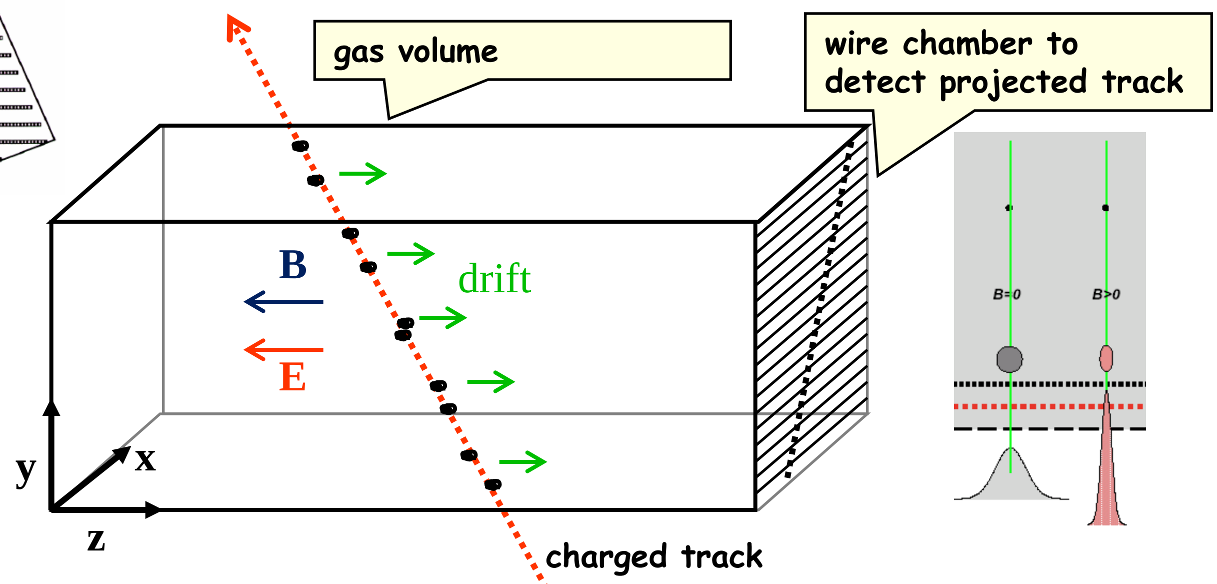

The family of gas detectors

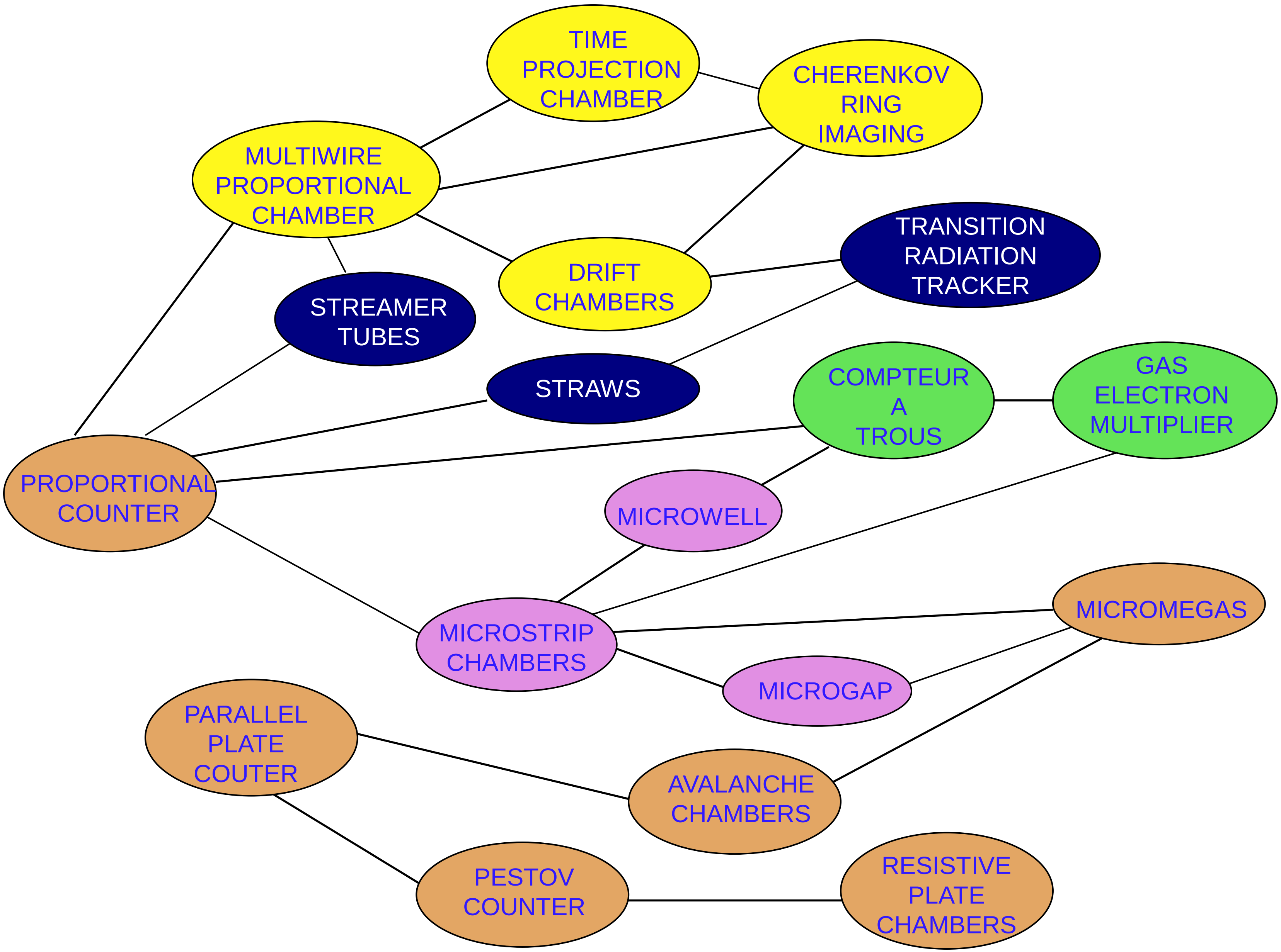

Solid State Detectors

In solid state detectors the charges produced by the ionization due to the incoming particle are sufficient to provide a measurable signal.

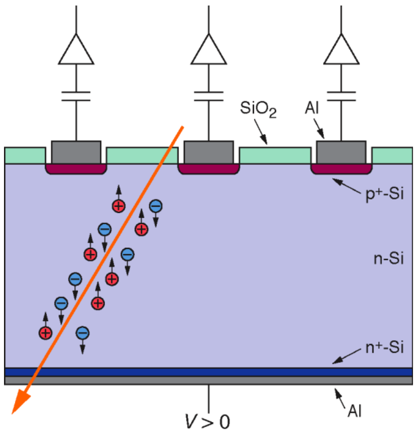

- ❑ Solid state detectors have a high density
  ➔ large energy loss in a short distance:
  116 (78) keV = mean (most probable) energy loss
  for 300μm Silicon thickness
- ❑ Low ionisation energy (few eV per e-hole pair) compared to gas detectors (20-40 eV per e-ion pair)
  3.6 eV for silicon to create an e-hole pair
  $\Rightarrow$ 72 e-h/μm (most probable); 108 e-h/μm (mean)
  $\Rightarrow$ most probable charge 300μm Silicon thickness:
  $\approx$ 21600 e $\approx$ 3.5 fC
- ❑ Drift velocity much faster than in gas detectors:
  ➔ Very fast signals of only a few ns length !
- ❑ Diffusion effect is smaller than in gas detectors:
  ➔ achievable position resolution of less than 10 μm

Si-Diode as Si-Detector

At the p-n junction the difference in the fermi levels cause diffusion of charge carries until thermal equilibrium is reached and the electric field thus created stops further diffusion. At this point the fermi level is equal.
A zone free of charge carries, called **depletion region**, is thus established .

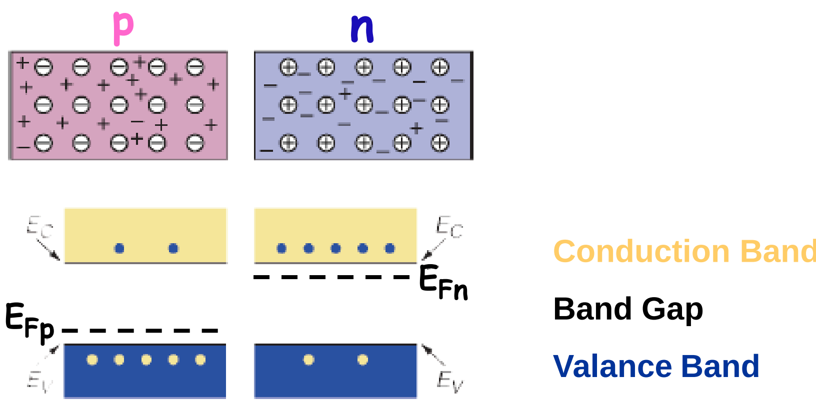

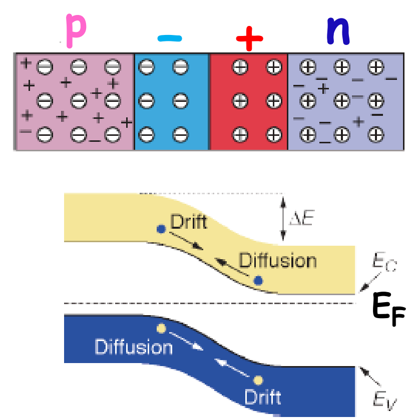

+ hole — ⊖ acceptor

– electron — ⊕ donator

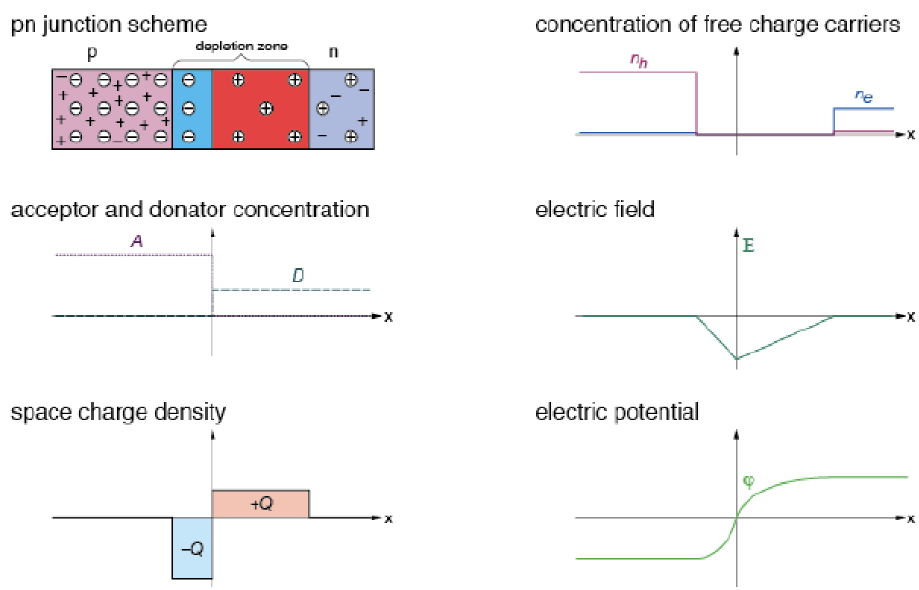

acceptor: p-doping atom (with 3 valence electron)
donator: n-doping atom (with 5 valence electron)

Si-Diode as Si-Detector

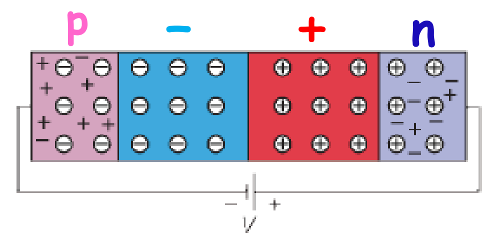

By applying an external voltage V, the depletion zone can be extended to the entire diode.

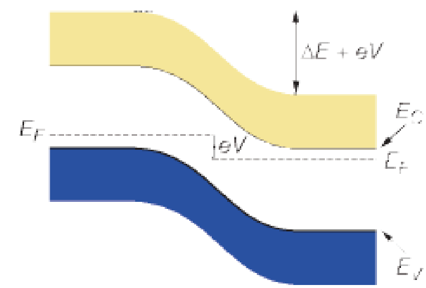

An incoming particle can then produce by ionization free charge carriers in the diode.
The charges carriers drift in the electric field and induce an electrical signal on the electrodes.

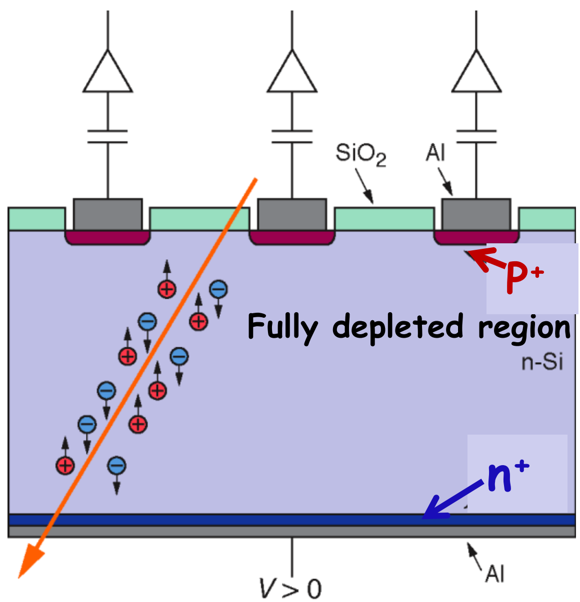

➔ That is the way a Silicon detector can work !

Detector Structures

Top view of a strip detector with polysilicon resistors:

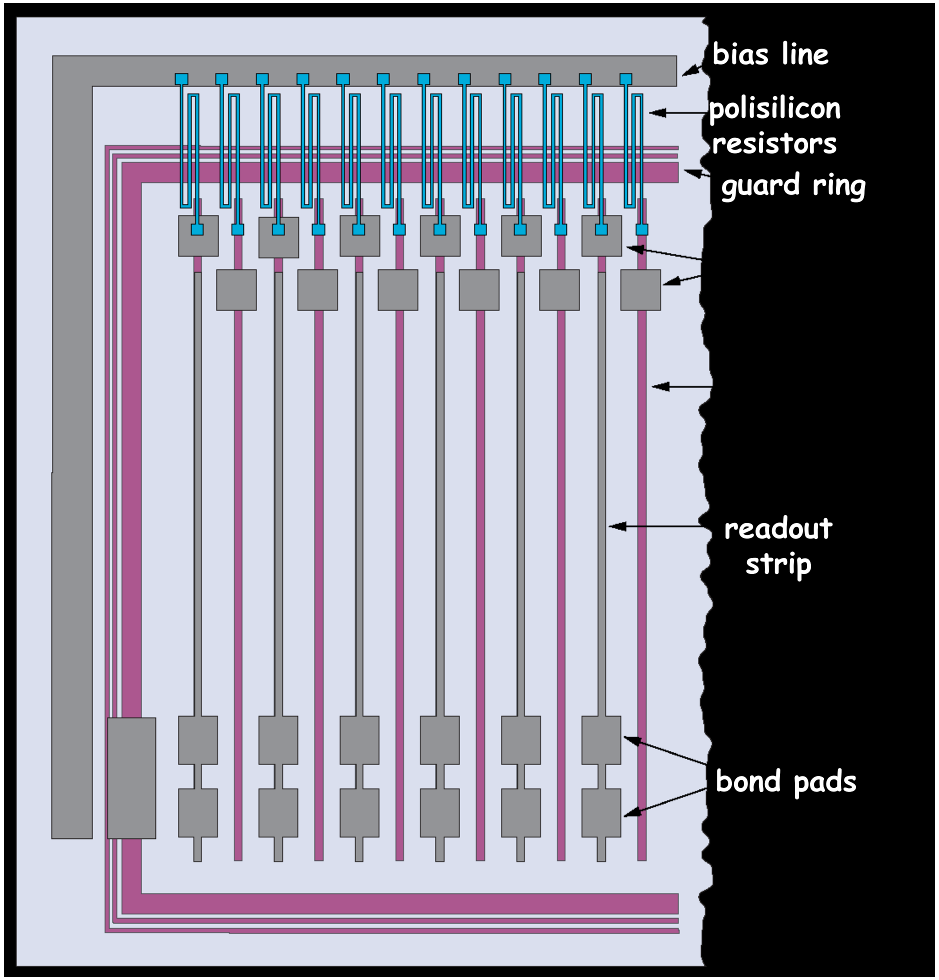

CMS-Microstrip-Detector: Close view of area with polysilicon resistors, probe pads, strip ends.

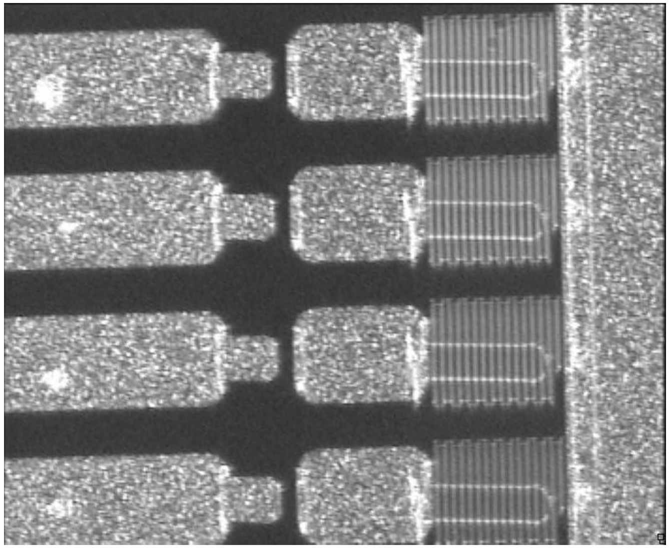

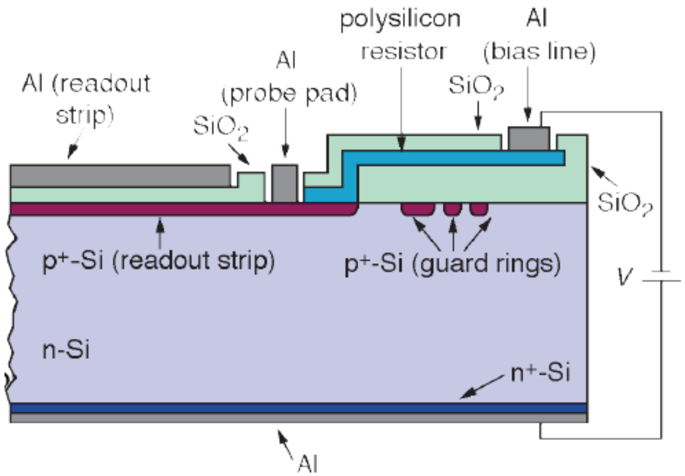

Double Sided Strip Detectors

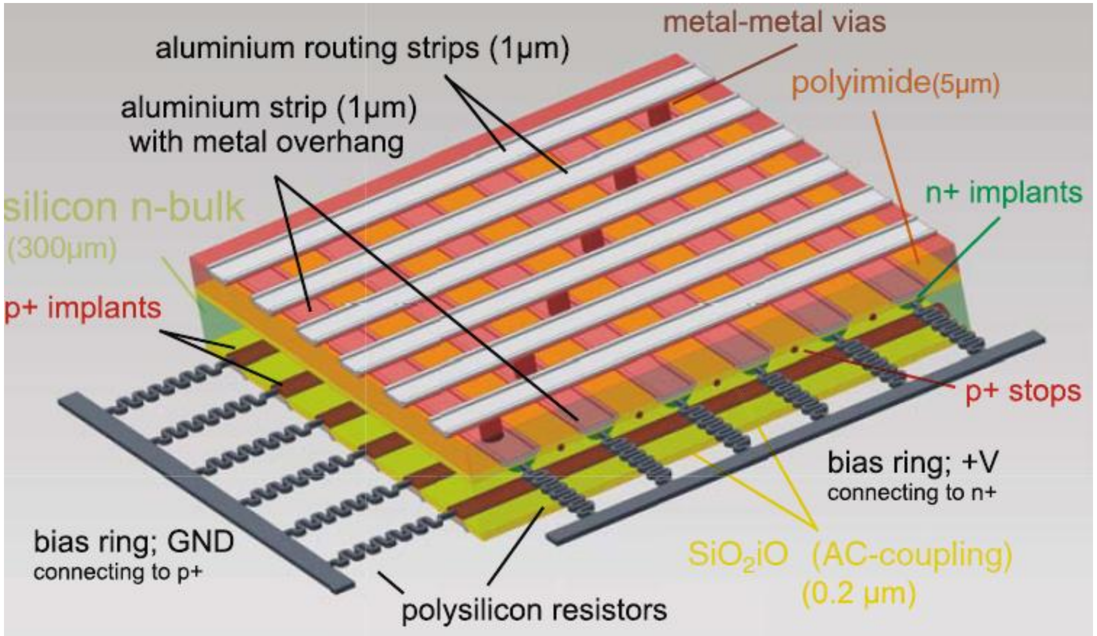

- Single sided strip detector measures only one coordinate.
  To measure second coordinate requires second detector layer.
- Double sided strip detector minimizes material measuring two coordinates in one detector layer.
- In n-type detector the n+ backside becomes segmented e.g. strips orthogonal to p+ strips.
- Drawback: Production, handling, tests are more complicated and hence double sided detector are expensive.

Double Sided Strip Detectors

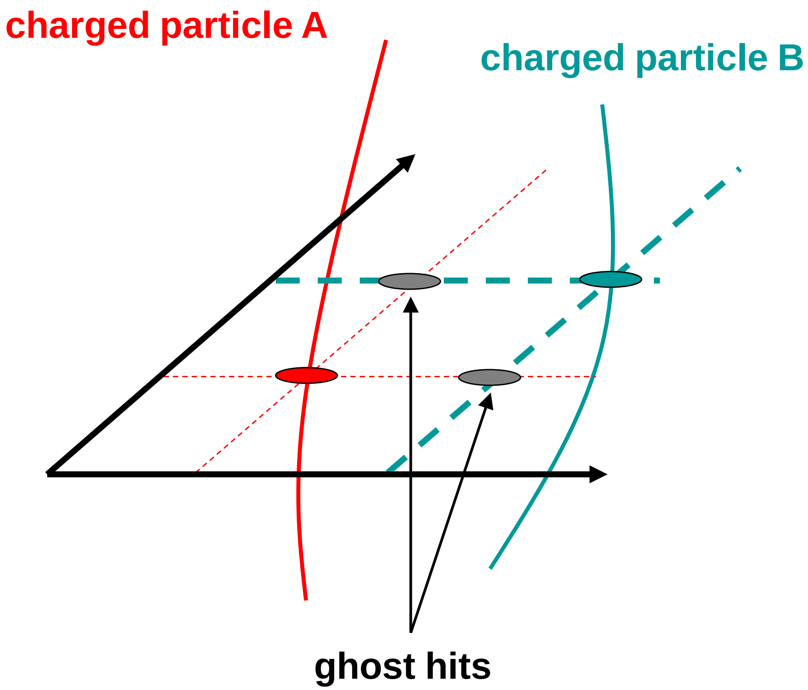

Double sided strip sensors measure the 2 dimensional position of a particle track. However, if more than one particle hits the strip detector the measured position is no longer unambiguous. “Ghost”-hits appear!

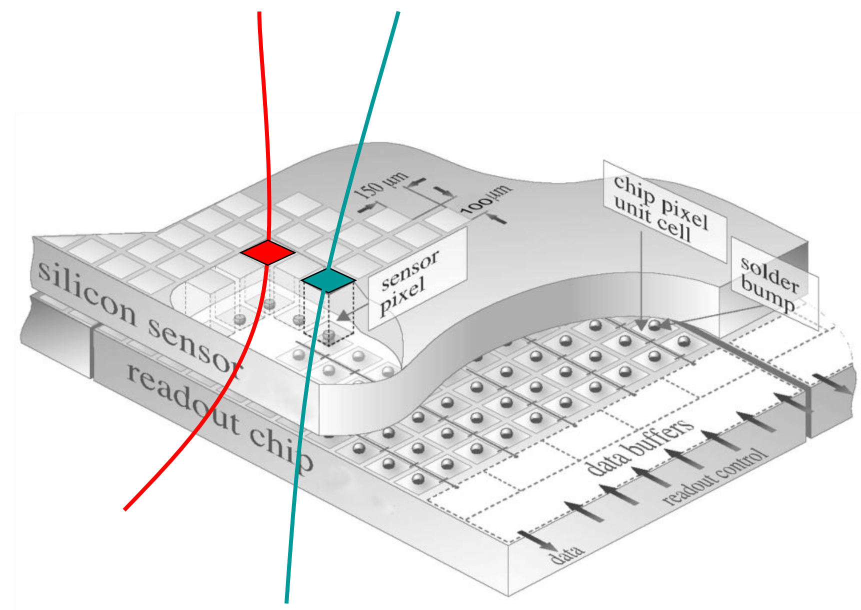

Pixel detectors produce 2-dimensional position measurements without ambiguity also in case of two particles crossing the detector!

Silicon Drift Detector (like gas TPC !)

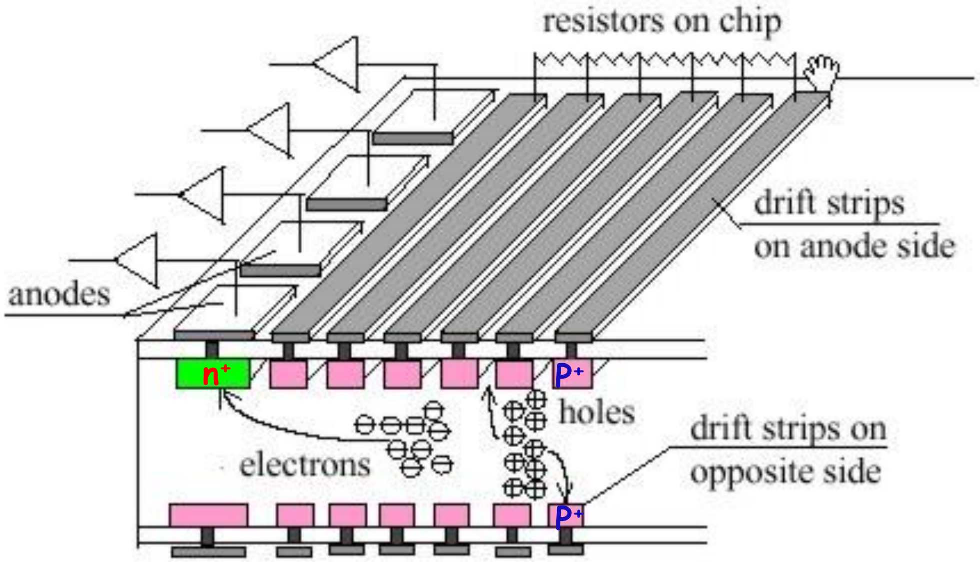

In silicon drift detectors the p+ strips and the backplane p+ implantation are used to fully deplete the bulk.

A drift field transports the generated electrodes to the readout electrodes (n+).

One coordinate is measured by signals on strips, the second by the drift time.

LHC: a very hostile environment for tracking

(high event rate, high multiplicity of charged tracks, high radiation flux)

Collisions at LHC

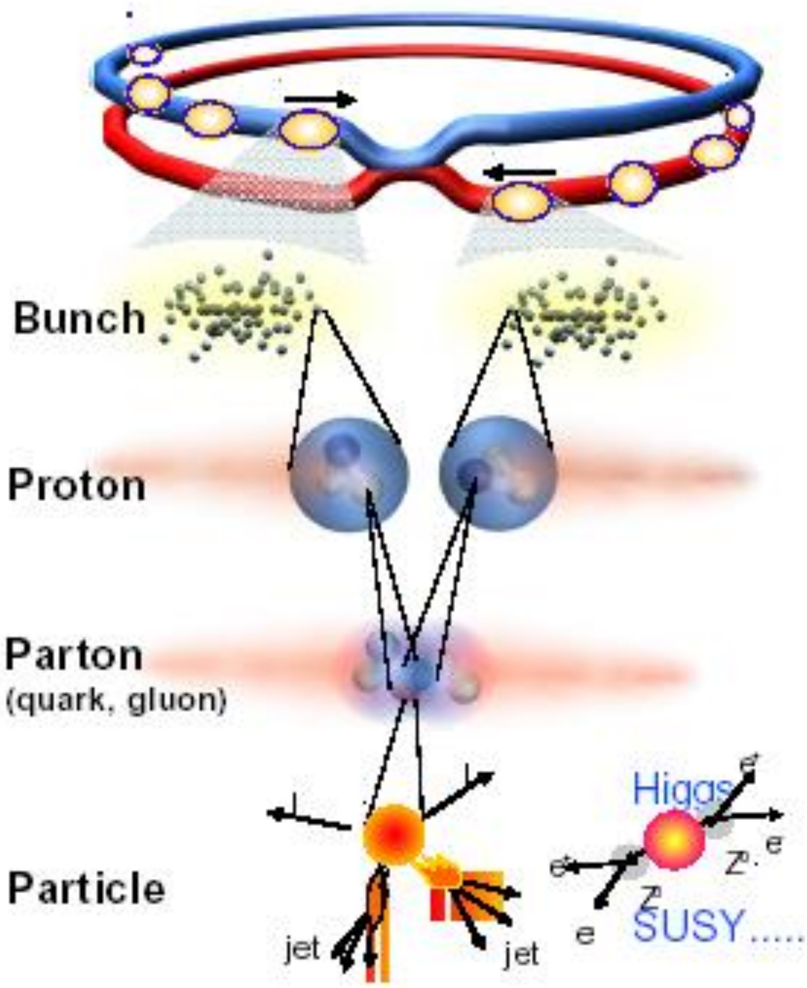

Proton-Proton	2835 bunch/beam
Protons/bunch	10^{11}
Beam energy	7 TeV (7×10^{12} eV)
Luminosity	10^{34} cm^{-2} s^{-1}
Crossing rate	40 MHz
Collisions rate ≈	10^{7} - 10^{9} Hz
New physics rate ≈	.00001 Hz

Event selection:
1 in 10,000,000,000,000

Signal and background → $\mathcal{L}=10^{34}\ cm^{-2}s^{-1}$

Cross sections for various physics processes vary over many orders of magnitude

Higgs (600 GeV/c^2): 1pb @10^{34} → 10^{-2} Hz
Higgs (100 GeV/c^2): 10pb @10^{34} → 0.1 Hz
t t production: → 10 Hz
$W \rightarrow \ell\nu$: → 10^2 Hz
Inelastic: → 10^9 Hz

Selection needed: 1:10^{10-11}
Before branching fractions...

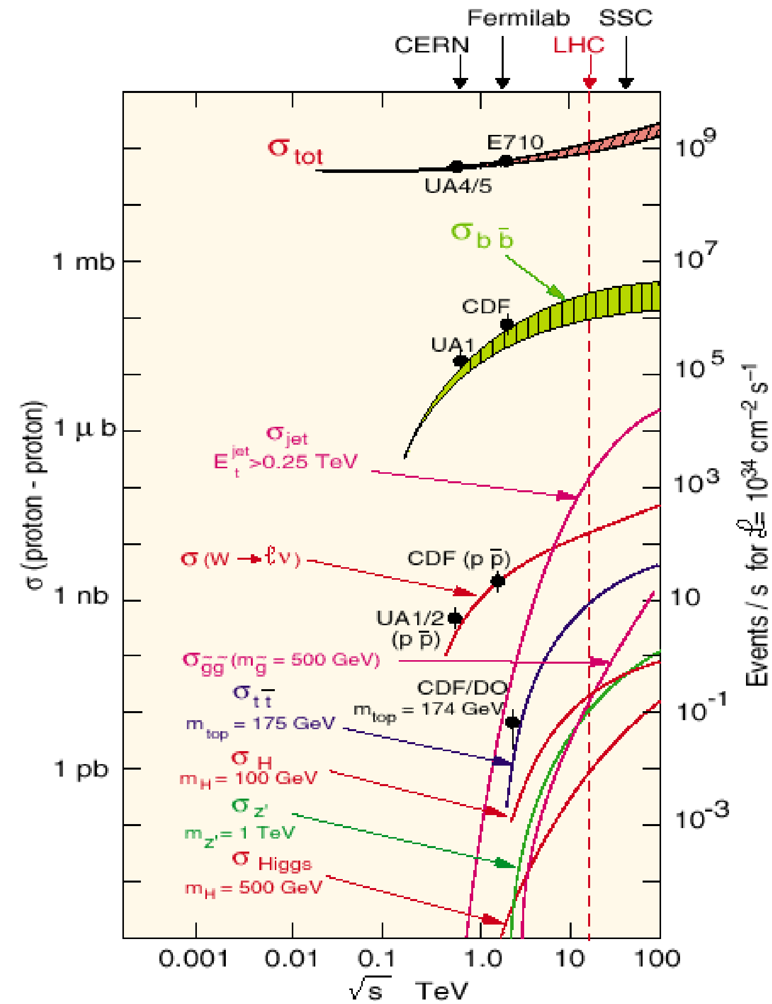

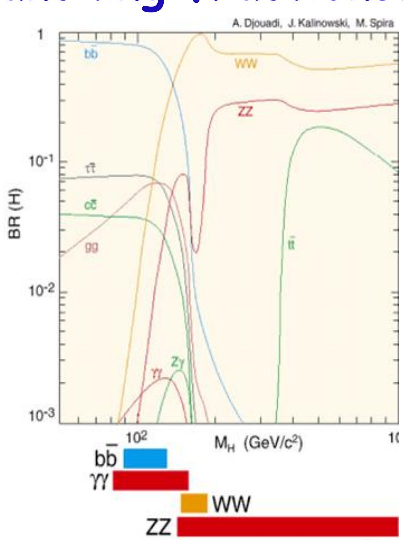

⇒ Needle in a Hay Stack

pp cross-sections and minimum bias

of interactions/crossing:

- Interactions/s:
  - Lum = 10^{34} $cm^{-2}s^{-1}$=$10^{7}mb^{-1}Hz$
  - $\sigma_{inel}(pp)$ = 80 mb
  - Interaction Rate, R = 8×10^{8} Hz
- Events/beam crossing:
  - Δt = 25 ns = 2.5×10^{-8} s
  - Interactions/crossing=20
- Not all p bunches are full
  - 2835 out of 3564 only
  - Interactions/"active" crossing =
  - = 20 x 3564/2835 = 25

$\sigma_{inel}(pp) \approx 80$ mb@14TeV

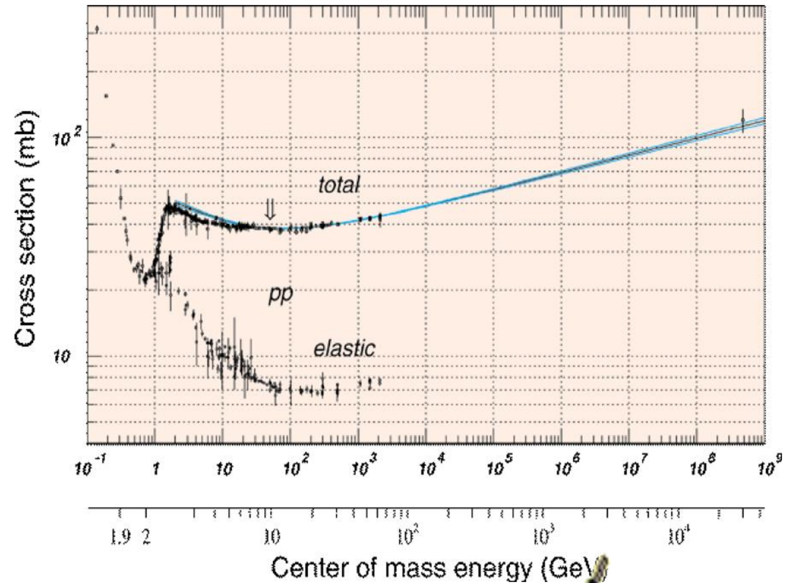

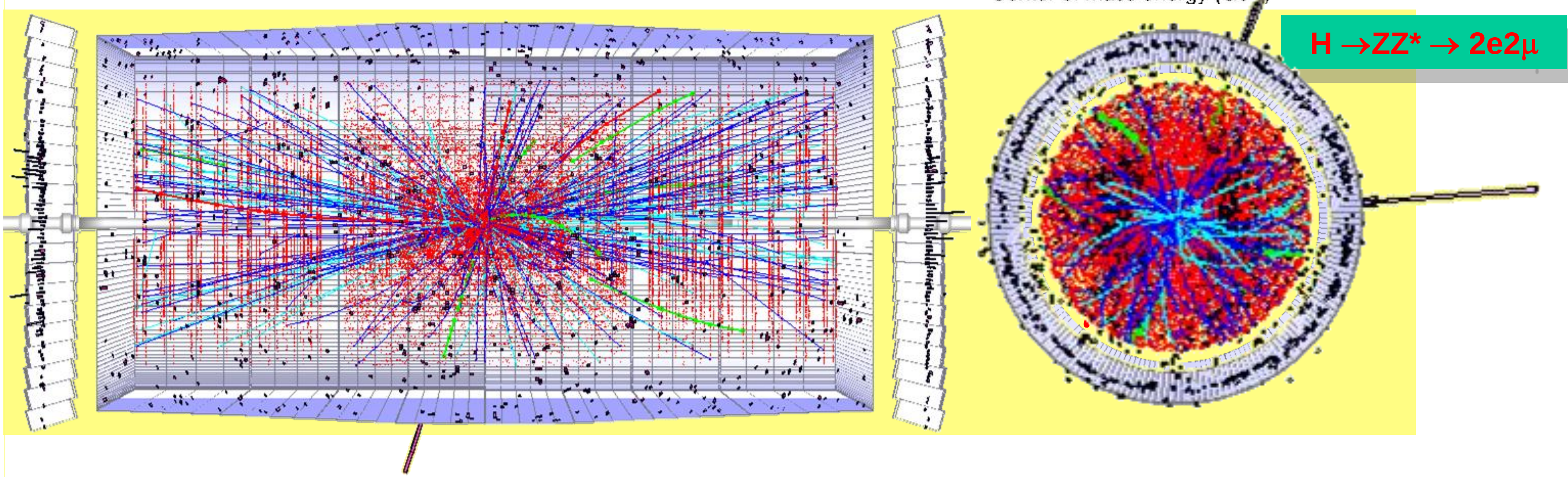

Impact on detector design

LHC detectors must have fast response

Otherwise will integrate over many bunch crossings

→ large "pile-up"

Typical response time : 20-50 ns

→integrate over 1-2 bunch crossings

→ pile-up of 25-50 min-bias

→ very challenging readout electronics

LHC detectors must be highly granular

Minimize probability that pile-up particles be in the same detector element as interesting object

→ large number of electronic channels

→ high cost

LHC detectors must be radiation resistant:

high flux of particles from pp collisions

→ high radiation environment

Evian, March 1992: first meeting on experimental program at LHC

Evian, November 2009: more than 17 years later ready to start…..

Towards the LHC Experimental Programme
General Meeting on LHC Physics & Detectors
5-8 March 1992
Evian-les-Bains, France

Expressions of Interest

ATLAS, CMS, ALICE, LHCb, TOTEM, LHCF

The LHC Detectors

ATLAS

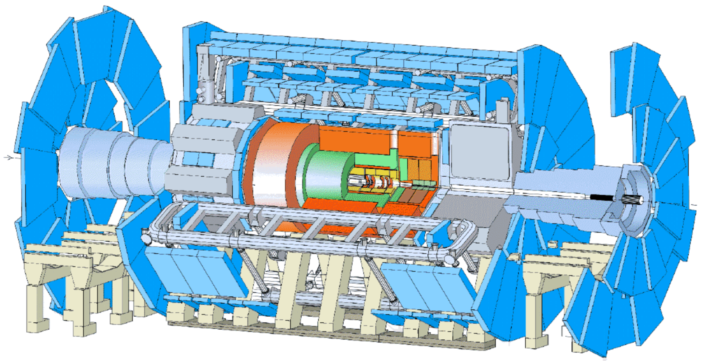

CMS

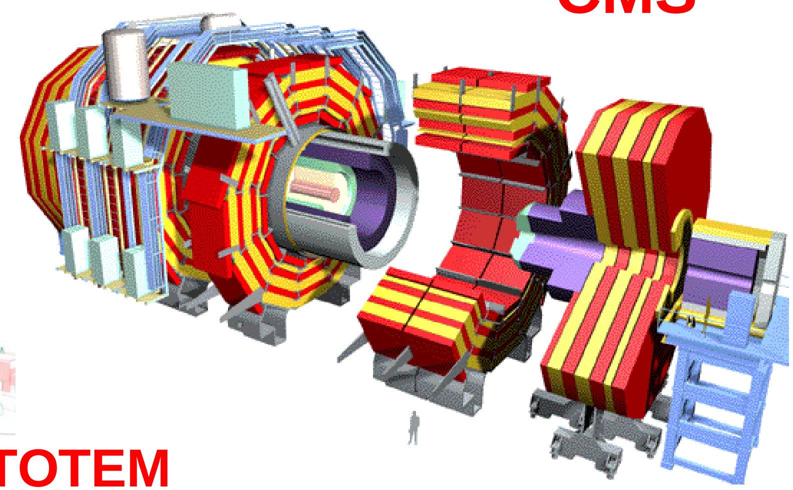

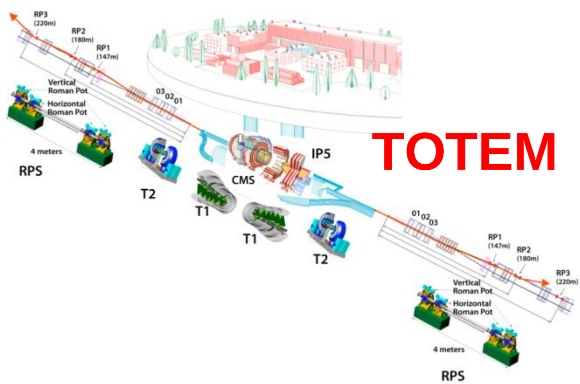

TOTEM

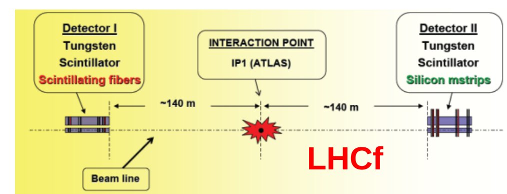

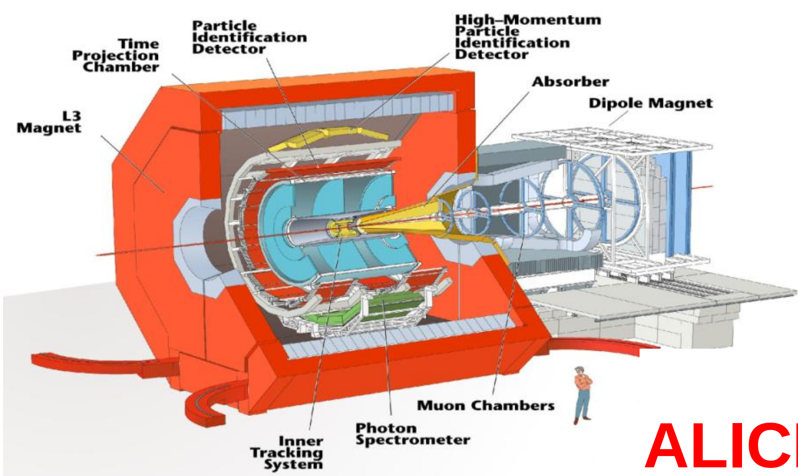

ALICE

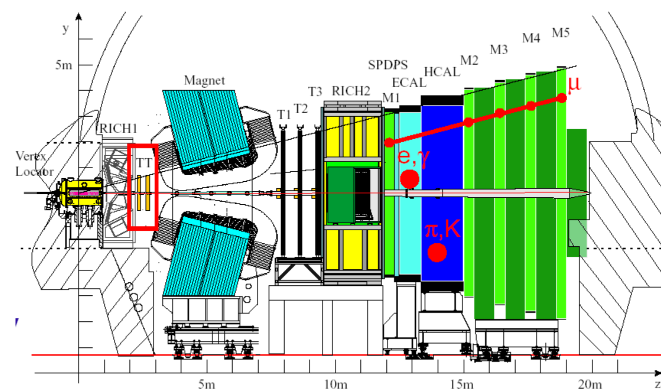

LHCb

Two general-purpose pp detectors with different strategies

ATLAS A Toroidal LHC ApparatuS

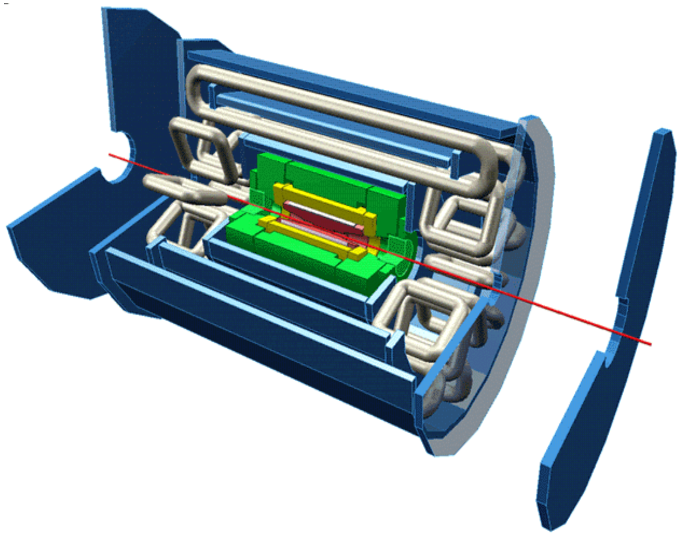

CMS Compact Muon Solenoid

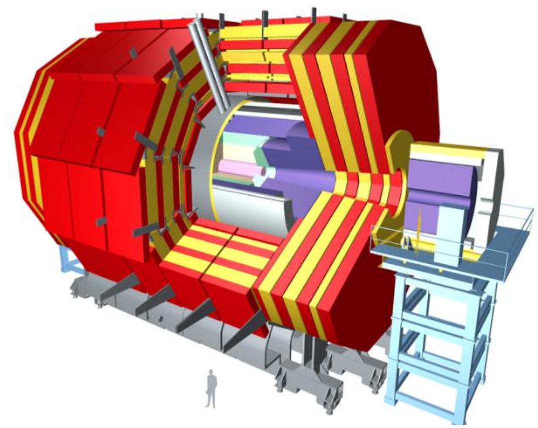

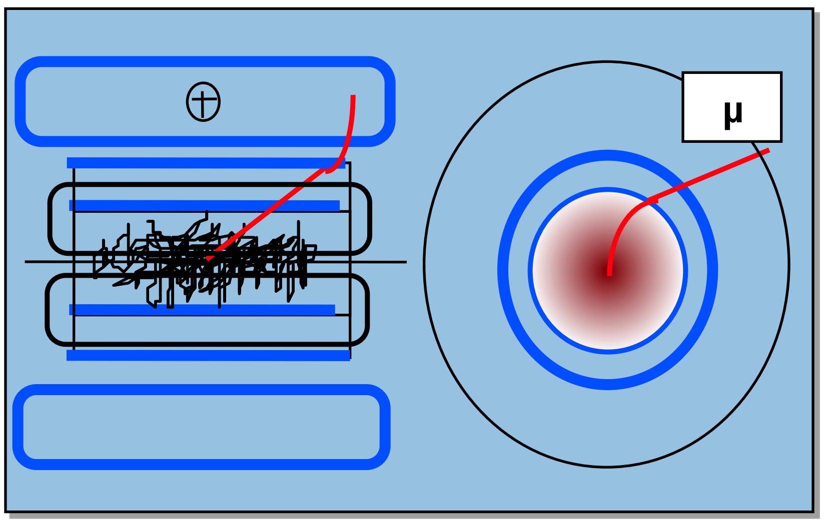

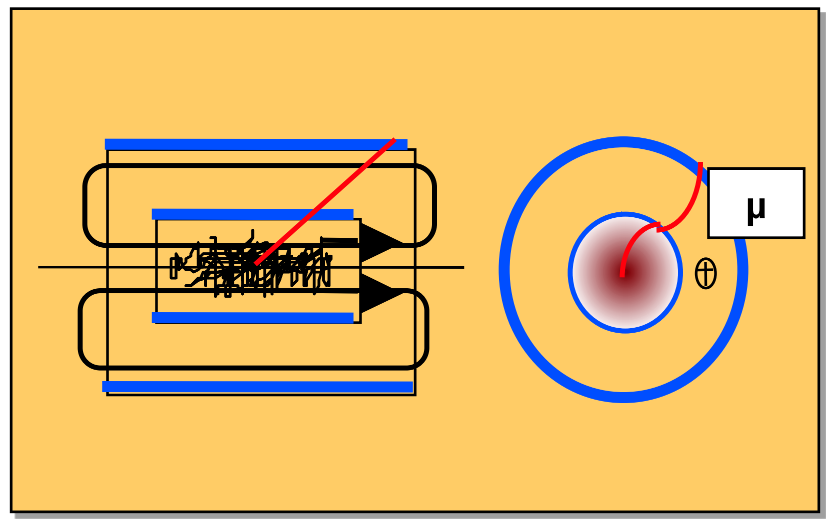

Different Strategies....

2.3mx5.3m Solenoid ~ 2 Tesla Field

End Cap Toroid

ATLAS

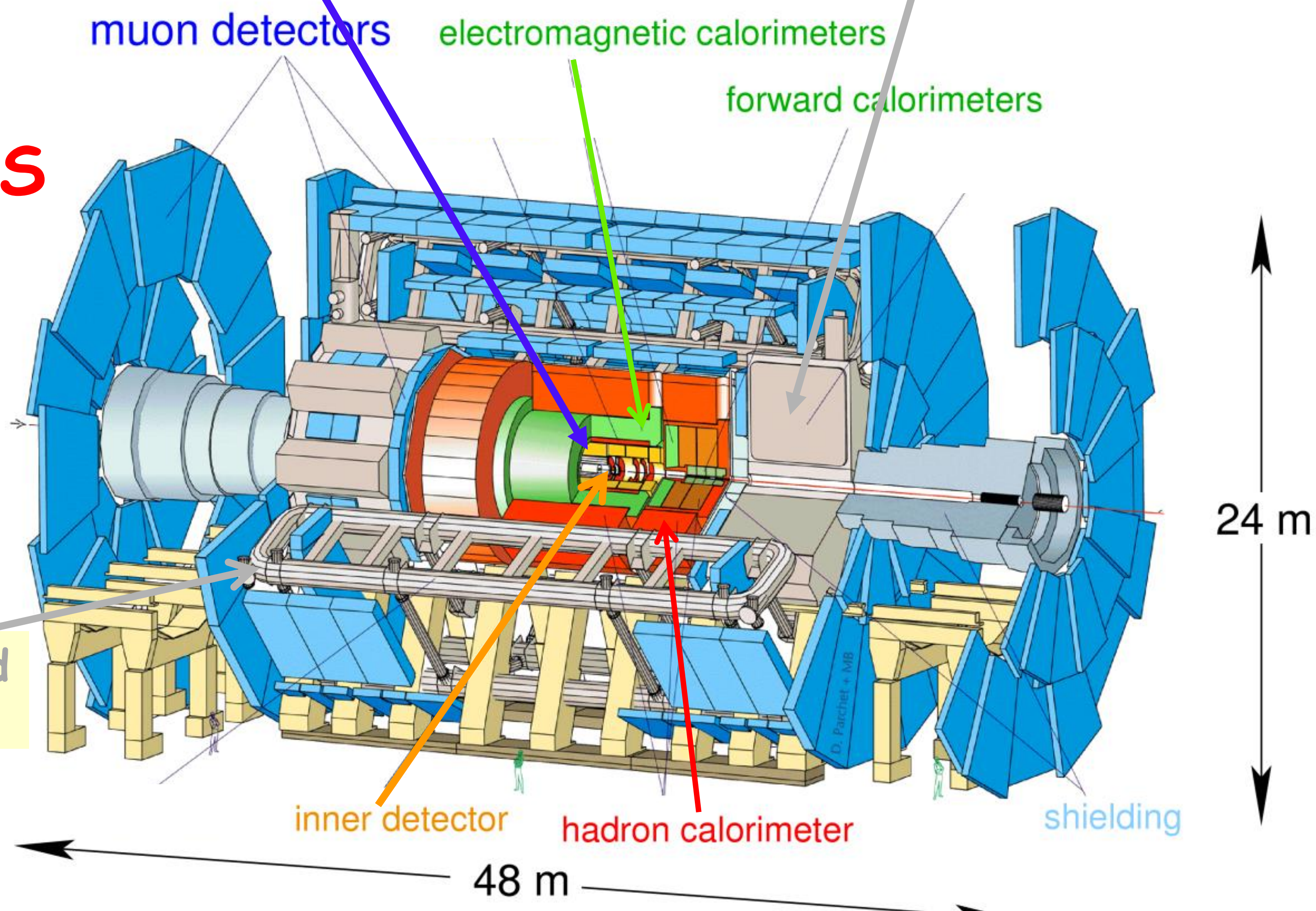

Barrel Toroid
<B> = 0.4 T

48m Long, 24m Diameter, 7'000 Ton Detector

Transverse slice of ATLAS

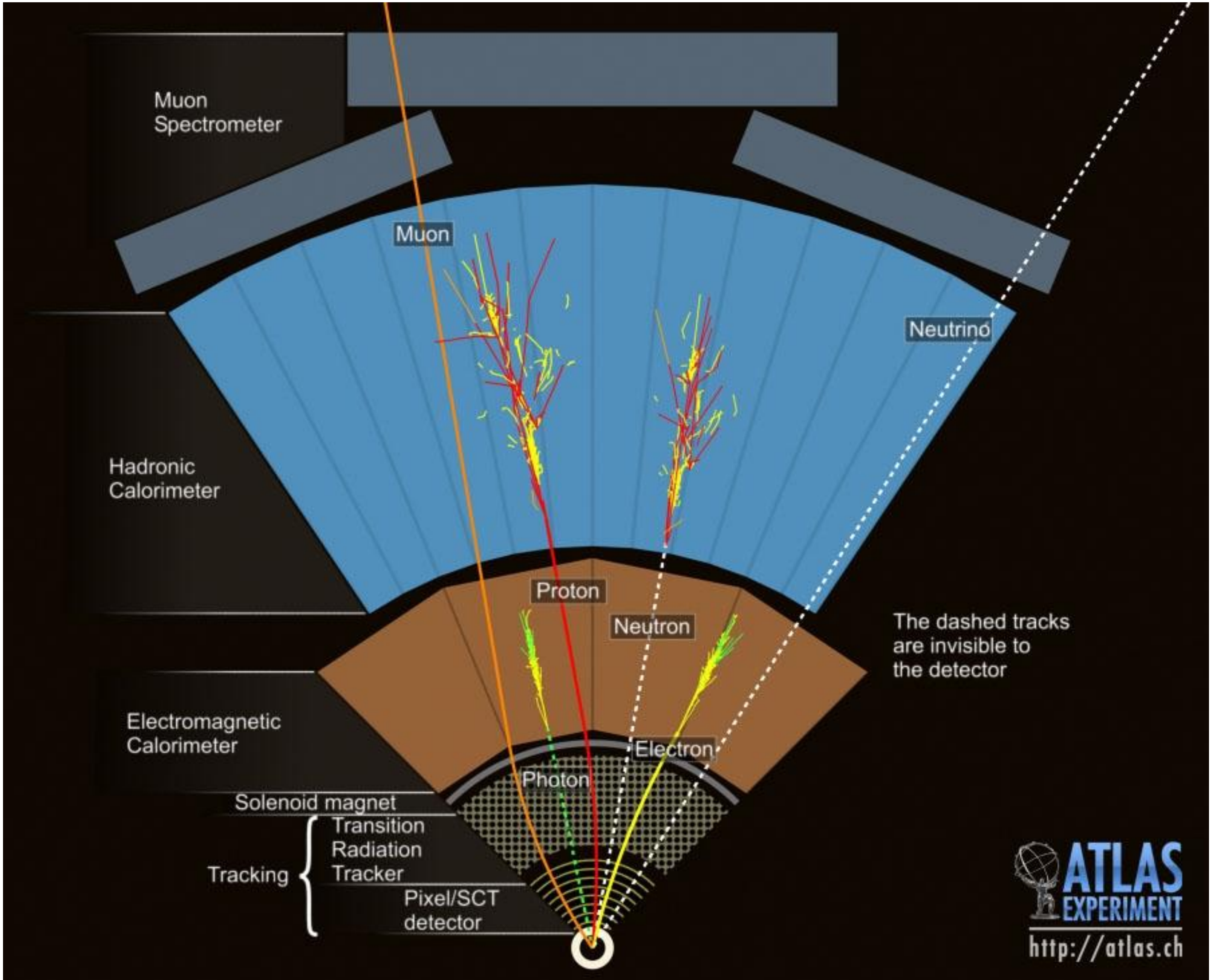

Different Strategies…

13m x 6m Solenoid: 4 Tesla Field

Tracking up to η ~ 2.4

Muon system in return yoke

First muon chamber just after solenoid → extended lever arm for p_t measurement

CMS

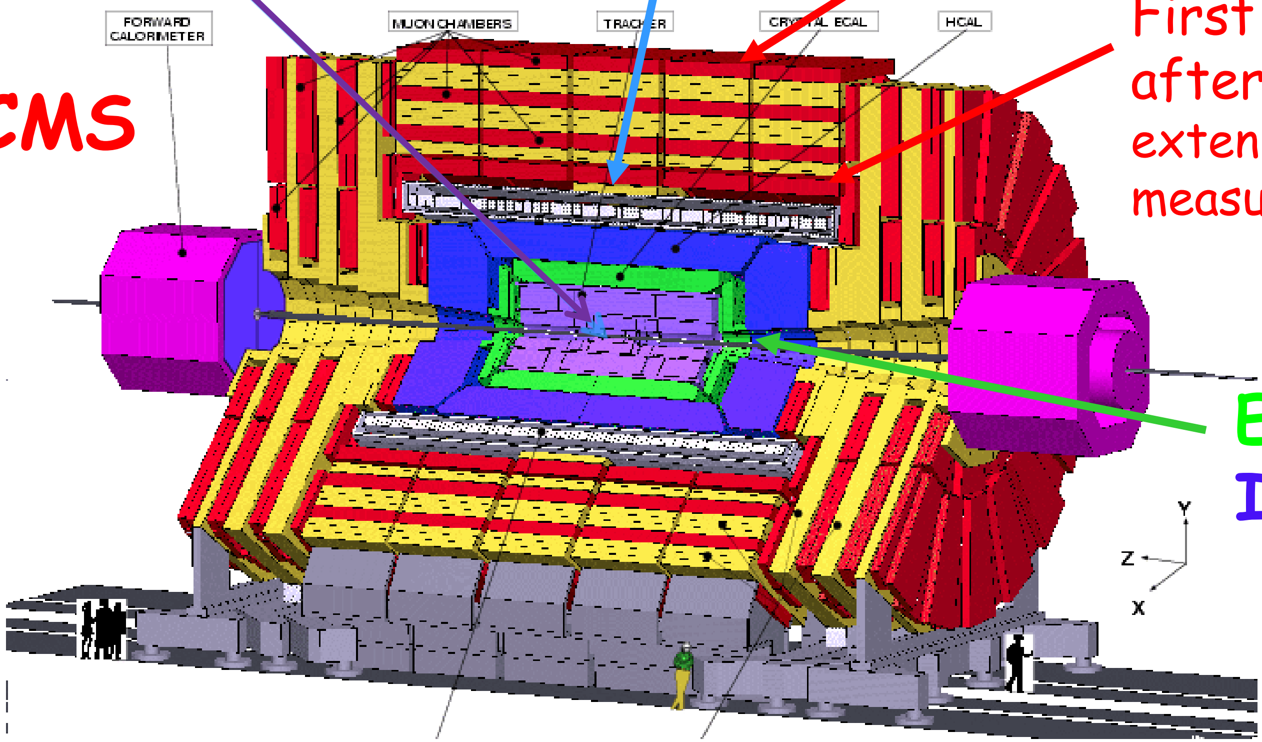

ECAL & HCAL Inside solenoid

22m Long, 15m Diameter, 14'000 Ton Detector

Transverse slice of CMS

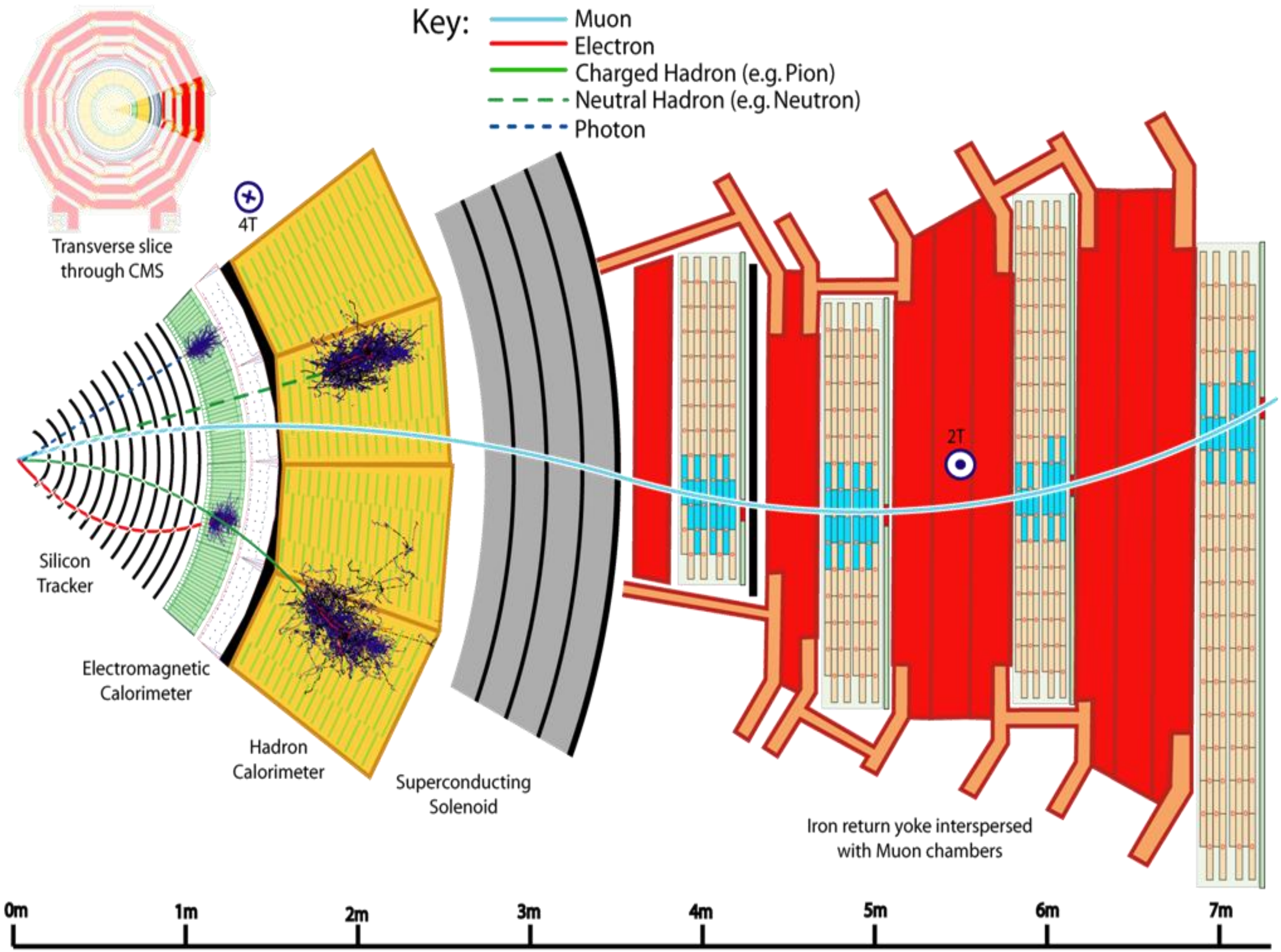

What a luminosity of $10^{34}cm^{-2}s^{-1}$ means on Tracking ...

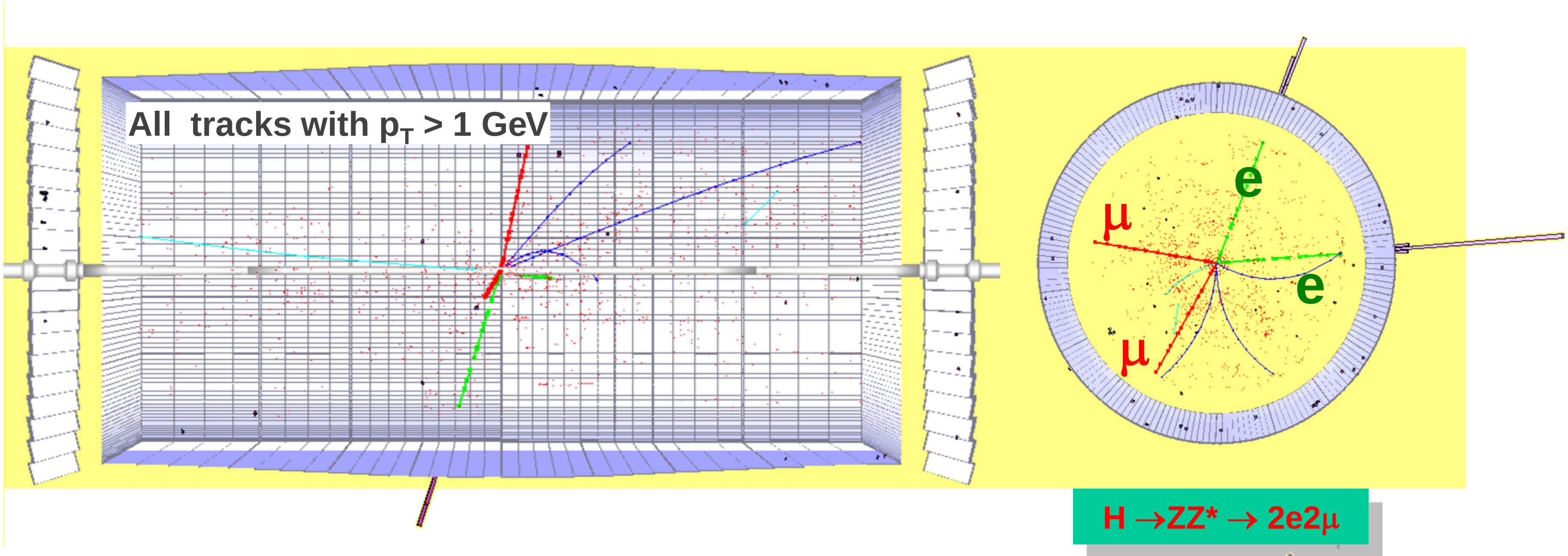

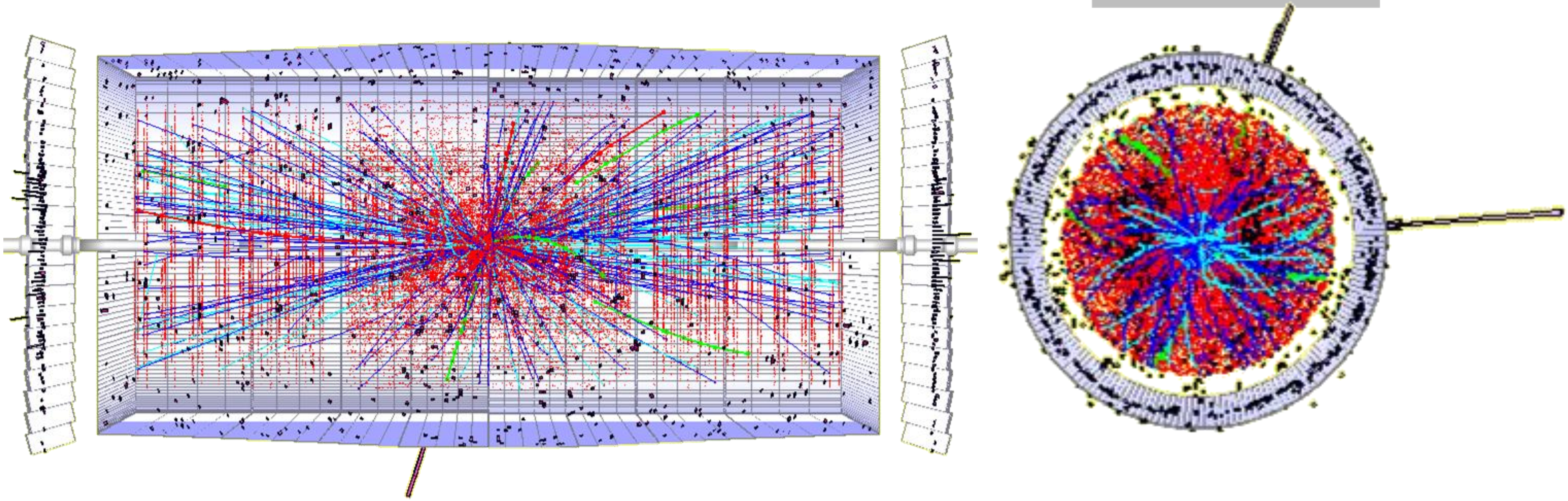

Tracking Requirements

Precise and efficient tracking at LHC is needed to extract physics signals from competitive but reducible background signals:

- Mass cut: precise invariant mass determination from precise momentum measurement of the decay products

- Isolation cut: high track reconstruction efficiency in dense environment (pile-up, jets…)

- Long-lifetime particles tagging: precise and efficient measurement of the track impact parameter and secondary vertices.

The approach

- Silicon microstrip detectors allow a very good point resolution (10-30 microns) that coupled to large lever arms in solenoidal field of 2-4T would allow an adequate momentum resolution, good impact parameter resolution for b-tagging and excellent measurement of the charge up to 1TeV and beyond.
- Single bunch crossing resolution is feasible in silicon (collection time <10ns) with fast read-out electronics.
- The real challenge is pattern recognition for track reconstruction: the high density of tracks typical of the inner regions of high luminosity hadronic colliders can be tackled with extreme segmentations both in r-phi and r-z : pixel detectors and silicon microstrip modules.
- Silicon detectors are well radiation resistant ($\Phi > 10^{14}$ n/cm^2) and can be produced in large scale at rather low cost.

⇒**Pixel detector** (in the radial region 5cm<r<20cm: 10^{14}cm^{-2}<Φ<10^{15}cm^{-2})

⇒**Silicon microstrip** (in the radial region r>20cm: 10^{13}cm^{-2}<Φ<10^{14}cm^{-2})

Two different strategies

This approach has been followed very aggressively by CMS who decided to build the first full silicon tracker in HEP

- more challenge in terms of technology and costs
- higher performance particularly in pattern recognition

ATLAS has adopted a more traditional approach based on a hybrid tracker:
pixel and silicon microstrip detectors in the innermost part and a large gaseous detectors in the outer part (straw tubes).

ATLAS Inner Detector

- **Transition Radiation Tracker (TRT)**
  - **4 mm diameter straw tubes**
  - **351 k channels**
  - **resolution 130 μm**
  - **polypropylene/polyethylene as transition radiation material: electron id 0.5 GeV<E<150 GeV**
- **SemiConductor Tracker (SCT)**
  - **4088 modules**
  - **80 μm strips (40 mrad stereo)**
  - **6 M channels**
  - **resolution 17 μm × 580 μm**
- **Pixel**
  - **1744 modules of 46080 pixels**
  - **mostly 50 μm × 400 μm**
  - **80 M channels**
  - **resolution 10 μm × 110 μm**

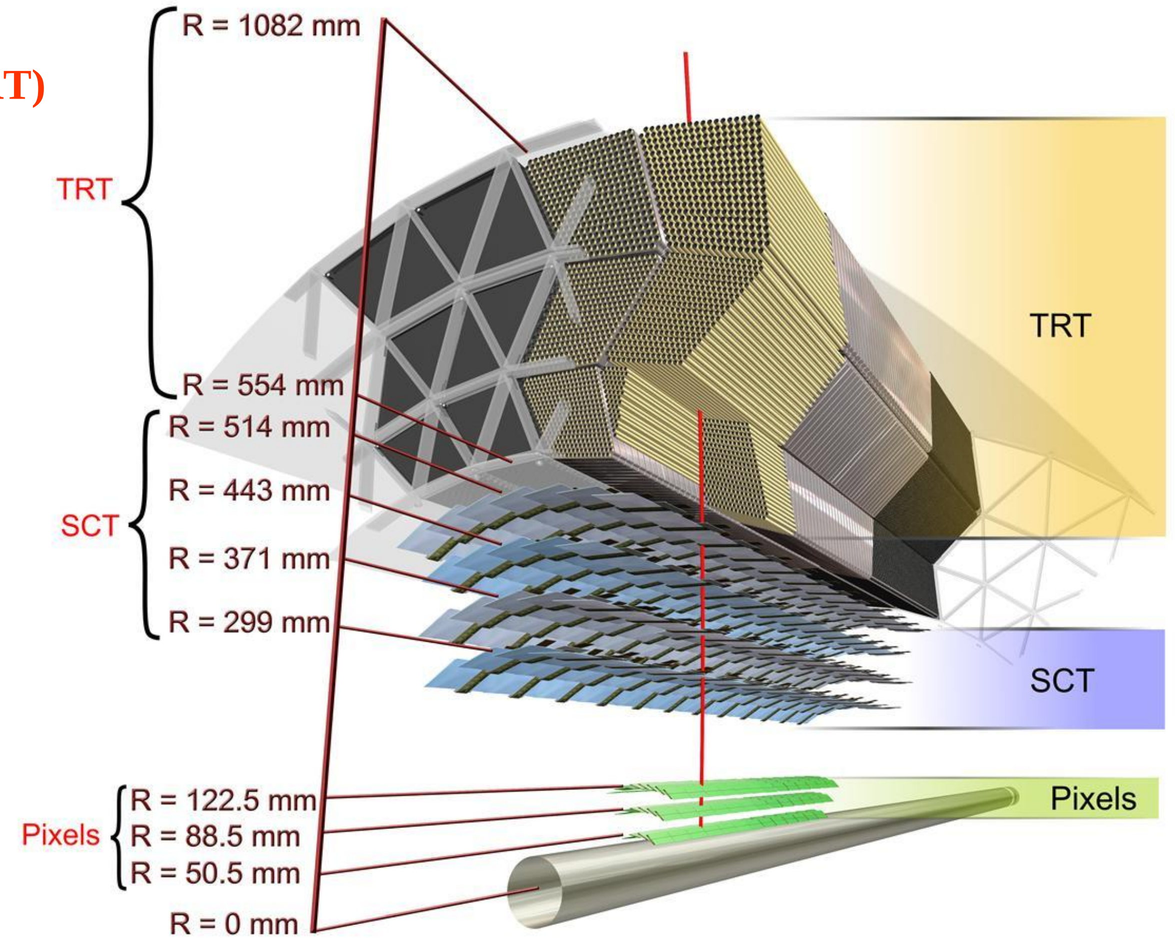

- **7-points silicon (pixels + strips) tracker (|η|<2.5)**
- **straw tubes quasi-continuous tracker (36 points +electron id) (TRT) (|η|<2).**
- **2 T solenoidal magnetic field**

- Momentum resolution:
  $\sigma(p_t)/p_t = 0.05\% \, p_t(GeV/c) \oplus 1\%$
- IP resolution:
  $\sigma(d_0) = 10\,\mu m \oplus 140\,\mu m / p_t(GeV/c)$

The ATLAS Pixel Detector

- **Requirements:**
  - Position resolution in rΦ-direction < 15μm
  - 3 track points for |η| < 2.5
  - Time resolution < 25 ns
  - Hit detection efficiency > 97%
- **3 barrel layers**
  - r = 5.05 cm, 8.85 cm, 12.25 cm
- **3 pairs of Forward/Backward disks**
  - z = 49.5 cm, 58.0 cm, 65.0 cm
- **Pixel size:**
  - 50 μm x 400 μm & 50 μm x 600 μm
- **~ 2.0 m^2 of sensitive area with 8 x 10^7 ch**
- **Modules are the basic building elements**
  - 1456 in the barrel + 288 in the endcaps
  - Active area 16.4 mm x 60.8 mm
  - Radiation tolerance 500 kGy / 10^{15} 1 $MeVn_{eq}cm^{-2}$

The same module is used in the barrel and in the disks:

- staves (13 modules along the beam axis) for the barrel.
- sectors (6 modules on a two-sided octant) for the disks.

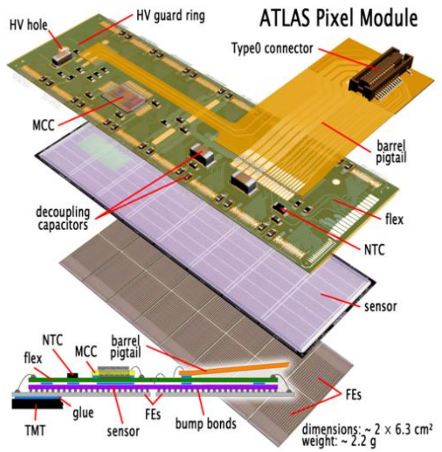

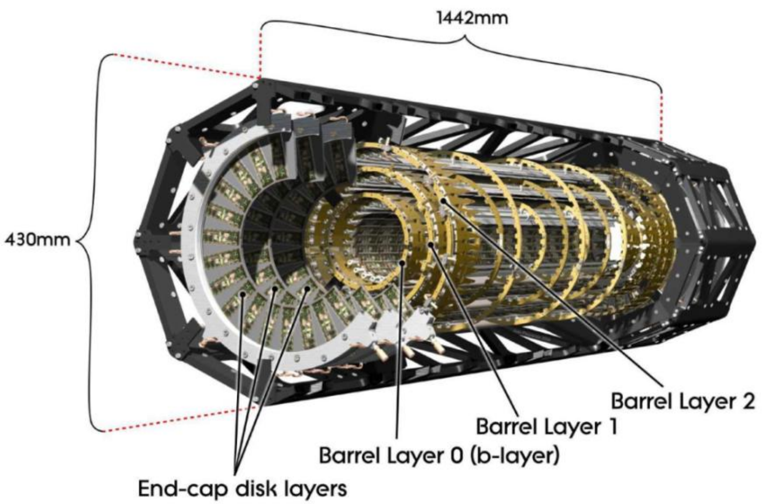

The ATLAS Semiconductor Tracker (SCT)

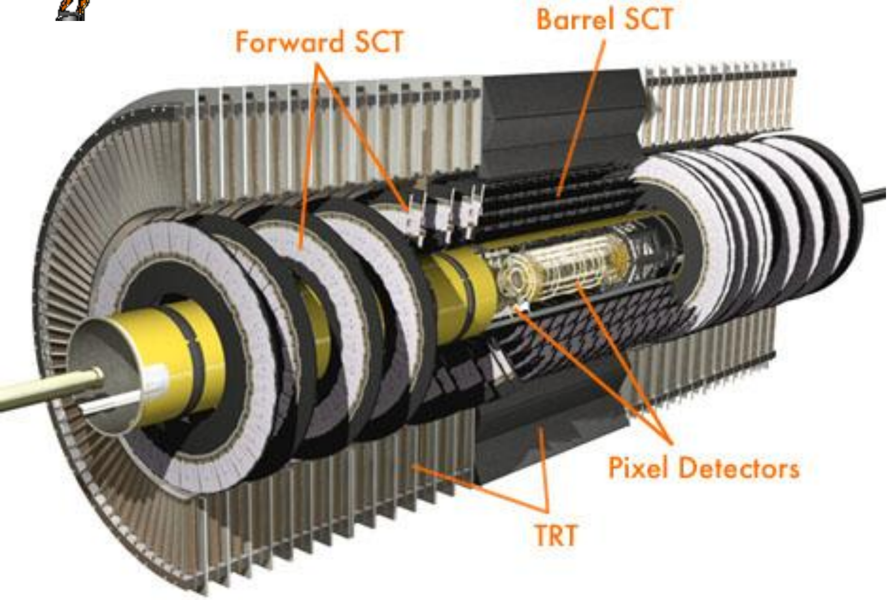

The SemiConductor Tracker (SCT) is a silicon strip detector. It's organized in 4 layers barrel, built with 2112 modules and two 9 disks end-caps, made of 1976 modules. The total number of strips is 6.3 10^6.

Physics requirements

- Resolution (x* y): 17 µm * 580 µm
- Alignment tolerances (x*y): 12 µm * 50 µm
- Noise occupancy: $< 5 * 10^{-4}$
- Efficiency: > 99%
- Radiation : ~ $2 * 10^{14}$ Neq cm^{-2} over 10 years

The barrel module consists of four single sided p-on-n strip detectors:

- Pitch 80 mm
- Strip length 120 mm
- Stereo angle 40 mrad

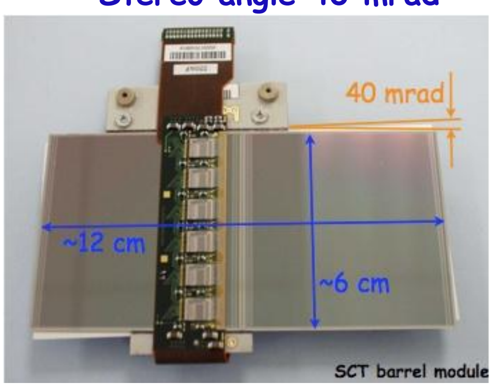

The end-caps are built with three different modules:

- Pitch 57-95 mm
- Strip length 55-120 mm

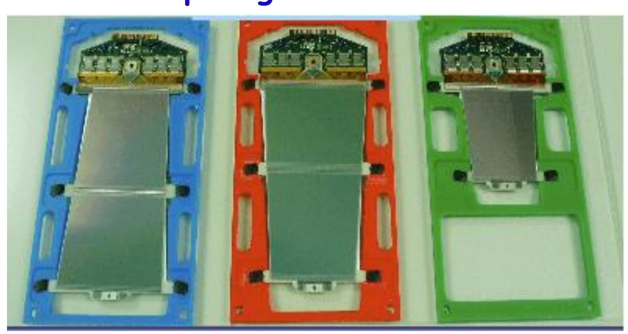

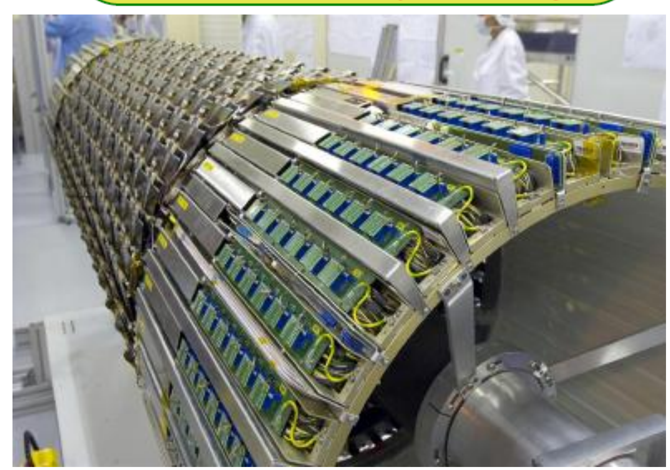

The ATLAS Transition Radiation Tracker (TRT)

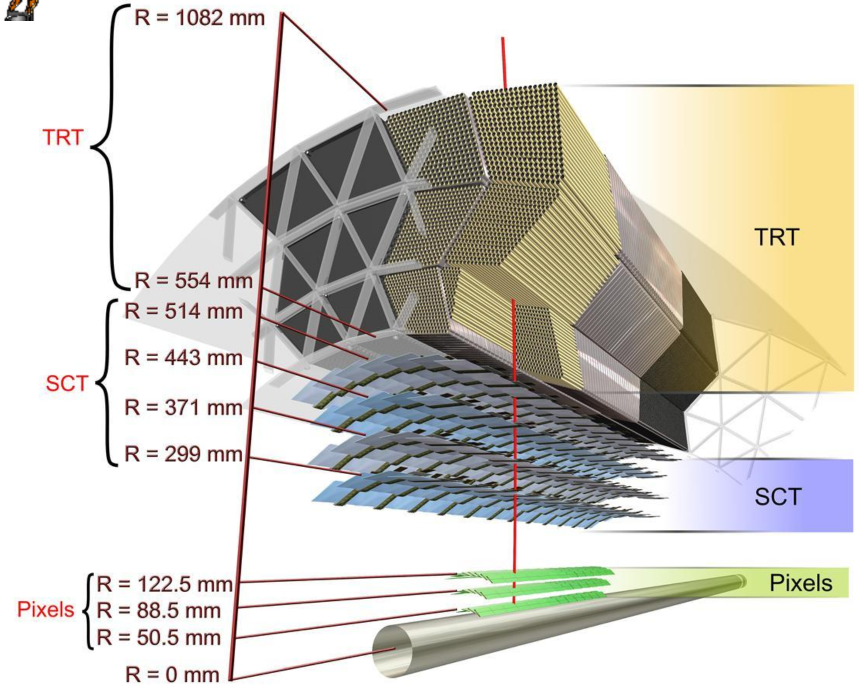

TRT: 4 mm straw tubes, arranged in 2·160 disks (end-cap) and 73 layers (barrel), 40 K channels, acceptance $|\eta|<2$

TR (polypropylene foils/fiber): pion-electron separation (TR γ's convert into e's in Xe)

TRT end-cap during assembly

\# Hits (Barrel): 3(Pixel)+4 (SCT)+<36>(TRT)

$\sigma/p_T \sim 5\times10^{-4}\, p_T \oplus 0.01$

Cosmic ray event in TRT

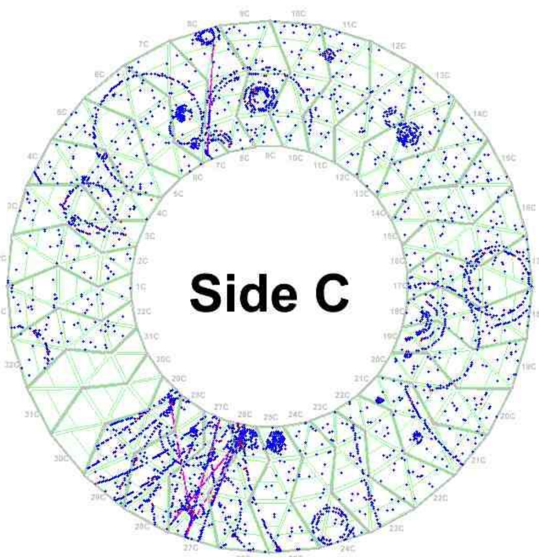

$\frac{1}{4}$ of TRT barrel during integration

CMS has chosen an all-silicon configuration

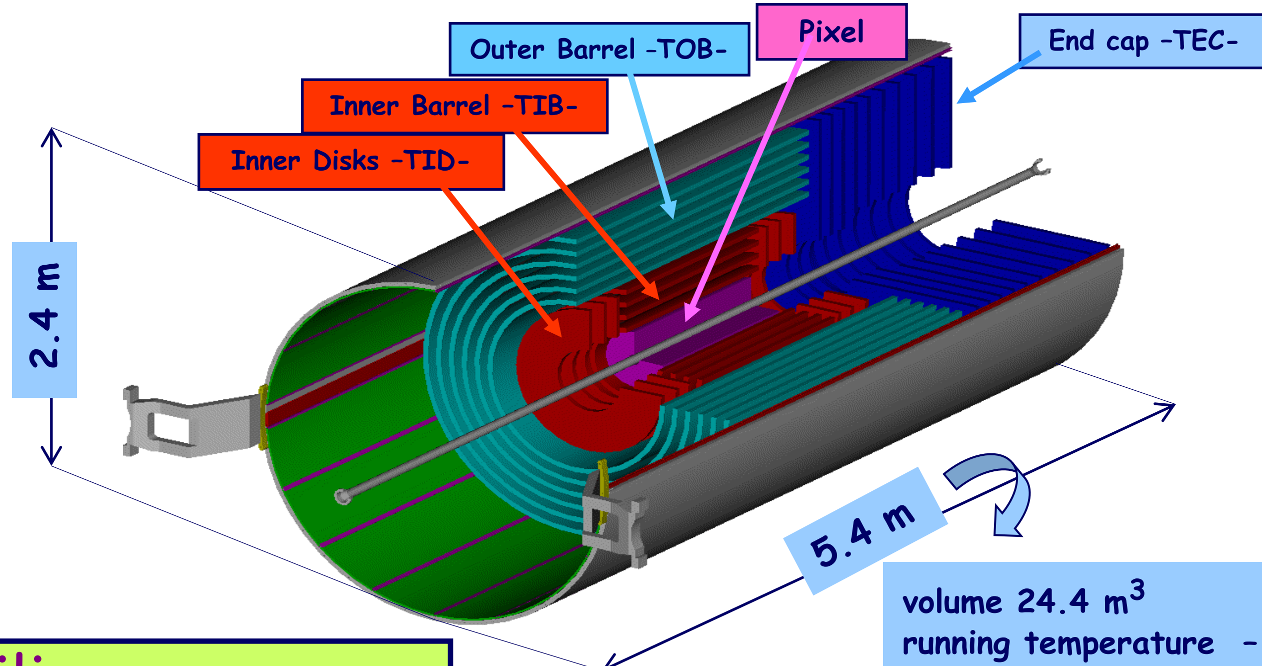

volume 24.4 m^3
running temperature – 10 ^0C

207m^2 of silicon sensors
10.6 million silicon strips
65.9 million pixels ~ 1.1m^2

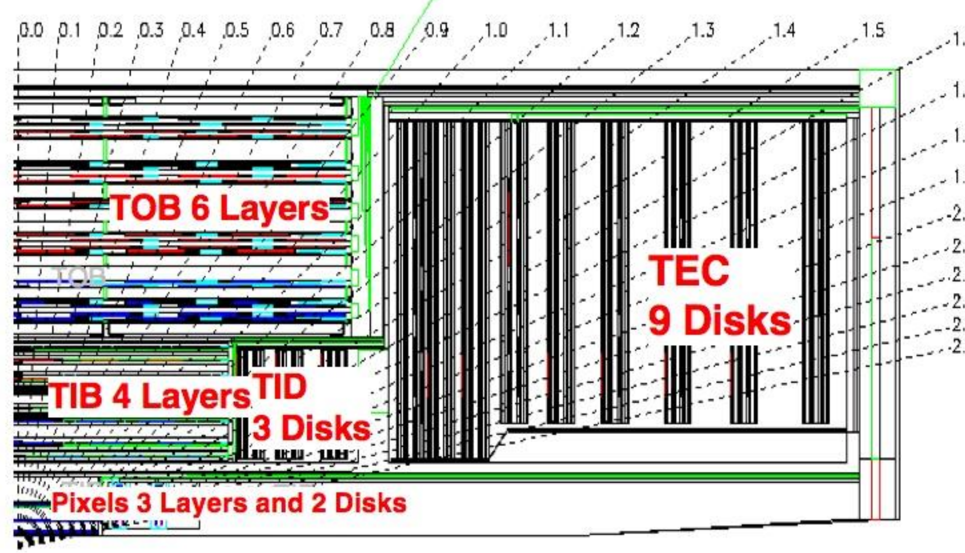

Strips:

Pitch: 80 μm to 180μm

Hit Resolution: 20 μm to 50μm

Pixels:

100 μm x 150μm

rφ and z resolution: ~15 μm

The CMS Silicon Strip Tracker

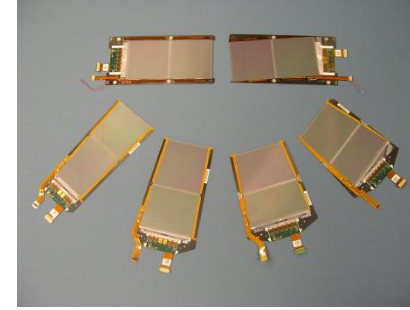

Outer Barrel (TOB): 6 layers
- Thick sensors (500 μm)
- Long strips

Endcap (TEC): 9 Disk pairs
- r < 60 cm thin sensors
- r > 60 cm thick sensors

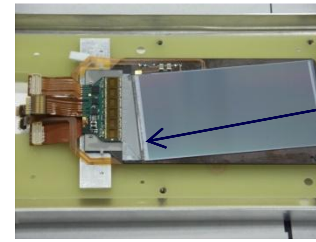

small angle tilt (100mrad) to provide second coordinate measurement

6 layers TOB

4 layers TIB

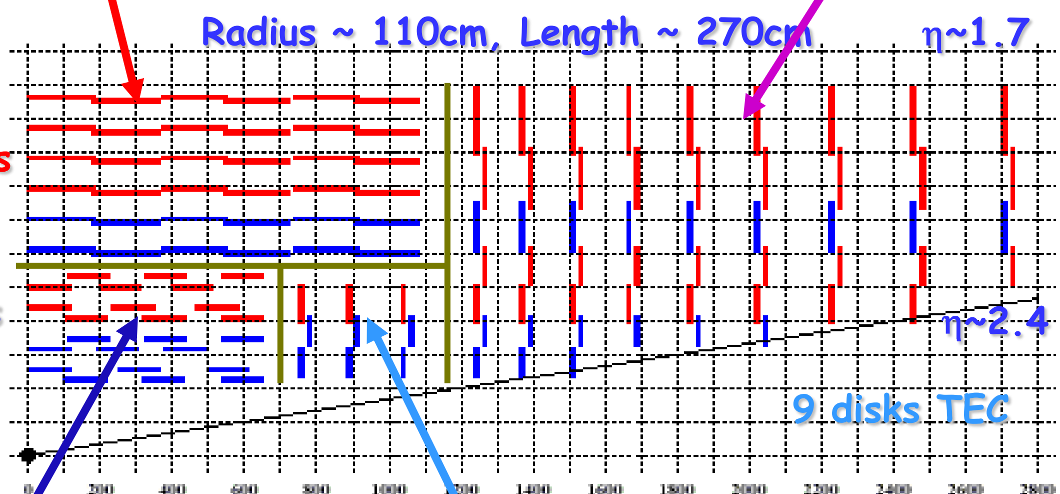

Inner Barrel (TIB): 4 layers
- Thin sensors (320 μm)
- Short strips

Inner Disks (TID): 3 Disk pairs
- Thin sensors

9'648'128 strips
75'376 APV chips
6'136 Thin sensors
18'192 Thick sensors
~17'000 modules
~25'000'000 Bonds

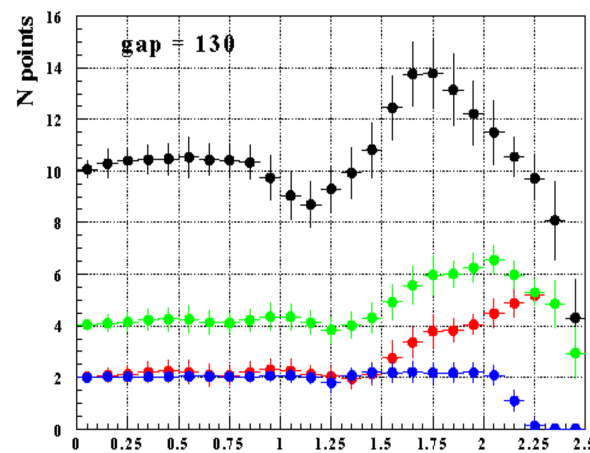

Black: total number of hits
Green: double-sided hits
Red: ds hits - thin detectors
Blue: ds hits - thick detectors

Strip length ranges from 10 cm in the inner layers to 20 cm in the outer layers.

Pitch ranges from 80μm in the inner layers to near 200μm in the outer layers

The CMS Silicon Strip Tracker

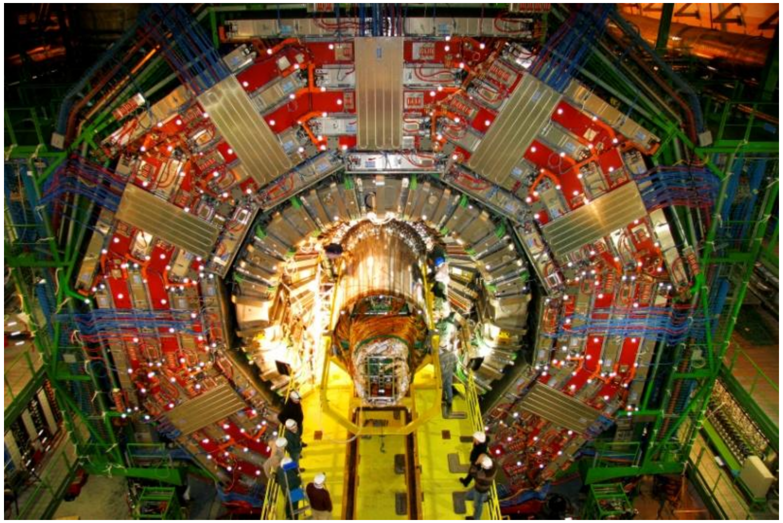

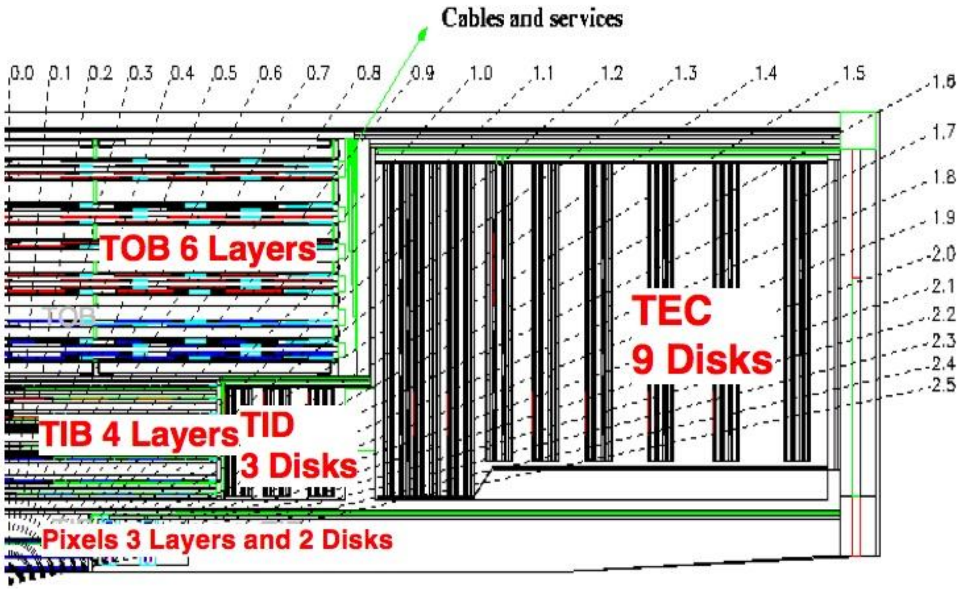

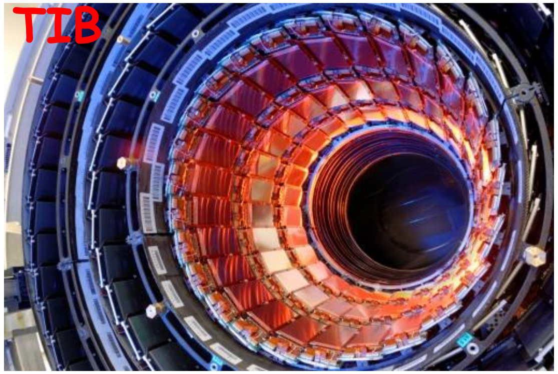

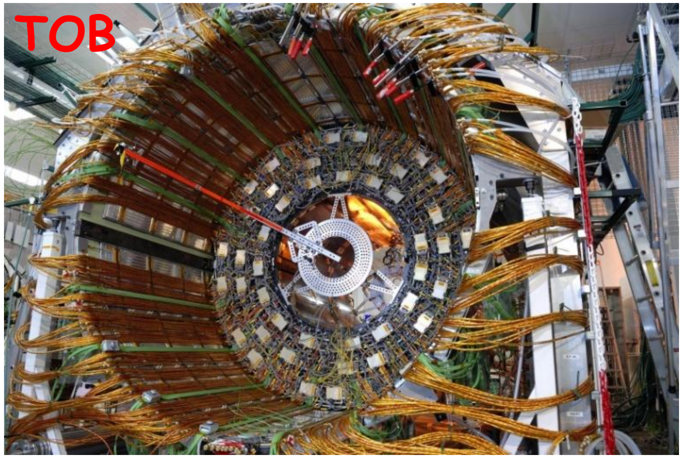

CMS modules of Silicon Strip Tracker

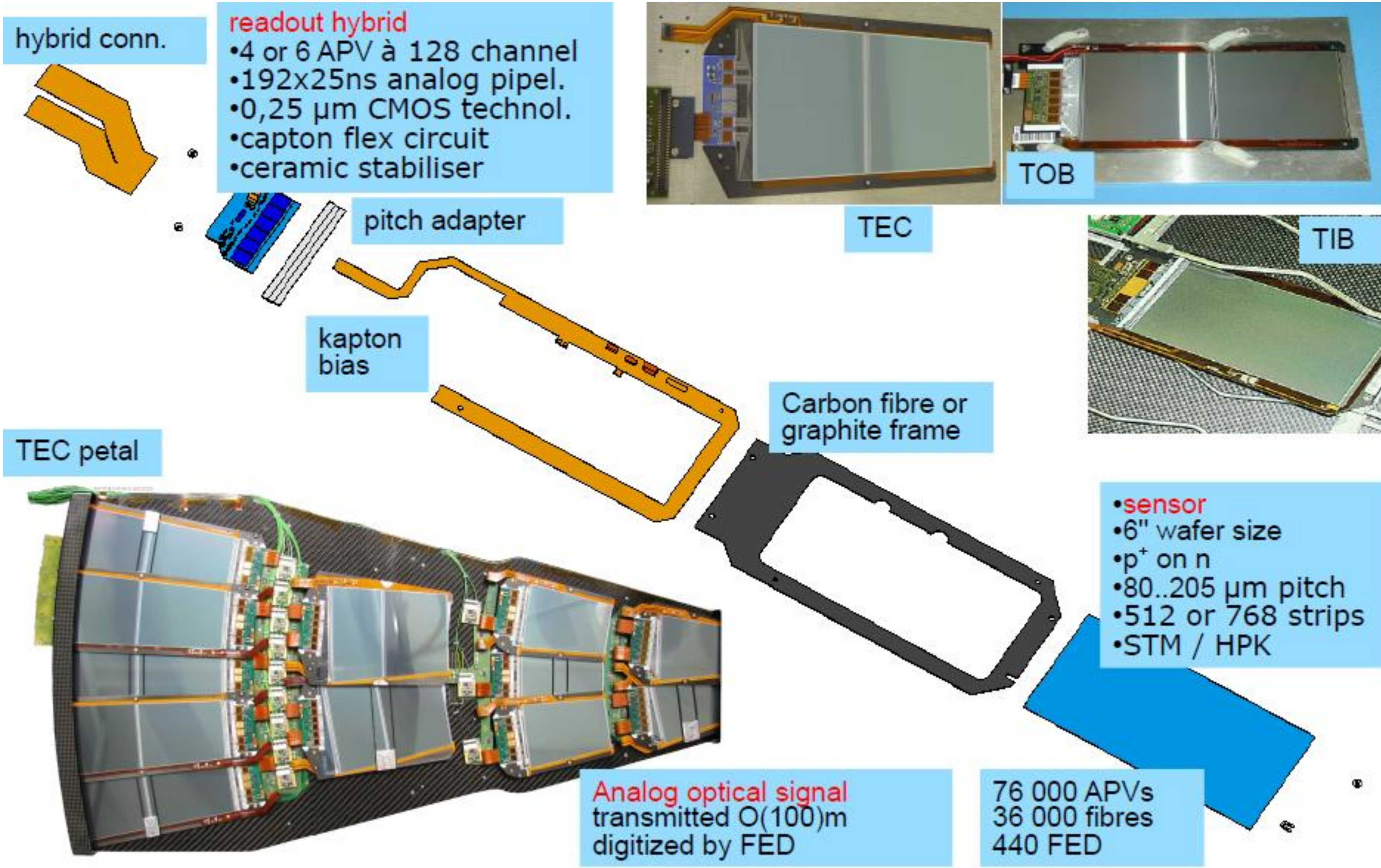

The CMS Pixel Detector

- 3 Barrel layers at 4.3, 7.2, 11.0 cm
- 2 Forward Disks
- 3-hit coverage for tracks $|\eta|<2.5$

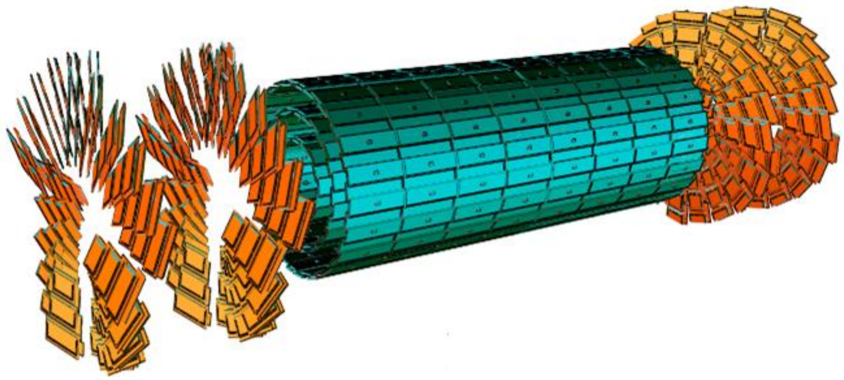

Total Area: 0.78+0.28 m^2
66 Million Pixels

Sensors: n on n Silicon 265 – 270 μm
150 x 100 μm pixels $\sigma(z) \sim \sigma(r\varphi) \sim 15\mu m$
Bump-bonded to PSI 46 Read Out Chips (analog readout)

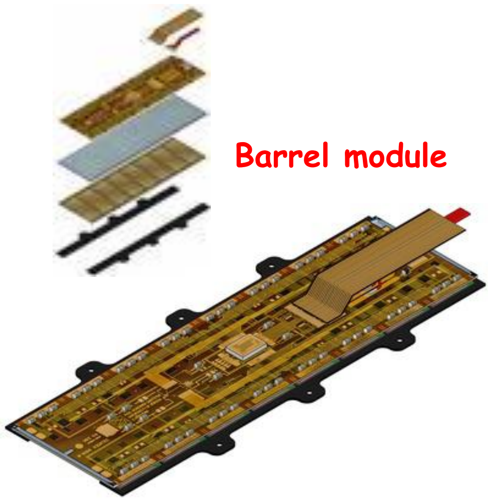

Barrel module

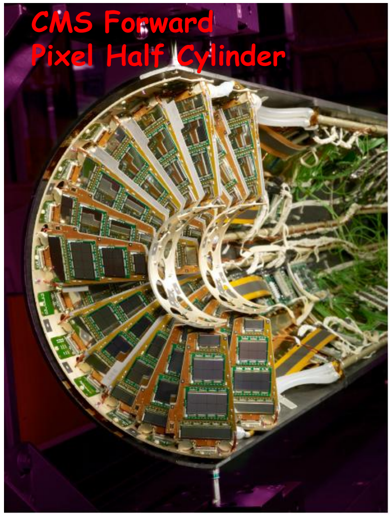

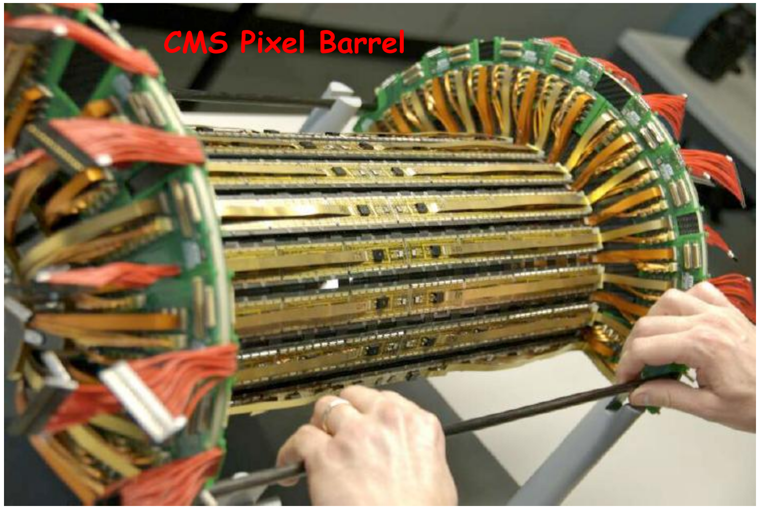

…and in ALICE tracking will not be easier….

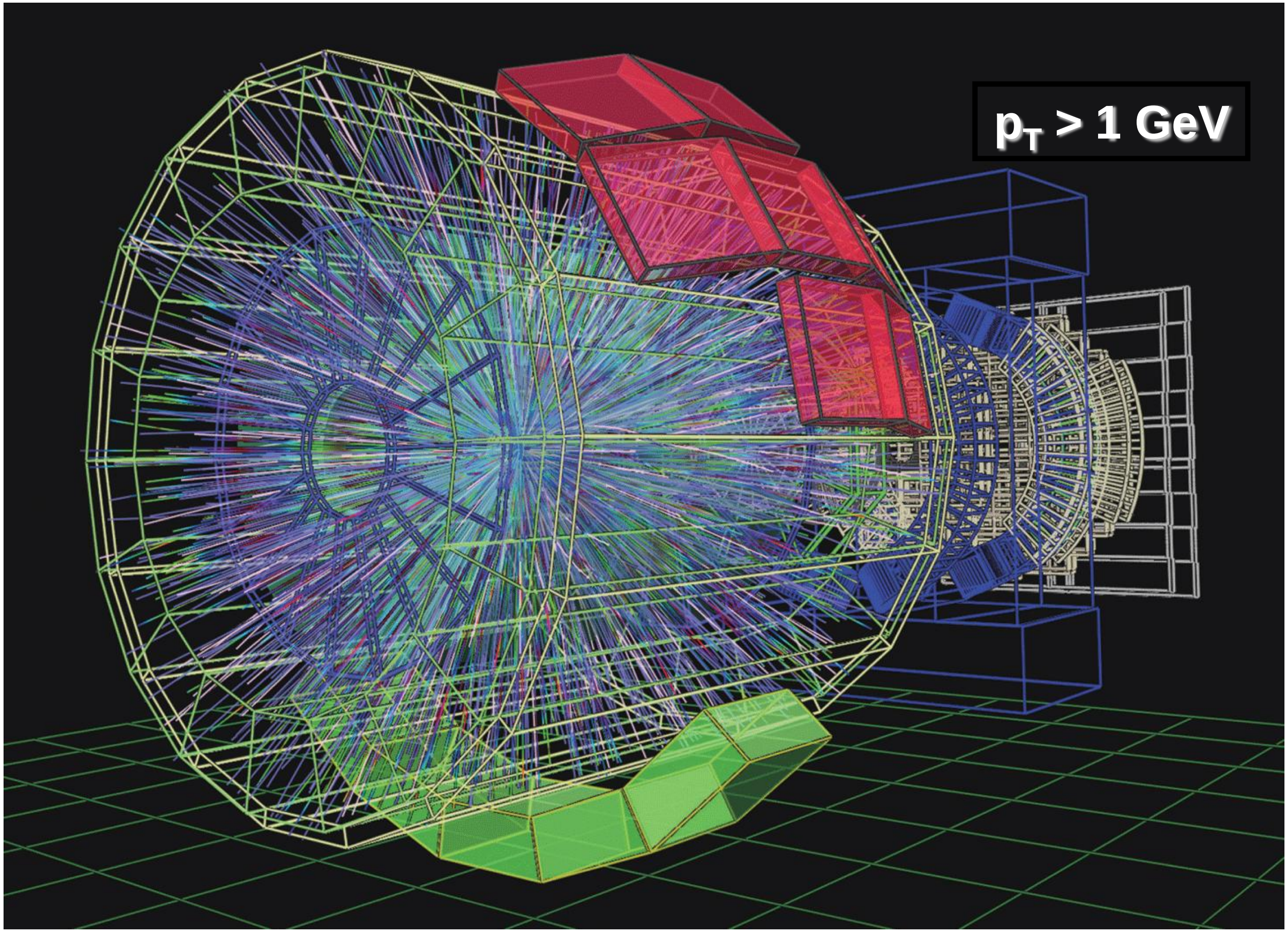

An ALICE PbPb Event

$N_{ch}(-0.5<\eta<0.5)=8000$!!

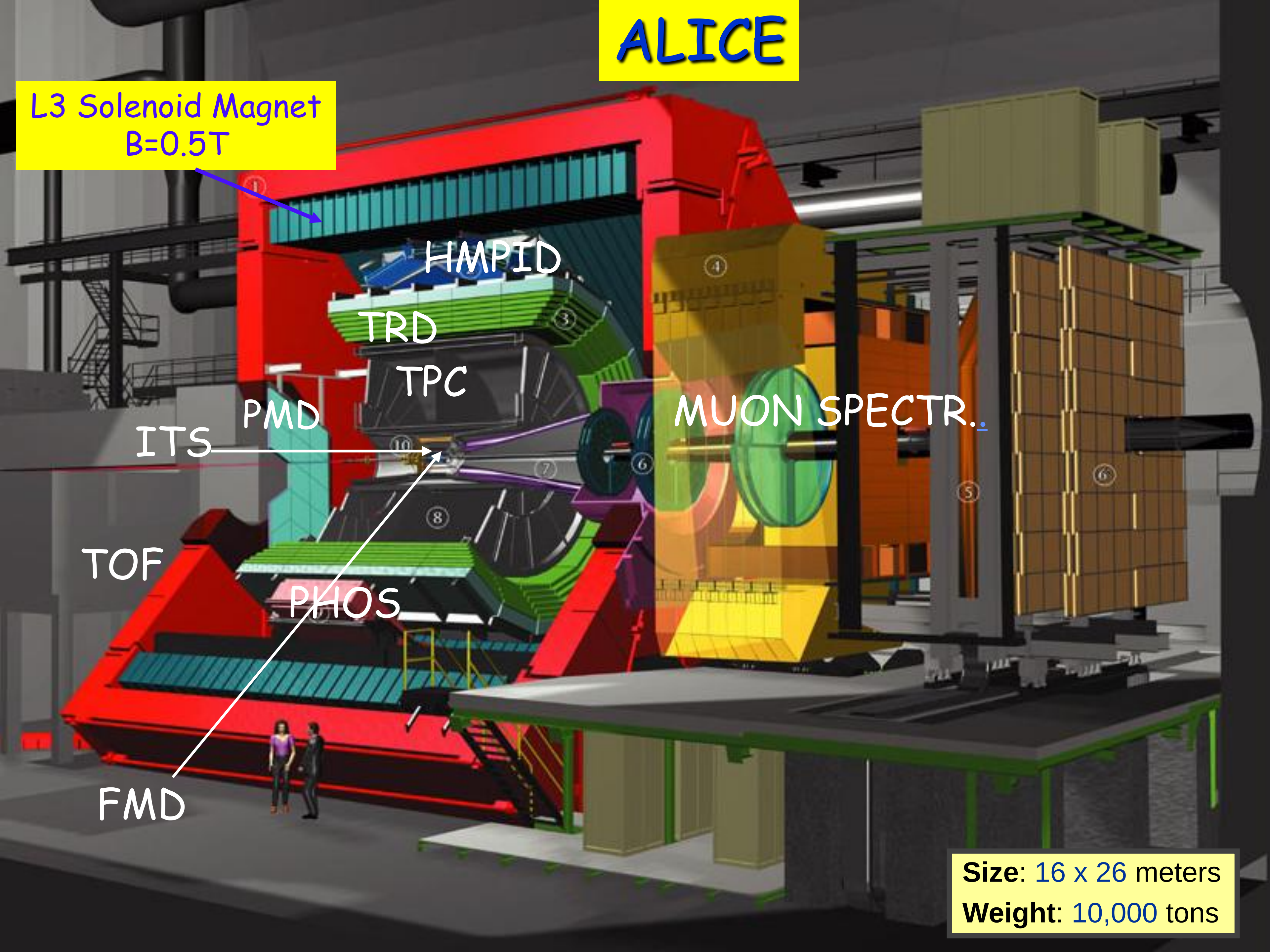
ALICE
L3 Solenoid Magnet
B=0.5T
HMPID
TRD
TPC
PMD
ITS
MUON SPECTR..
TOF
PHOS
FMD
Size: 16 x 26 meters
Weight: 10,000 tons

ALICE Tracking Layout

Inner Tracking System (ITS):
6 Si Layers (pixels, drift, strips)
Vertex reconstruction, dE/dx
$-0.9<\eta<0.9$

TPC

Tracking, dE/dx

$-0.9<\eta<0.9$

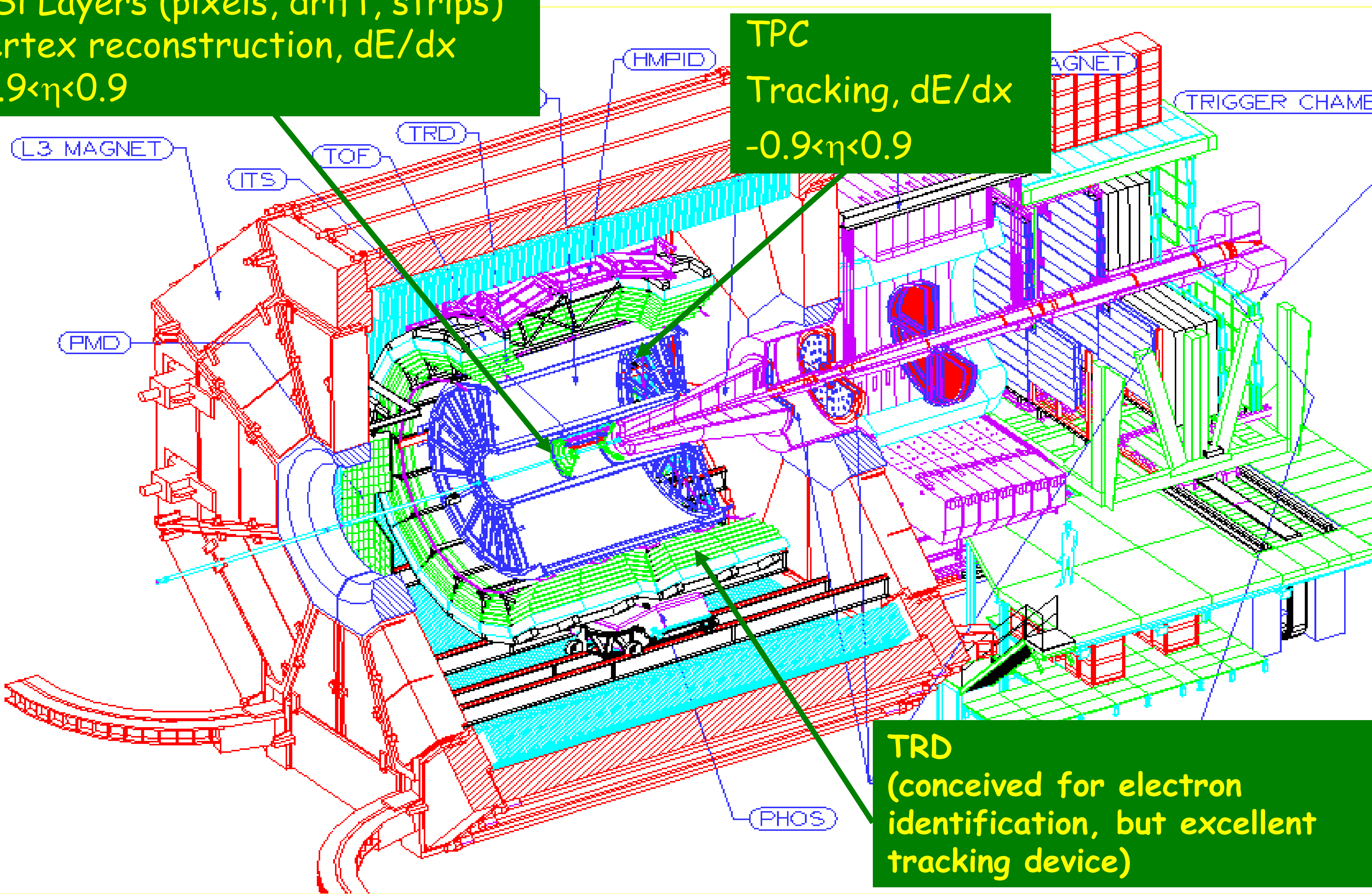

TRD
(conceived for electron identification, but excellent tracking device)

ALICE Inner Tracking System

- **6 barrel layer**
- **3 different silicon detector technologies,**

  2 layers each, as seen by produced particles:

  - Pixels (SPD), Drift (SDD), double-side Strips (SSD)

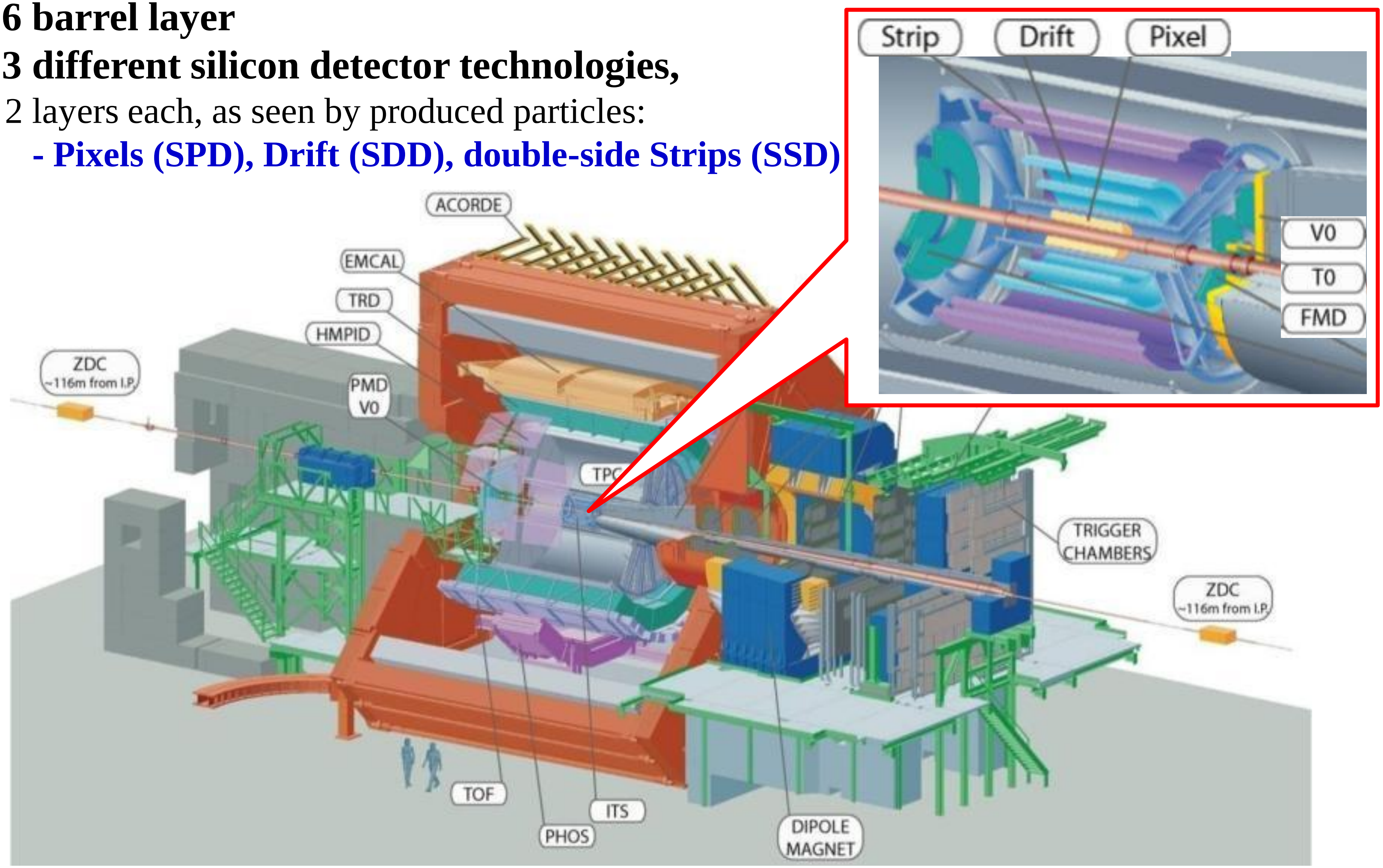

Inner Tracking System (ITS)

- Six layers of silicon detectors
  - ⇨ Coverage: $|\eta|<0.9$
- Three technologies
  - ⇨ Pixels (SPD)
  - ⇨ Drift (SDD)
  - ⇨ Double-sided Strips (SSD)
- Design goals
  - ⇨ Optimal resolution for primary vertex and track impact parameter
    - ✓ *Minimize distance of innermost layer from beam axis ($\langle r \rangle \simeq 3.9$ cm) and material budget*
  - ⇨ Maximum occupancy (central PbPb) < few %
  - ⇨ 2D devices in all the layers
  - ⇨ dE/dx information in the 4 outermost layers for particle ID in $1/\beta^2$ region

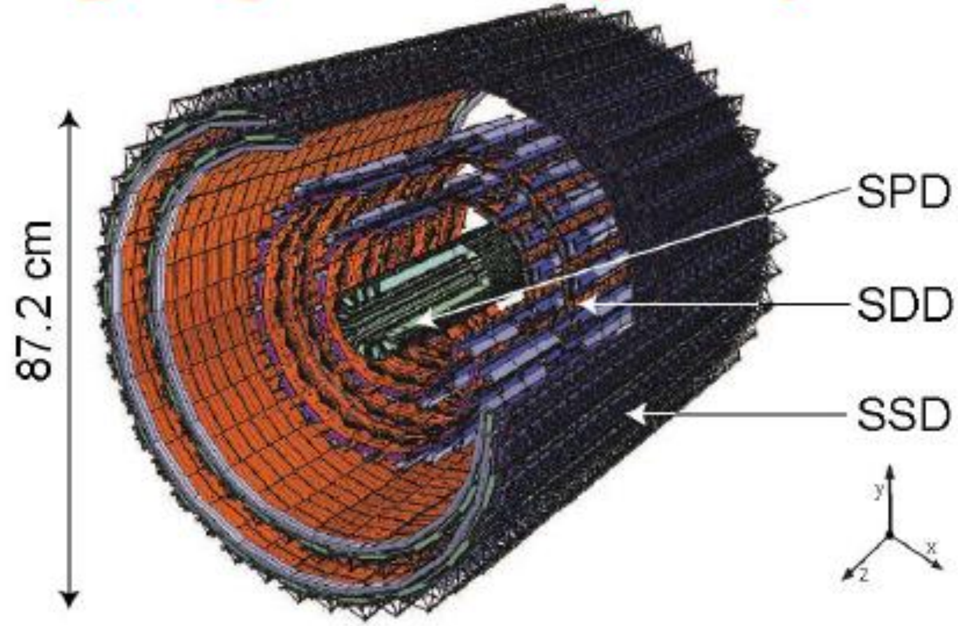

Layer	Det. Type	Radius (cm)	Length (cm)	Resolution (μm) $r\phi$	Z
1	SPD	3.9	28.2	12	100
2	SPD	7.6	28.2	12	100
3	SDD	15.0	44.4	35	25
4	SDD	23.9	59.4	35	25
5	SSD	38.0	86.2	20	830
6	SSD	43.0	97.8	20	830

Inner Tracking System

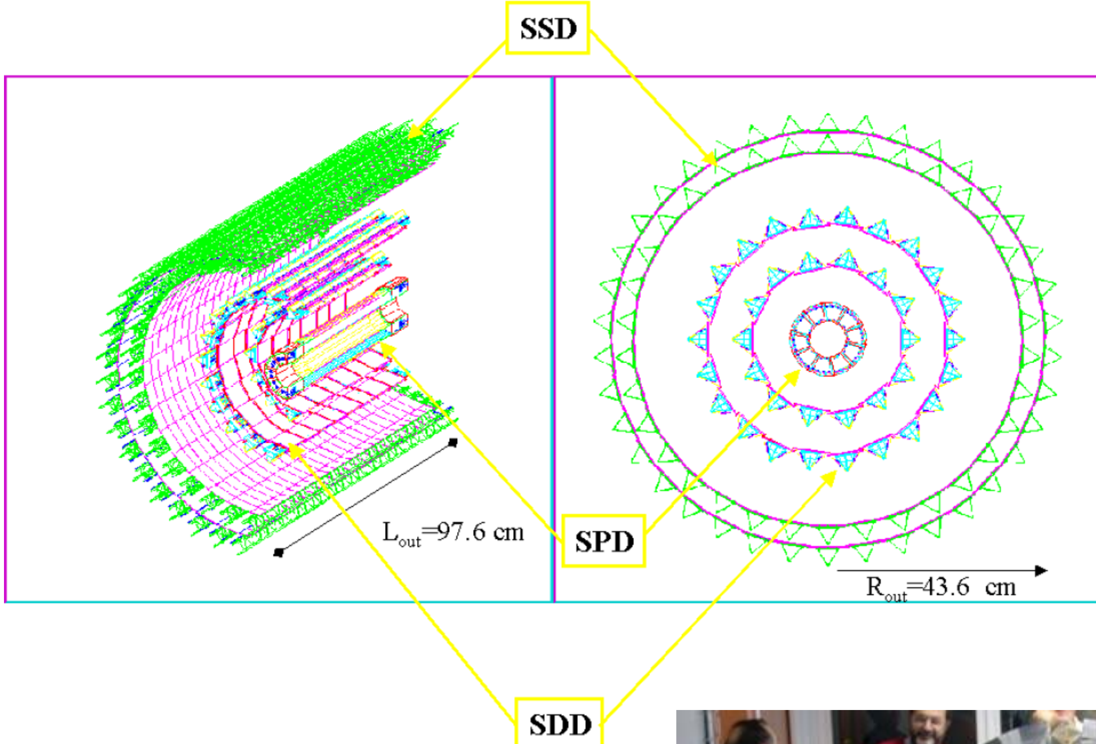

Silicon Pixel Detector (SPD):
- **~10M channels**
- **240 sensitive vol. (60 ladders)**

Silicon Drift Detector (SDD):
- **~133k channels**
- **260 sensitive vol. (36 ladders)**

Silicon Strip Detector (SSD):
- ~2.6M channels
- 1698 sensitive vol. (72 ladders)

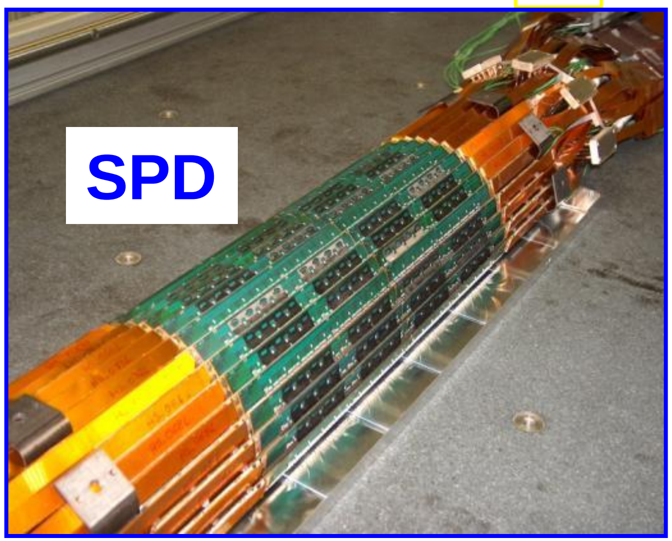

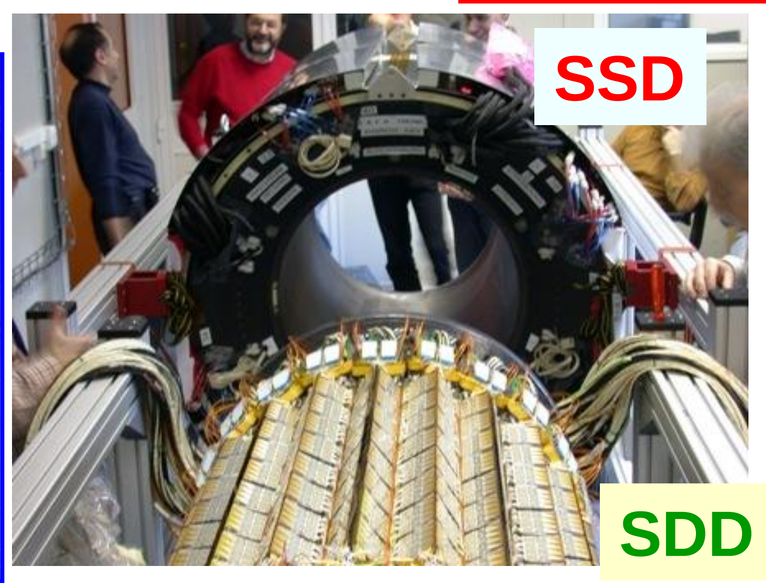

ITS total:
2198 alignable sensitive volumes
→ 13188 d.o.f.

Pixel

- 2 layer barrel
- Total surface: ~$0.24m^2$
- Power consumption ~1.4kW
- Evaporative cooling C_4F_{10}
- Operating at room temperature
- Material budget per layer ~1% X_0

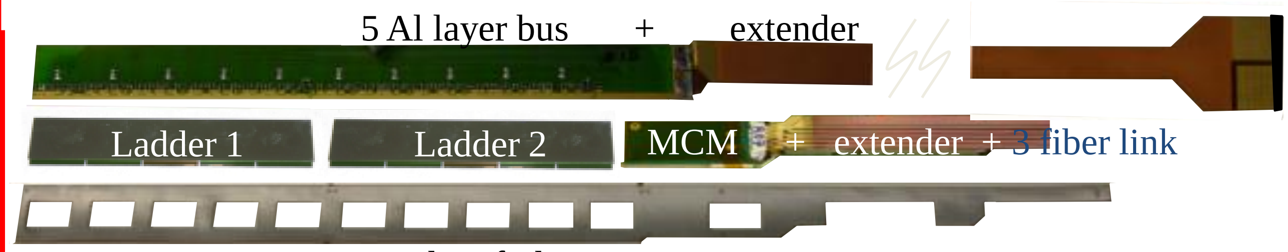

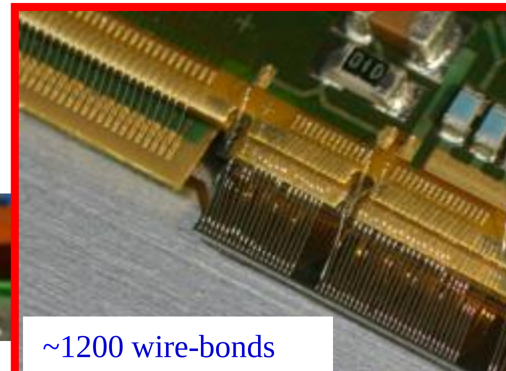

Outer surface: 80 half-staves

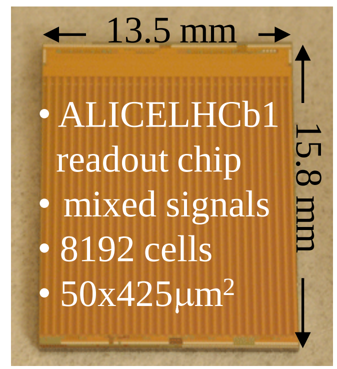

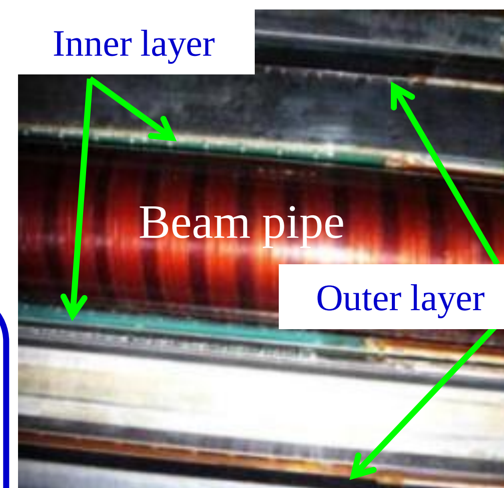

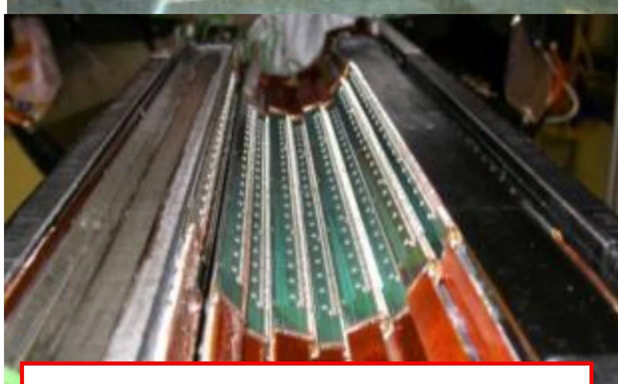

Unique L0 trigger capability
- Prompt FastOR signal from each chip
- Extract and *synchronize* 1200 FastOR signals from the 120 half-staves
- User defined programmable algorithms

Minimum distance inner layer-beam pipe ≈5 mm

Inner surface: 40 half-staves

Silicon Drift Detector

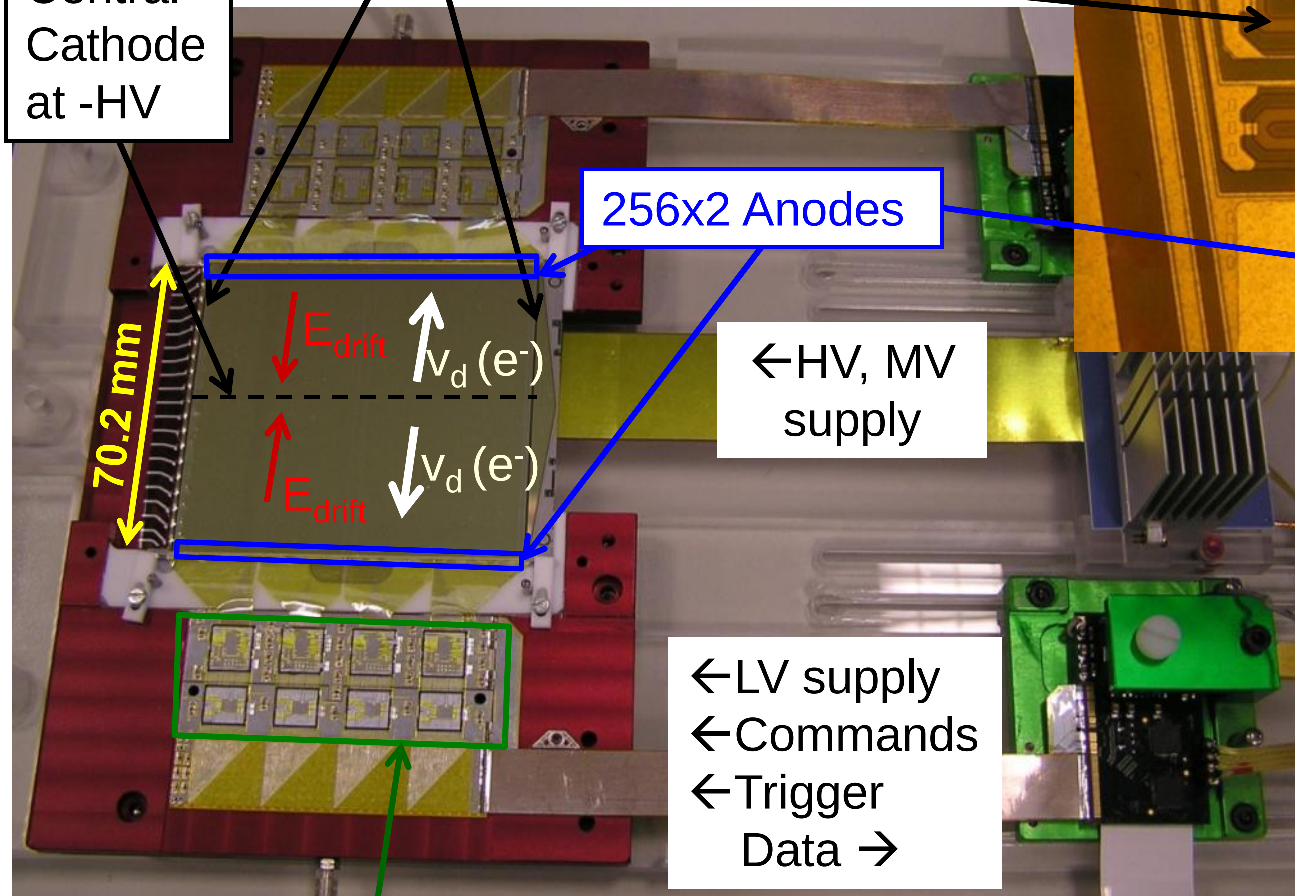

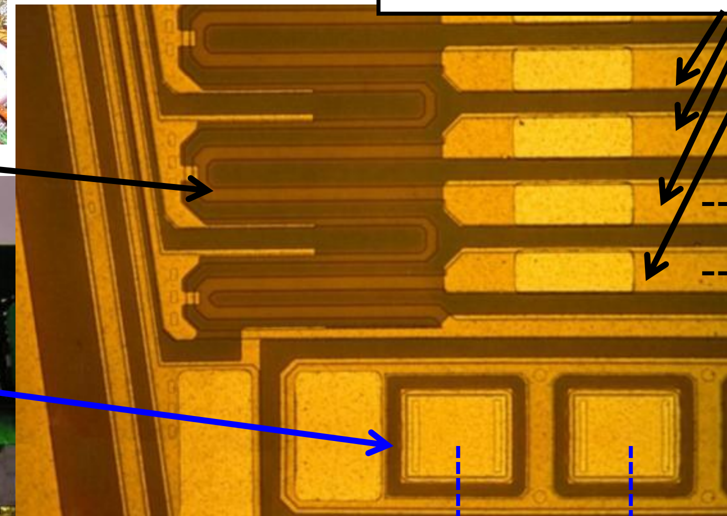

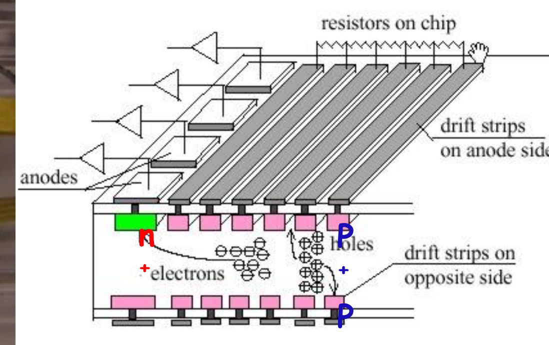

double-side Strip

$r\phi$- overlap: { L5: 34 ladders, L6: 38 ladders }

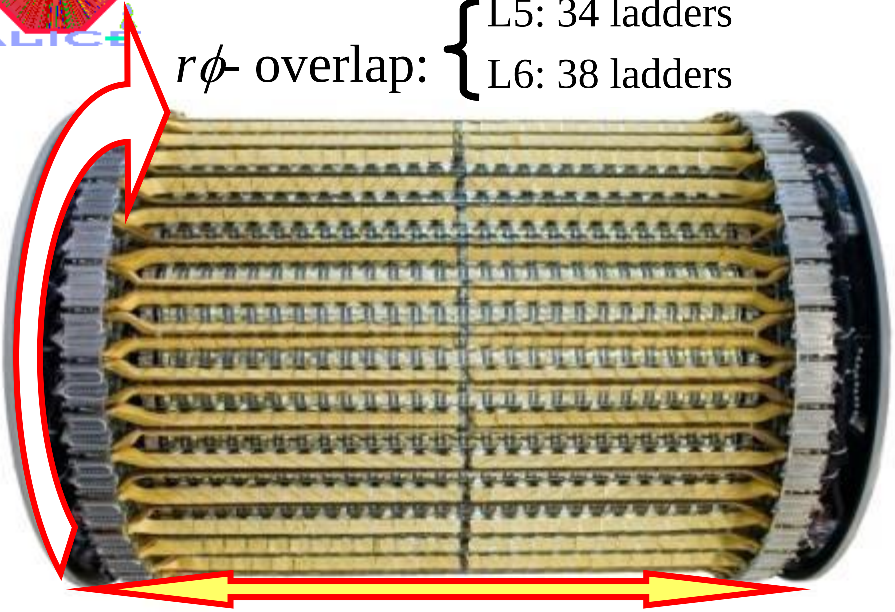

z - overlap: { L5: 22 modules, L6: 25 modules }

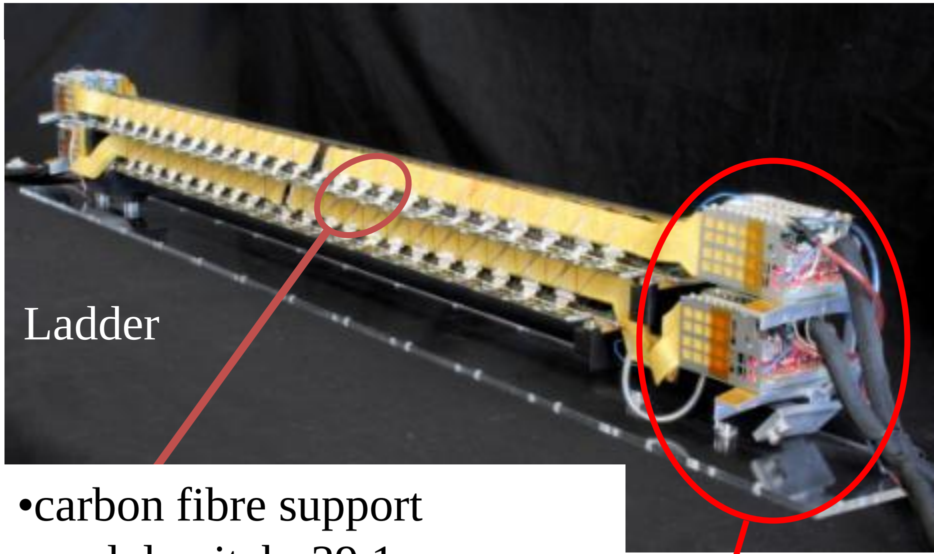

•carbon fibre support
•module pitch: 39.1 mm
•Al on polyimide laddercables

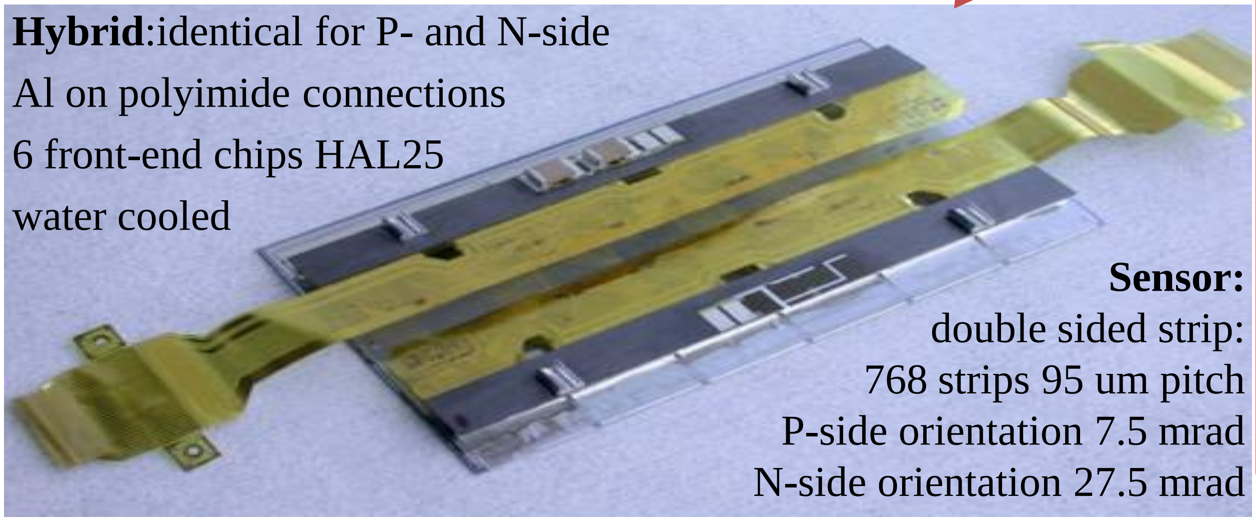

Hybrid:identical for P- and N-side
Al on polyimide connections
6 front-end chips HAL25
water cooled

Sensor:
double sided strip:
768 strips 95 um pitch
P-side orientation 7.5 mrad
N-side orientation 27.5 mrad

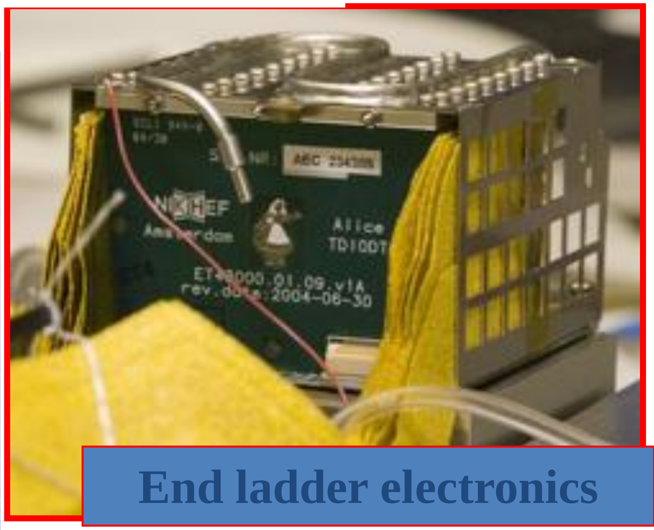

End ladder electronics

TPC layout

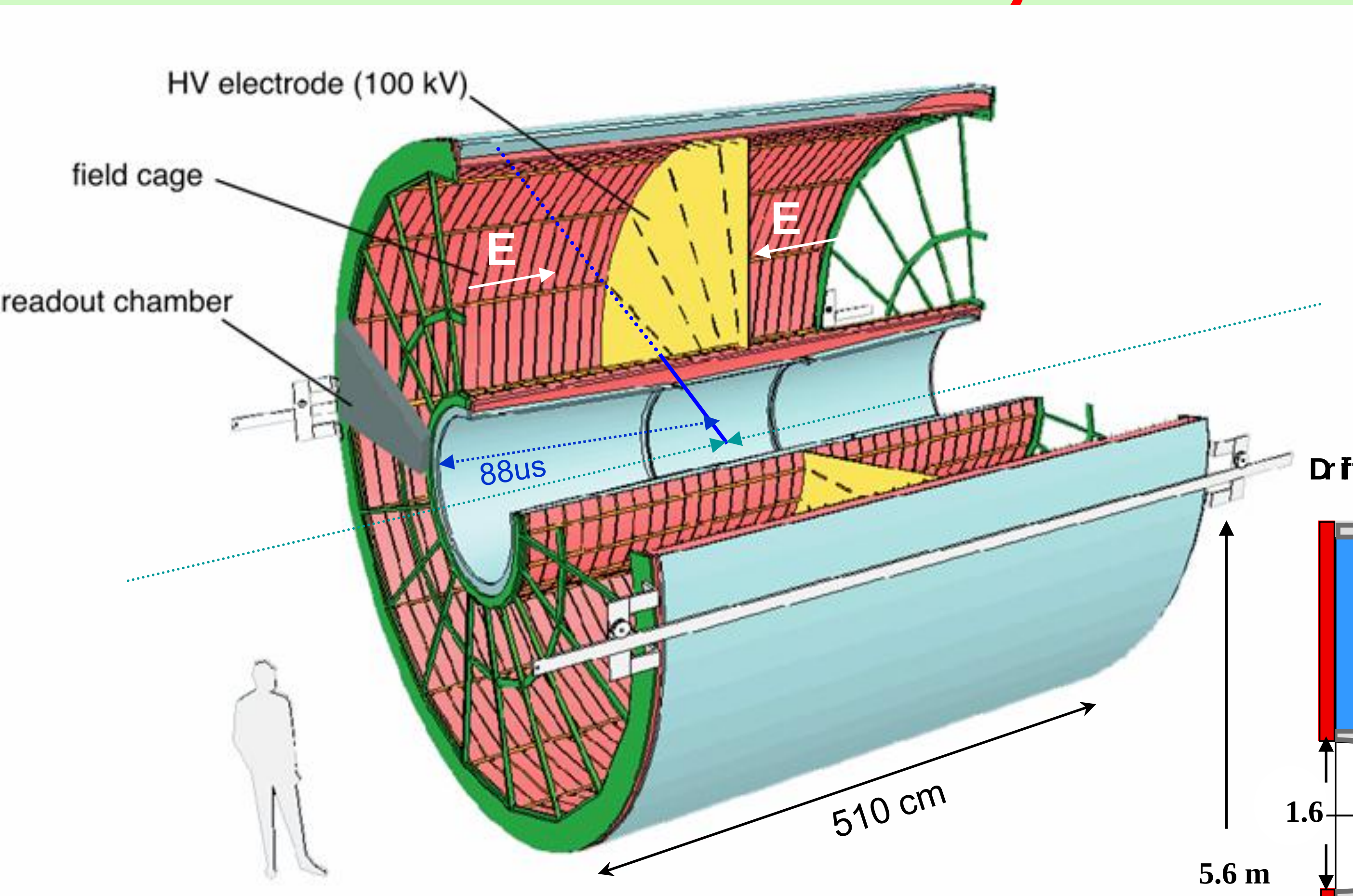

GAS VOLUME
88 m^3

DRIFT GAS
90% Ne - 10%CO_2

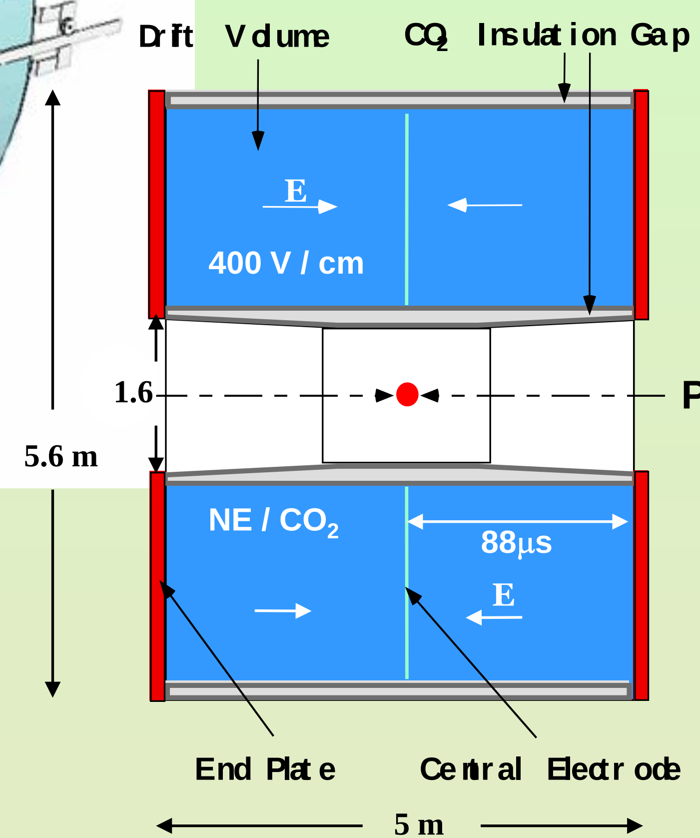

<u>Readout plane segmentation</u>

18 trapezoidal sectors

each covering 20 degrees in azimuth

570k channels

Time Projection Chamber (TPC)

- Characteristics:
  - ⇨ 85 m^3 - $NeC_2O_2N_2$ gas mixture
  - ⇨ 557,568 readout channels
  - ⇨ Maximum drift time = 92 μs
  - ⇨ Many (>90) 3D points (+dE/dx) per track
- Installation in ALICE since 2007
- Running continuously from May to October 2008 and since August 2009
- Calibration:
  - ⇨ >750 million events (cosmics, krypton, and laser) recorded, with and without B
  - ⇨ First round of calibrations (dE/dx, momentum, alignment, gain) completed before p-p collisions

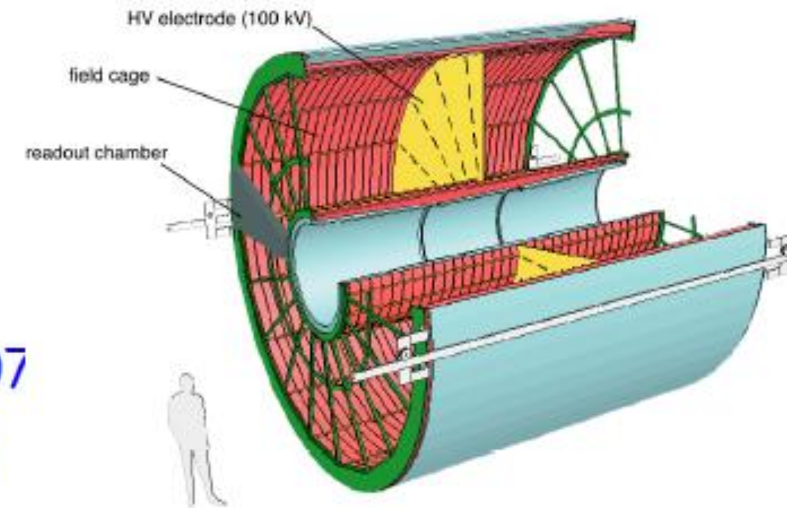

Laser event

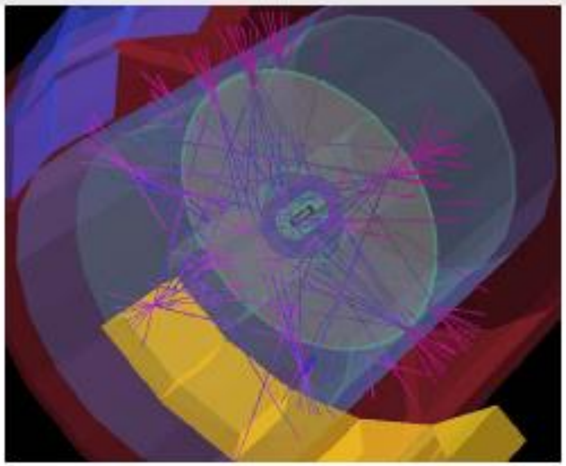

J. Alme et al., TPC collab., arXiv:1001.1950

TPC

Largest TPC ever: R=2.5 m, length=5m

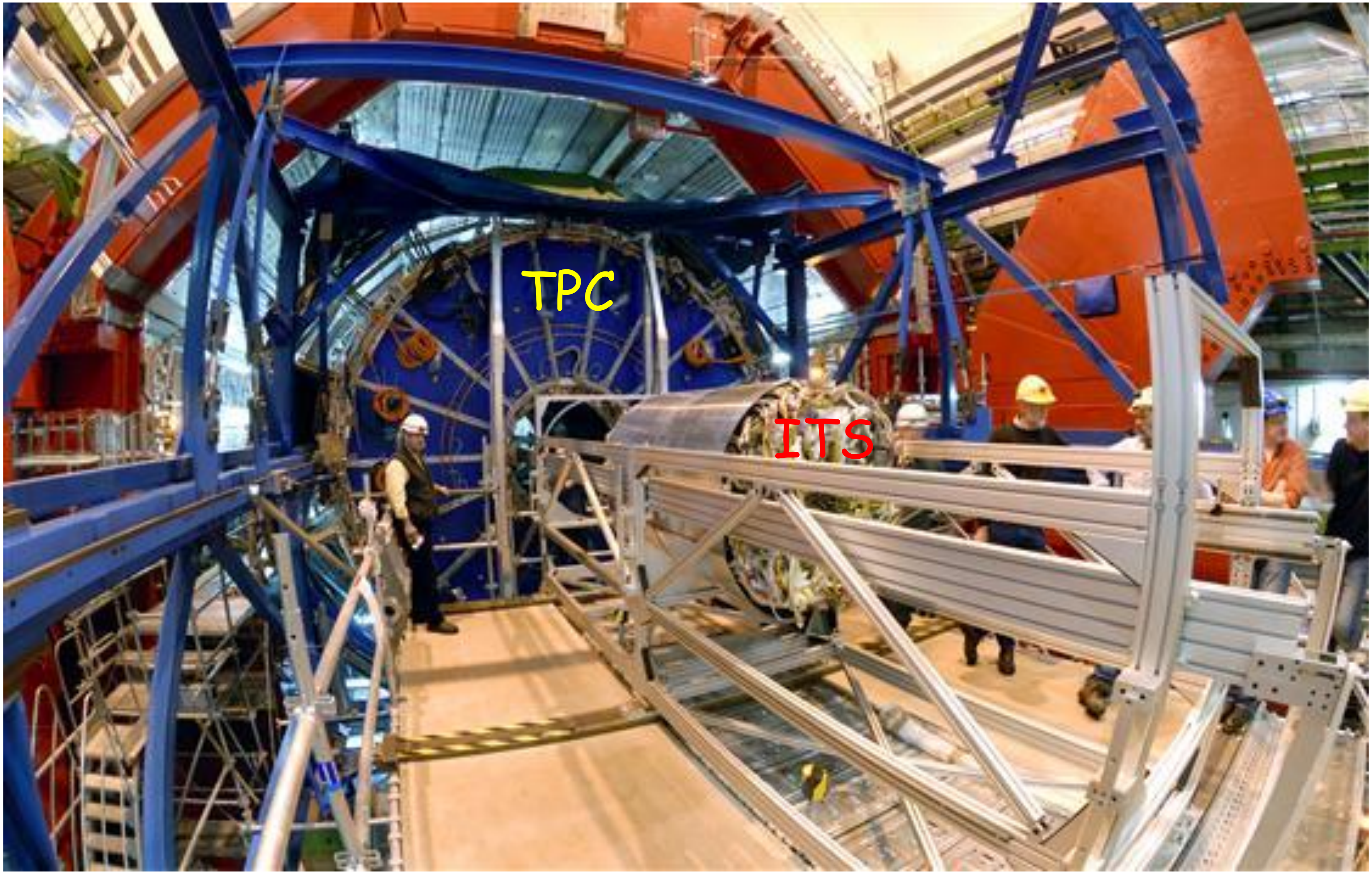

ALICE installation

SPD, SDD+SSD, TPC 'Russian Doll', sliding one after the other

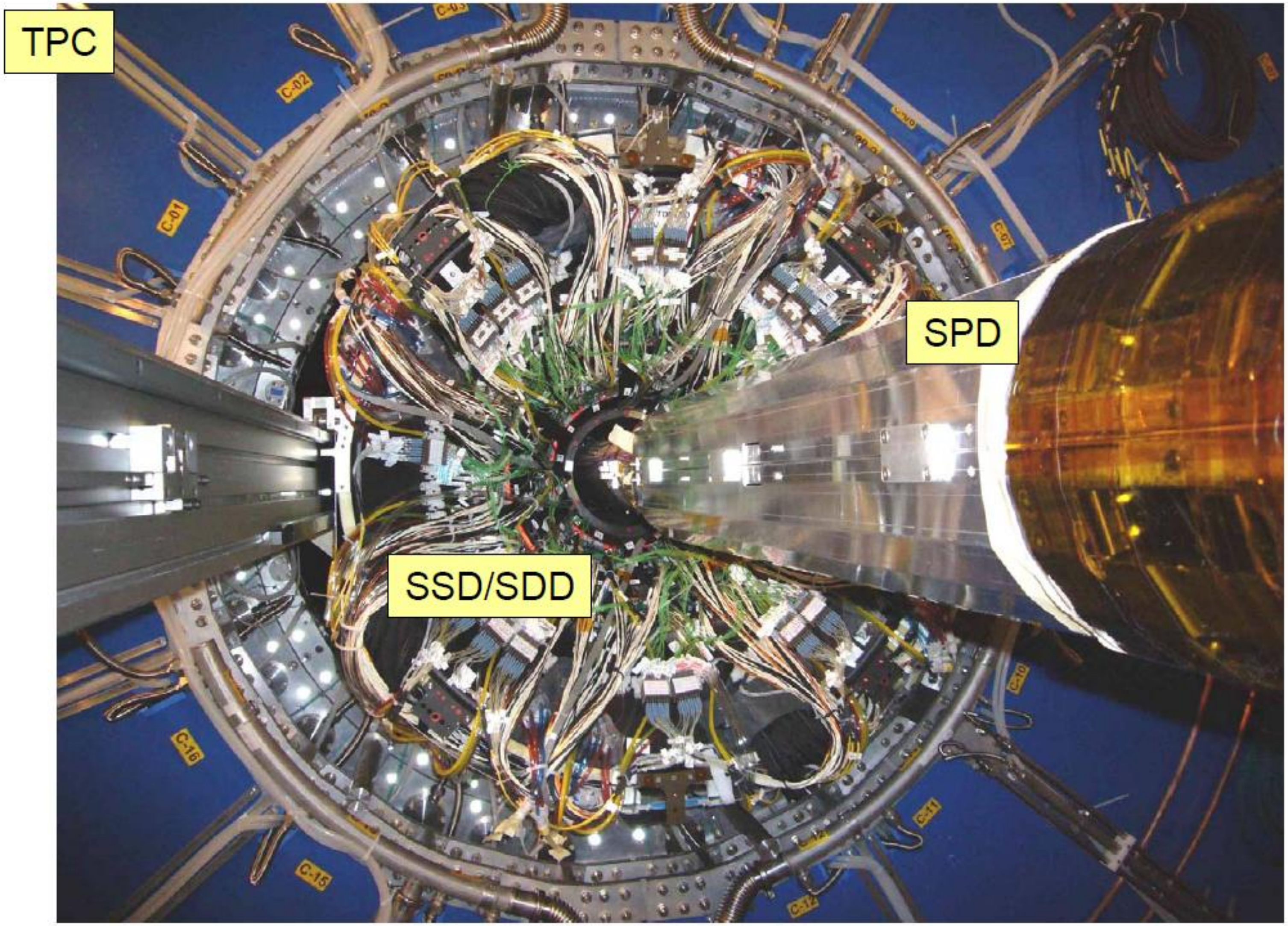

The LHCb Detector

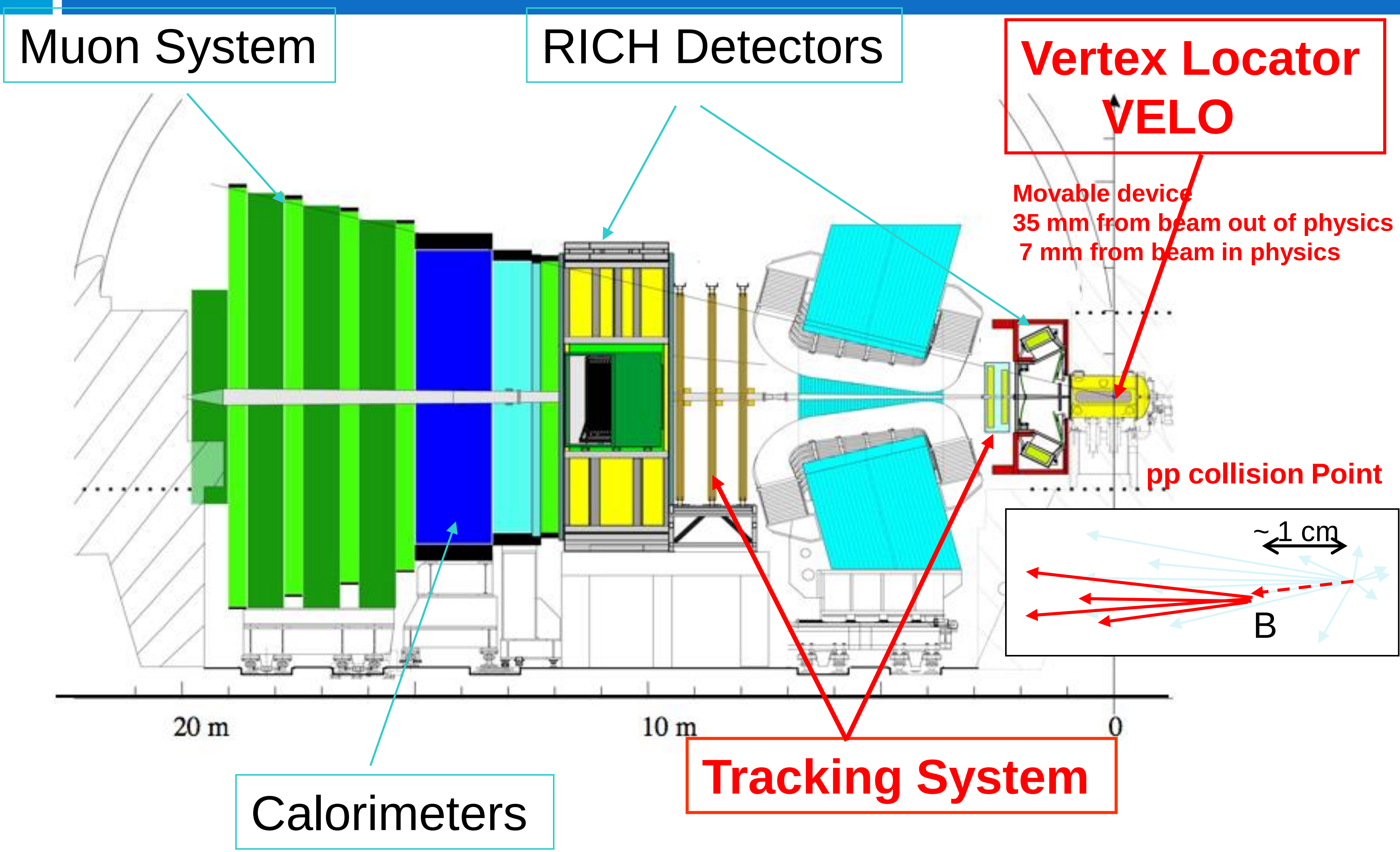

The LHCb Detector

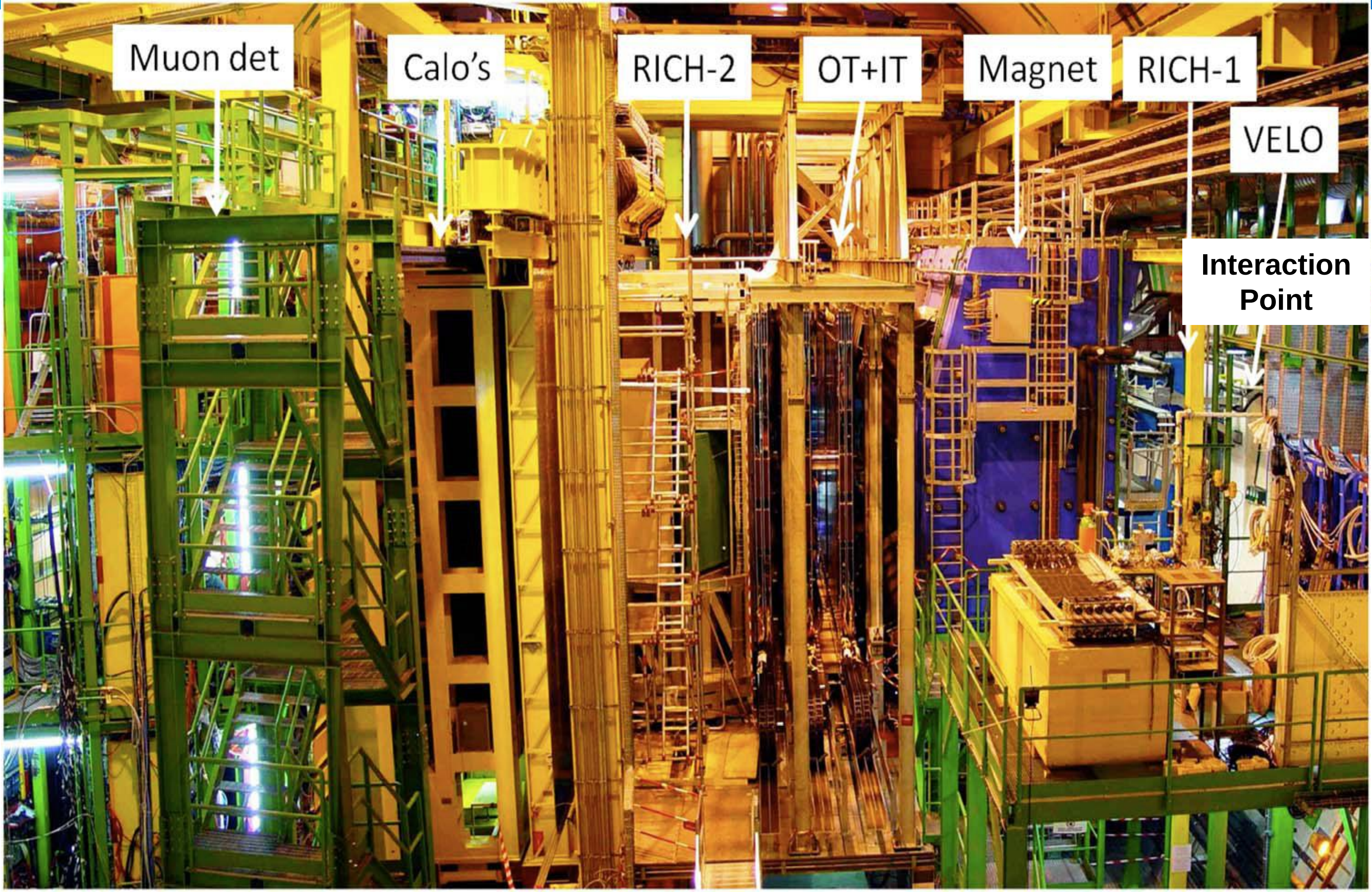

B-Vertex urement

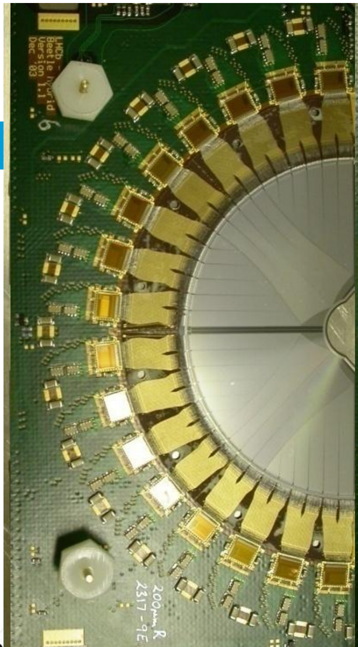

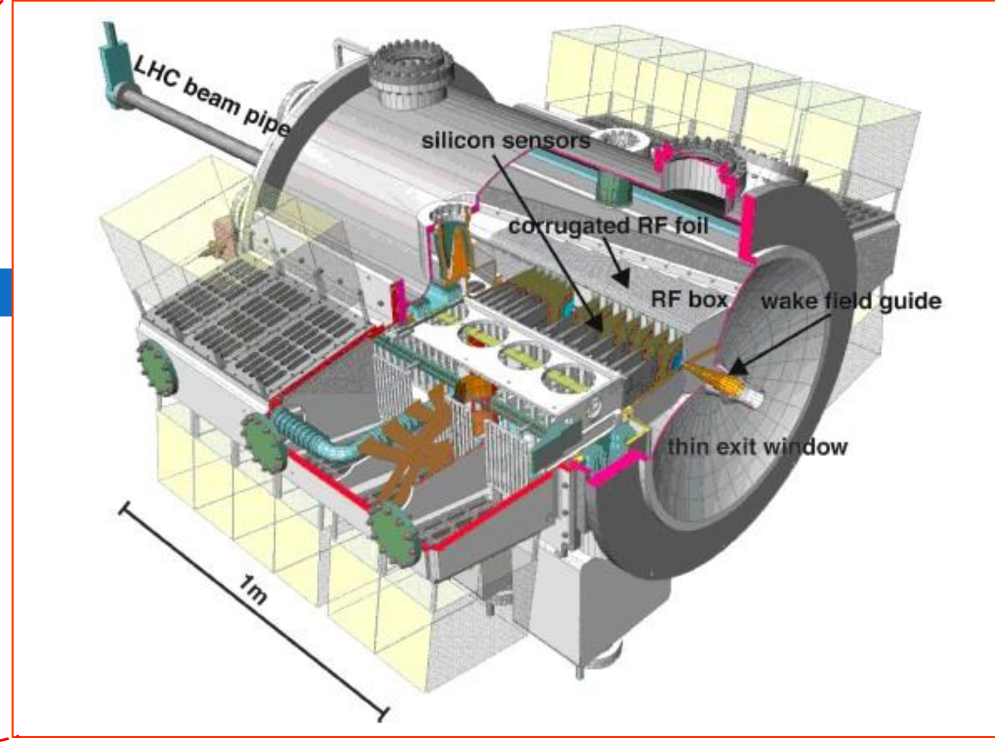

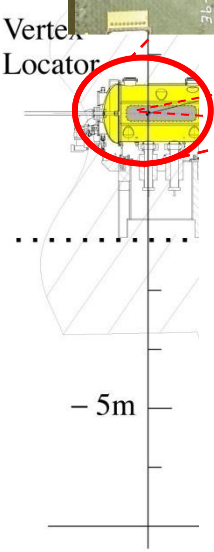

Vertex Locator (Velo)

21 stations of silicon strip detectors (r-ϕ)

~ 8 μm hit resolution

~25 μm IP resolution

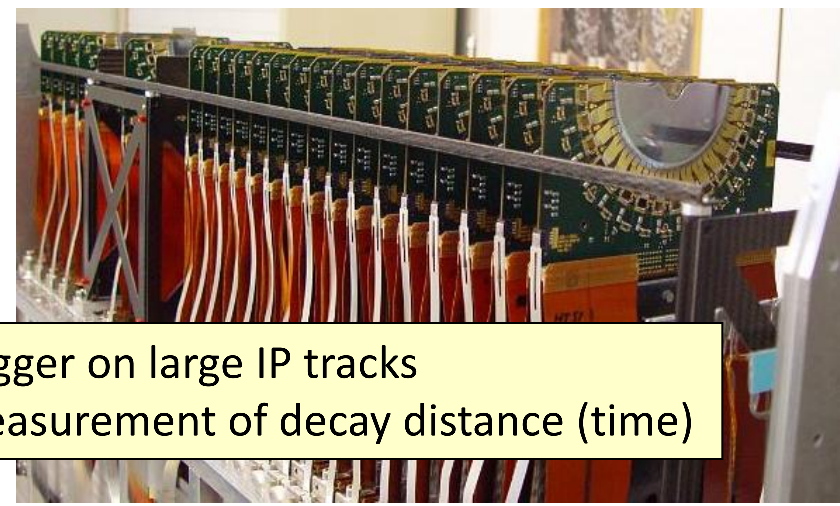

- Trigger on large IP tracks
- Measurement of decay distance (time)

VELO – VErtex LOcator

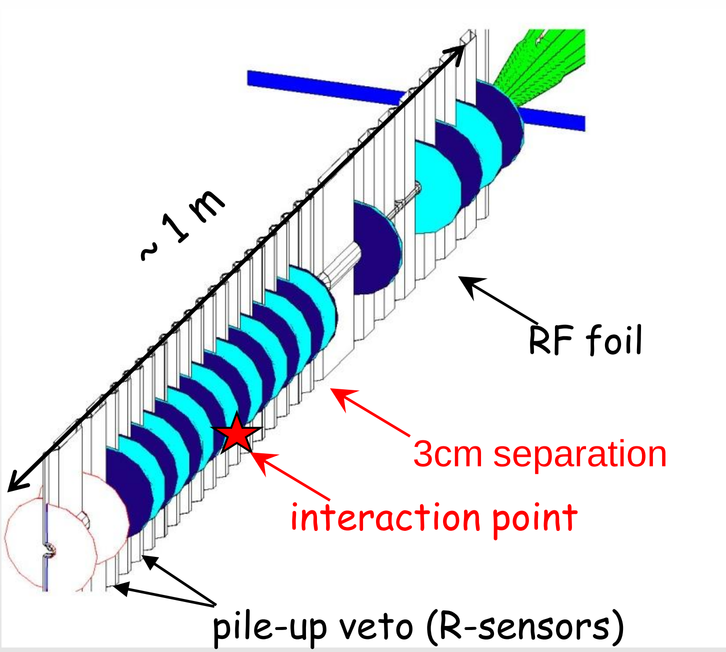

- Detector halves retractable (by 30mm) from interaction region before LHC is filled (to allow for beam excursions before injection and ramping)
- 21 tracking stations
- Unique R-Φ geometry, 40–100μm pitch, 300μm thick
- Optimized for
  - tracking of particles originating from beam-beam interactions
  - fast online 2D (R-z) tracking
  - fast offline 3D tracking in two steps (R-z then Φ)

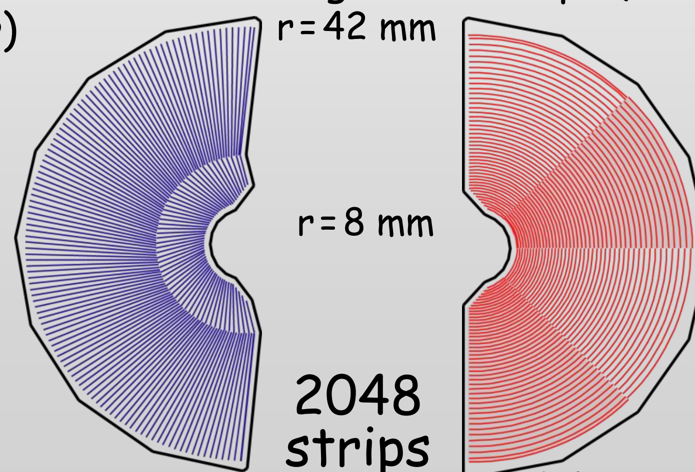

Tracking System

TT + 3 stations (T1,T2,T3), each with 4 detection planes (0°,+5°,-5°,0°)

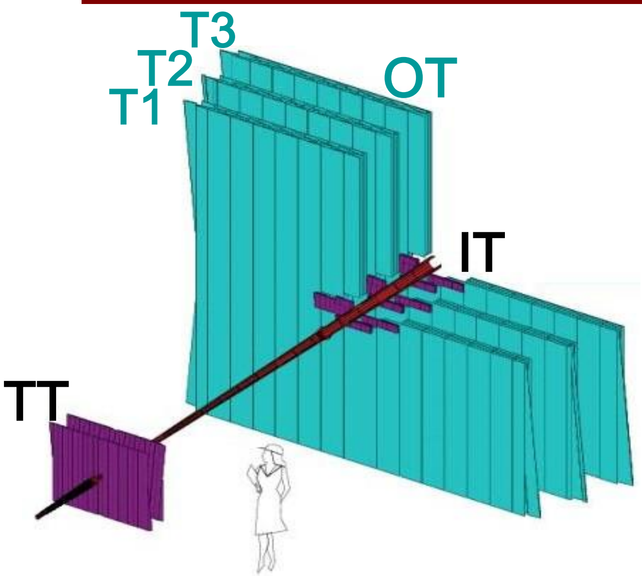

Trigger Tracker
~1.4×1.2 m^2 (144k ch)

Inner Tracker
~0.5 m^2 around beam pipe (130k ch)

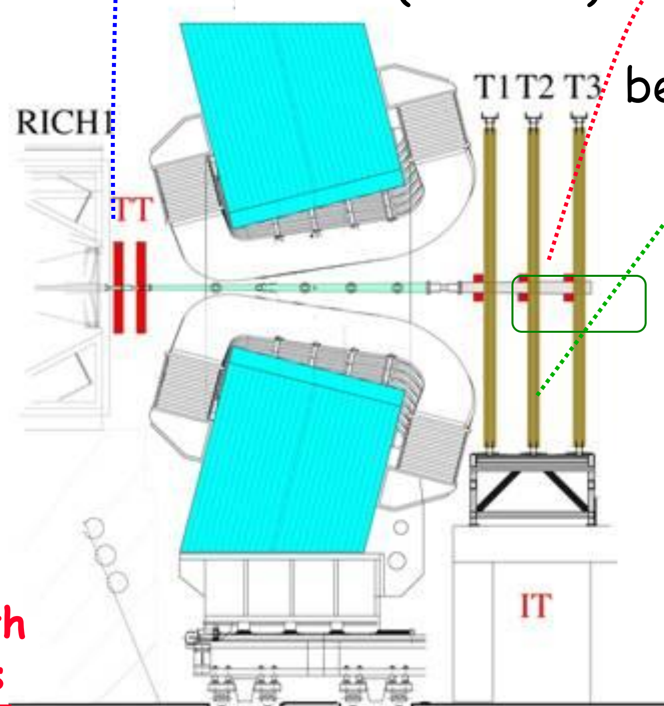

Outer Tracker
Straw Tubes
(56 k ch)

Similar sensors for TT & IT:
Si μ-strip with pitch ~ 200 μm

TT: 128 Modules (7 Si sensors)

IT: ladders with 1 or 2 sensors

Silicon Trackers

Trigger Tracker:

- 500 μm thick Si μ-strip sensors
- 7-sensor long ladders, 183 μm pitch
- Area of 8.2 m^2 covered with 896 sensors, 280 r/o sectors,
- 99.7% of channels functional

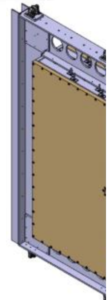

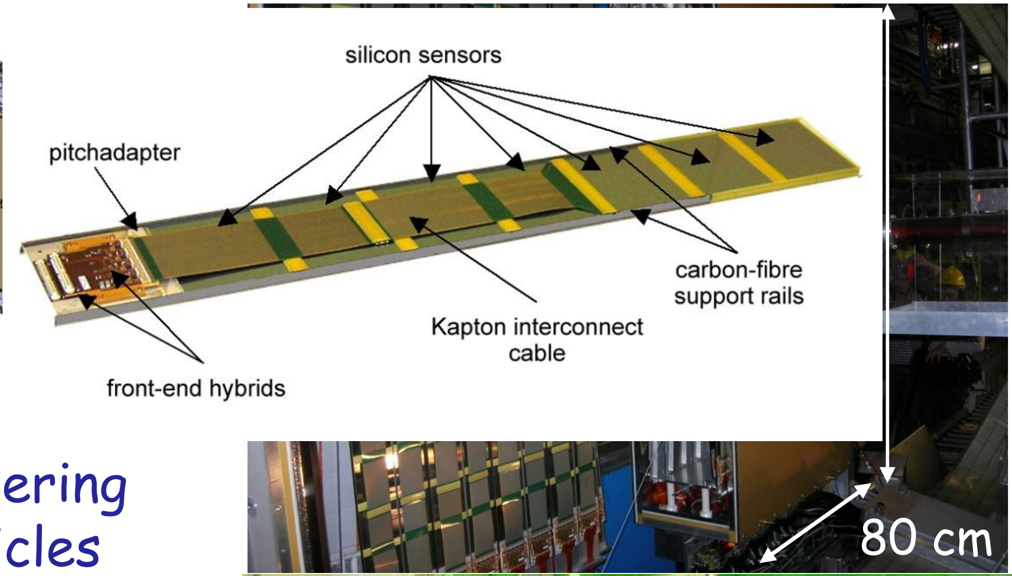

→ Provides tracking info for triggering
→ Tracking of low momentum particles

Inner Tracker:

- 320 (410) μm for 1 (2)-sensor ladders
- Readout pitch 198 μm pitch
- Area of 4.2 m^2 covered with 504 sensors, 336 ladders
- 99.4% of channels functional

→ Provides tracking in high flux region ($5x10^5 cm^{-2}s^{-1}$), 2% of area 20% of tracks

Experimental layout

T1: $3.1 < \eta < 4.7$

T2: $5.3 < \eta < 6.5$

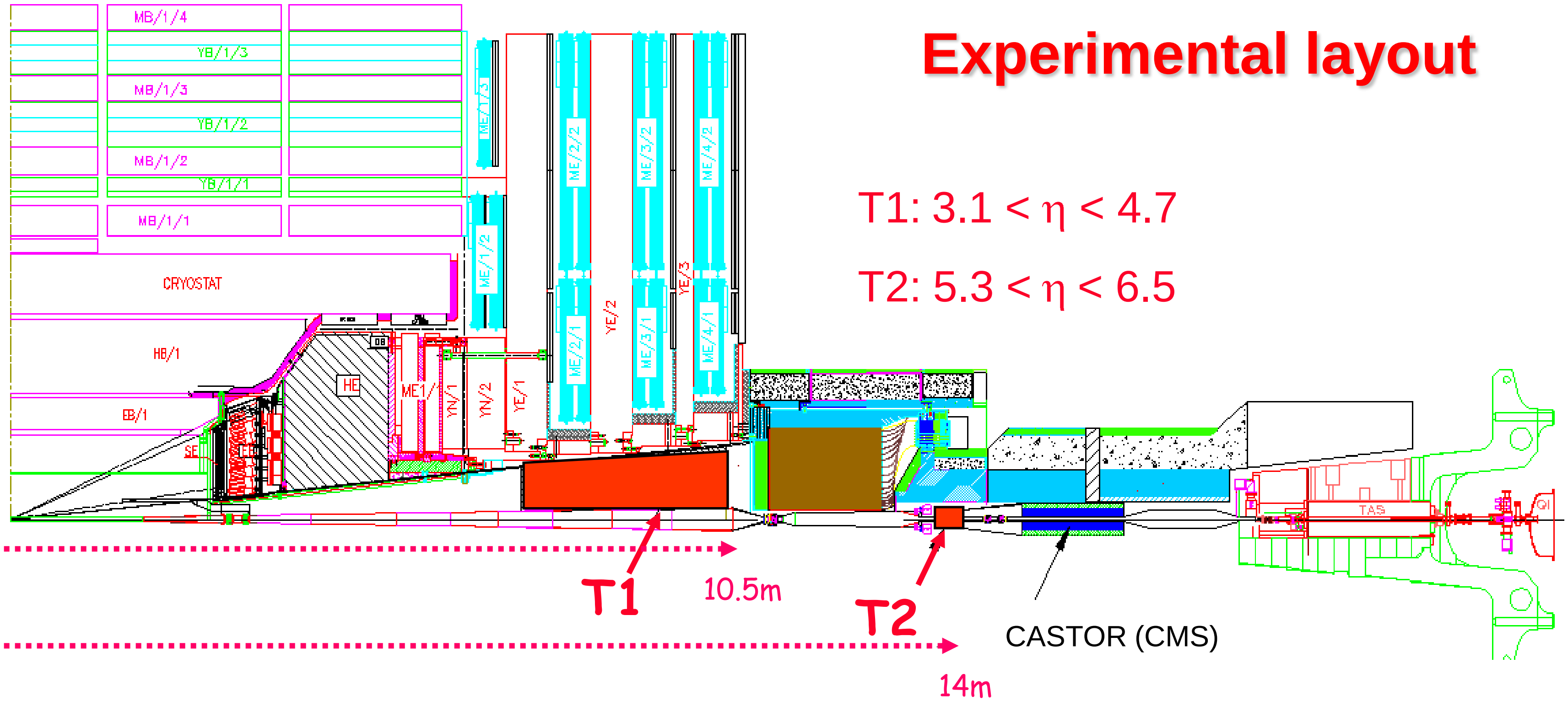

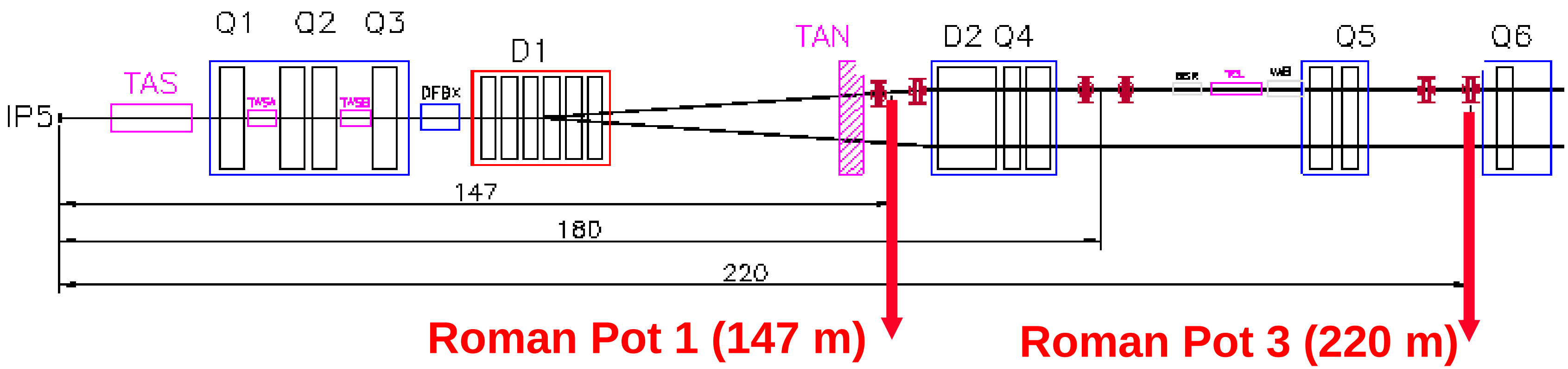

TOTEM

T2 Telescope

- Gas Electron Multiplier (GEM)
- $5.3 < |\eta| < 6.5$
- 10 half-planes @ 13.5 m from IP5
- Half-plane:
  - 512 strips (width 80 µm, pitch of 400 µm), radial coordinate
  - 65*24=1560 pads (2x2 mm^2 -> 7x7 mm^2), radial and azimuth coord.
  - Resolution: $\sigma(R) \sim 100$ µm, $\sigma(\varphi) \sim 1°$
- Primary vertex reconstruction (beam-gas interaction removal)
- Trigger using (super) pads

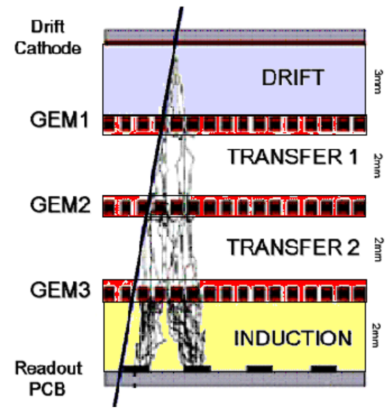

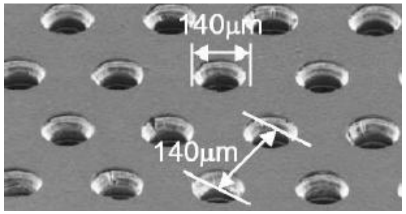

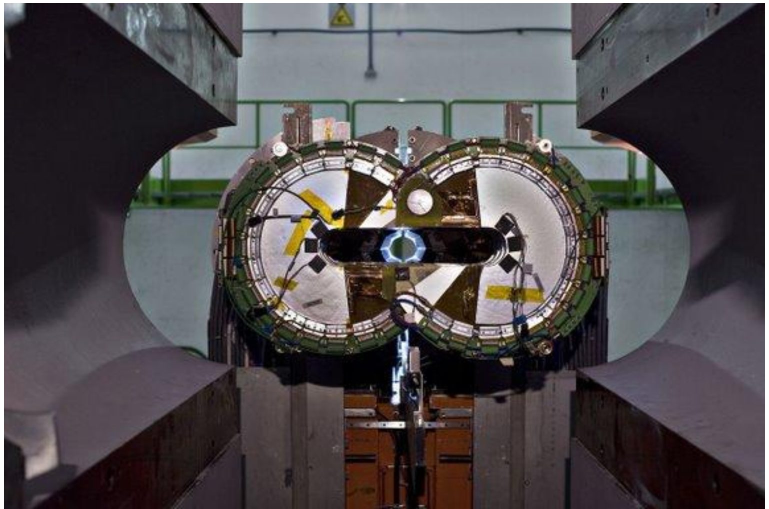

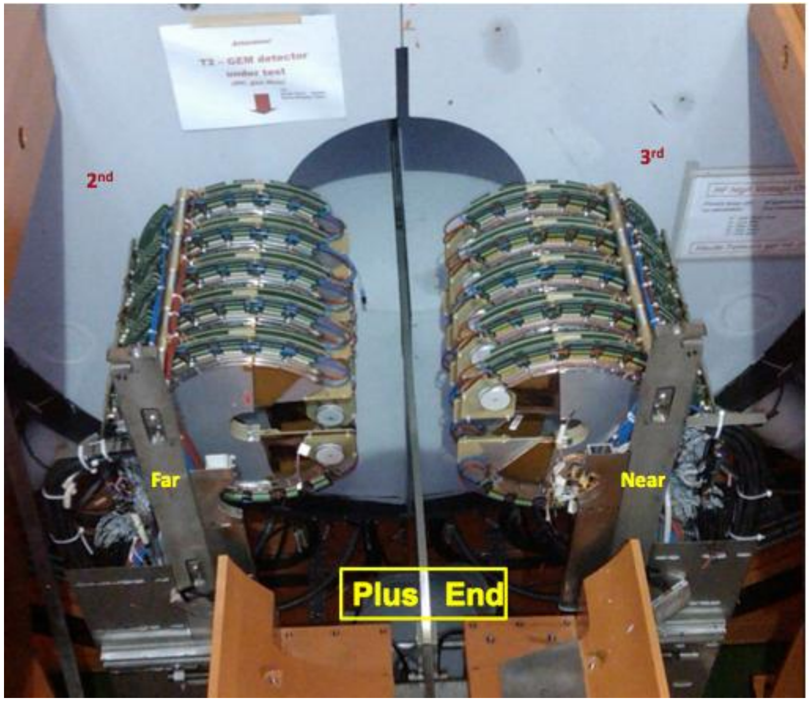

Leading Proton Detection: TOTEM Roman Pots

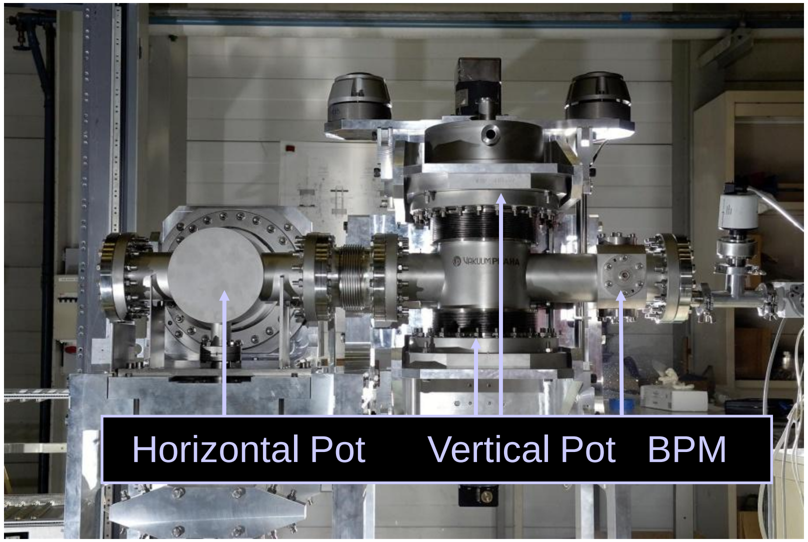

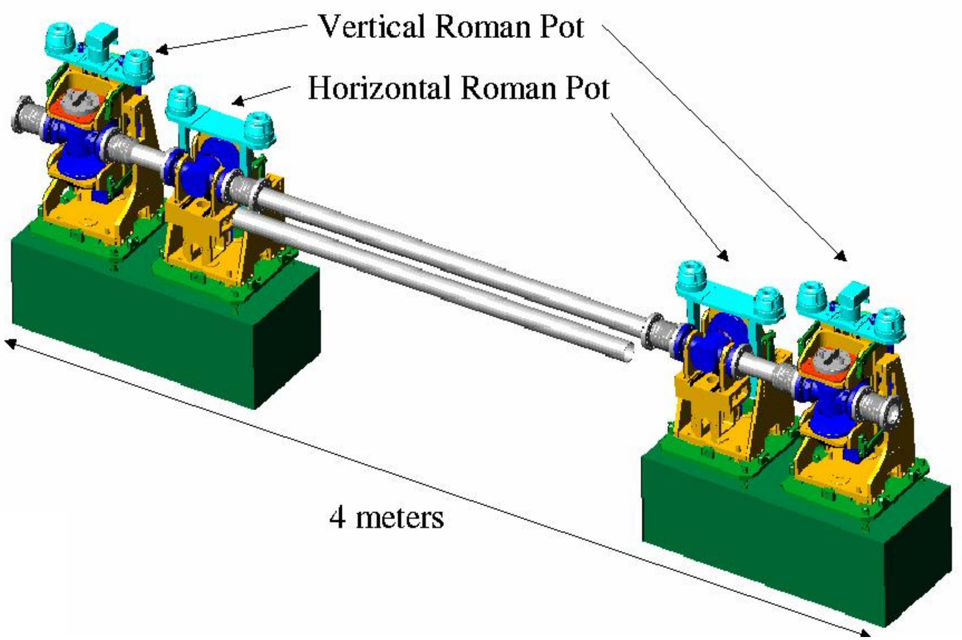

“edgeless” Si strip detectors
(10 planes per pot)

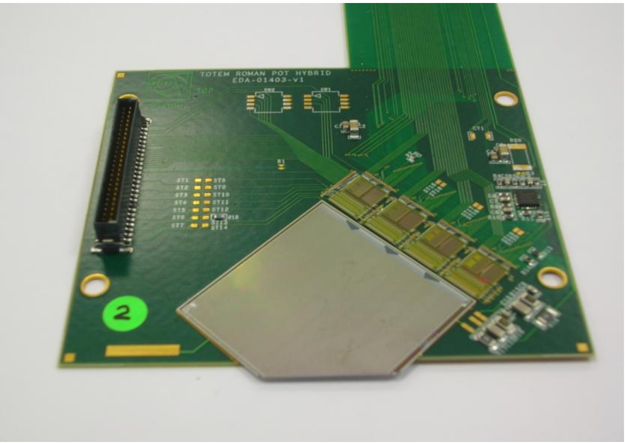

Leading proton detection at distances down 10 $\sigma_{beam} + d$

Need “edgeless” detectors (efficient up to physical edge) to minimise width d of dead space.

TOTEM: specially designed silicon strip detectors (CTS), efficient within 50 μm from the edge

T1 Telescope

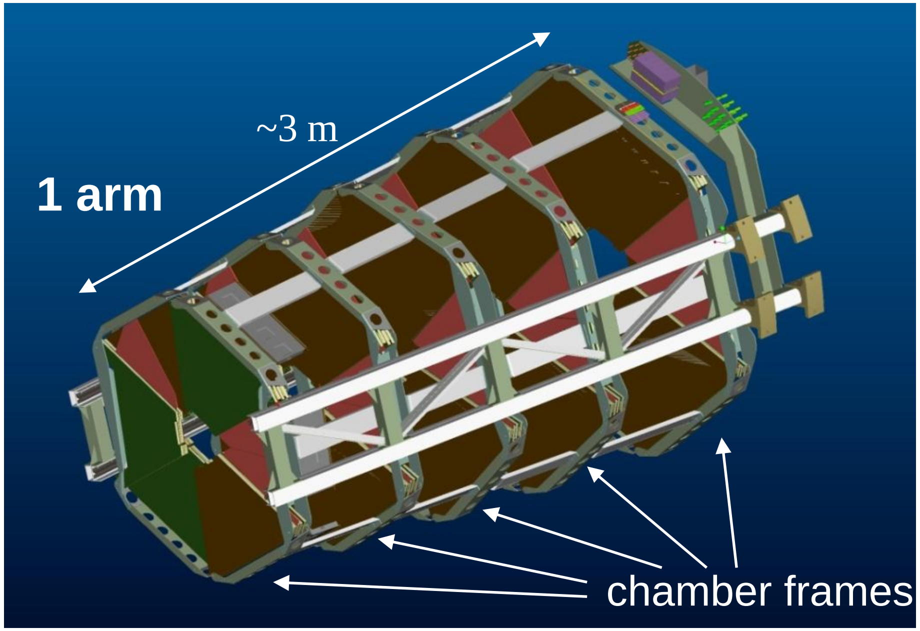

- Cathode Strip Chambers (CSC)
- $3.1 < |\eta| < 4.7$
- 5 planes with measurement of three coordinates per plane, $\sigma \sim 1$ mm
- Primary vertex reconstruction (beam-gas interaction removal)
- Trigger with anode wires
- Connected to VFAT chips
- Successful ageing studies

(~ 5 years at $L_{inst}=10^{30}$ cm^{-2}s^{-1})

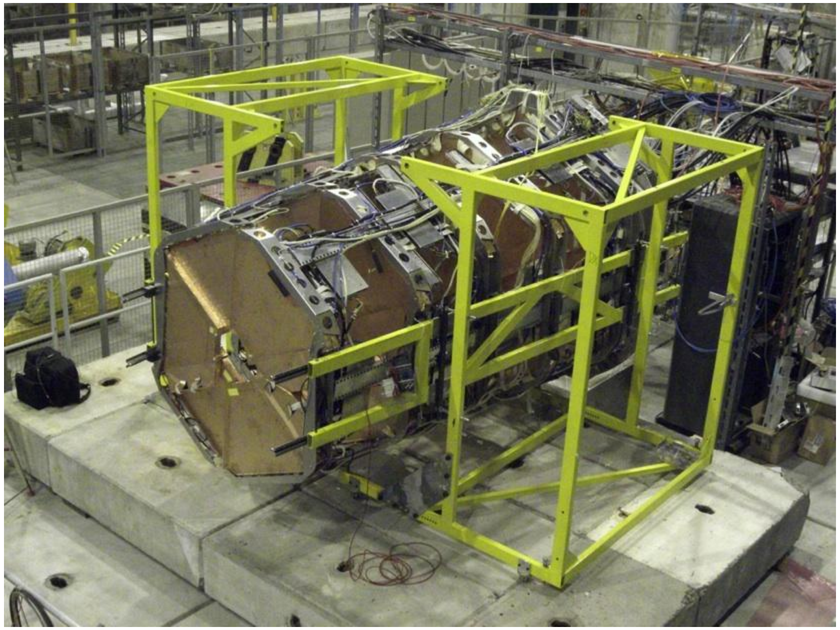

Installation as soon as possible

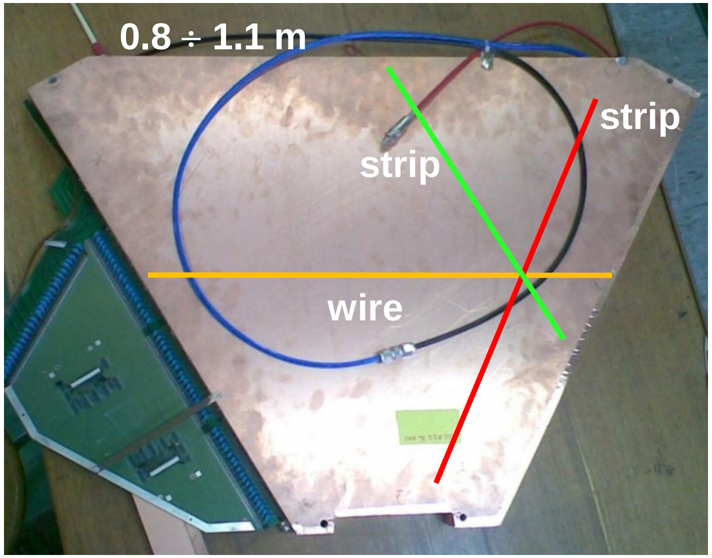

Backup slides

Several drawings of this presentation have been borrowed (sometimes with small changes only for the sake of my presentation) from very good lectures that can be found in the Web.

See for instance:

W. Riegler; Summer Student Lectures 2009
M. Krammer; XI ICFA School on Instrumentation

Muon Energy Loss

(Limits of applicability for Bethe Bloch)

μ at minimum ionization

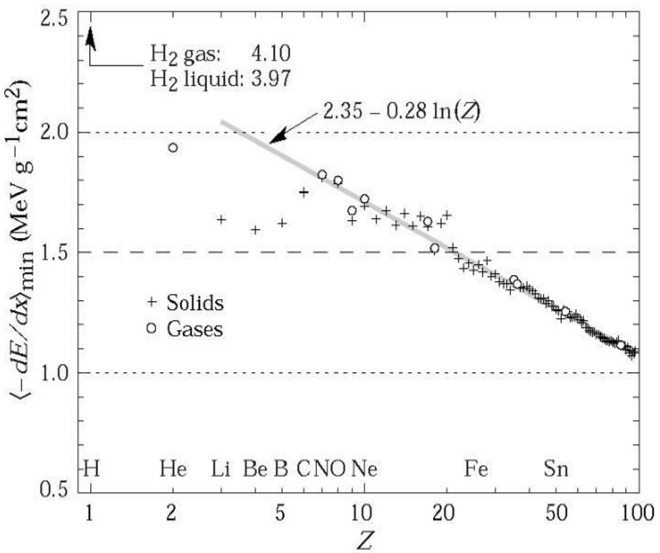

Example: a 1 GeV μ in Iron

Fe: Thickness = 100 cm; ρ = 7.87 g/cm^3

dE ≈ 1.4 * 100* 7.87 = 1102 MeV

→ a 1 GeV μ can traverse 1m of Iron

a 1TeV muon hitting copper is not a MIP !

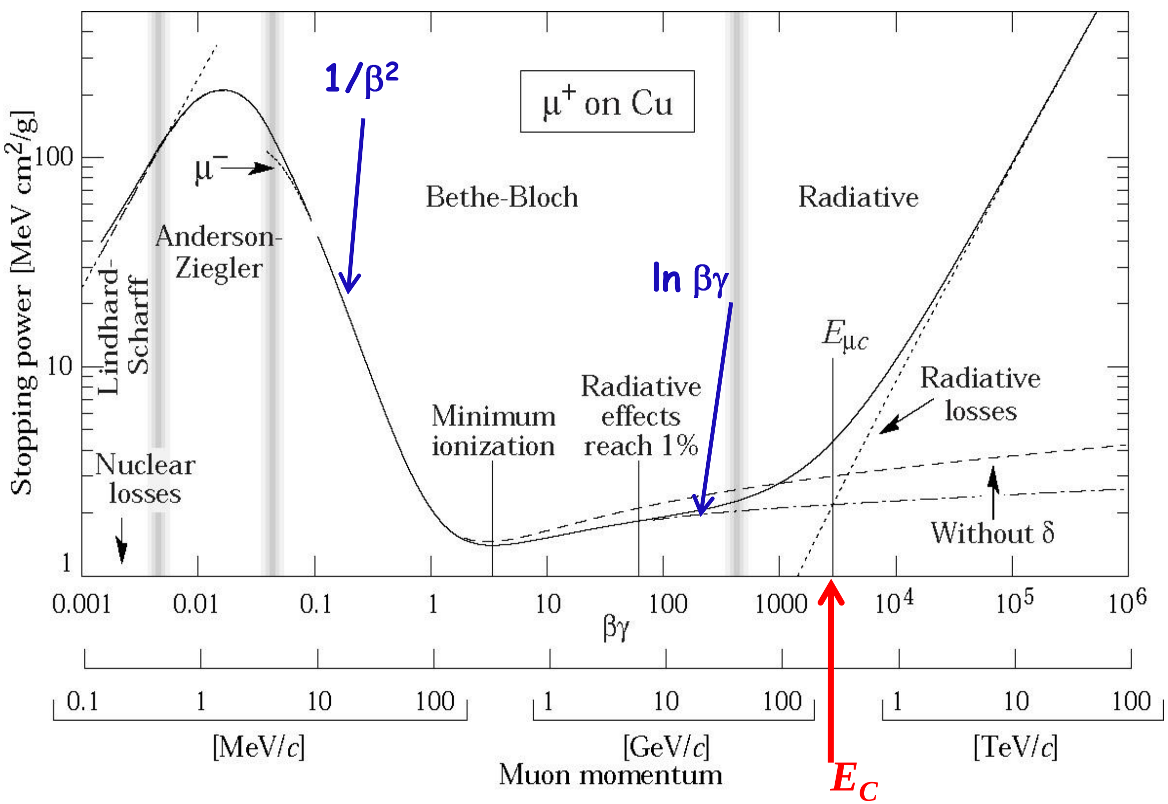

E_c = energy for which ionization matches bremsstrahlung

Bremsstrahlung

A charged particle of mass m and charge q traversing material not only interacts with the atomic electrons loosing energy via ionization and excitation, but also can be deflected by the atomic nuclei of charge Z of the material. This deflection (Rutherford scattering) results in an acceleration of the charge q that causes emission of photons. The radiation energy (Bremsstrahlung) emitted by the accelerated particle for a given momentum transfer can be evaluated by the Maxwell's equations and comes out to be:

- proportional $1/m^2$ of the incoming particle
- proportional to q^4 of the incoming particle
- proportional to Z^2 of the material
- proportional to ρ of the material

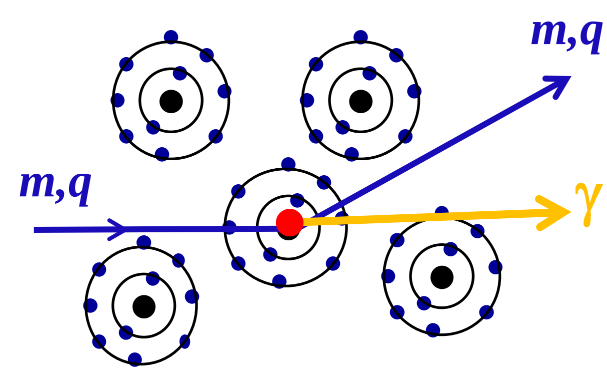

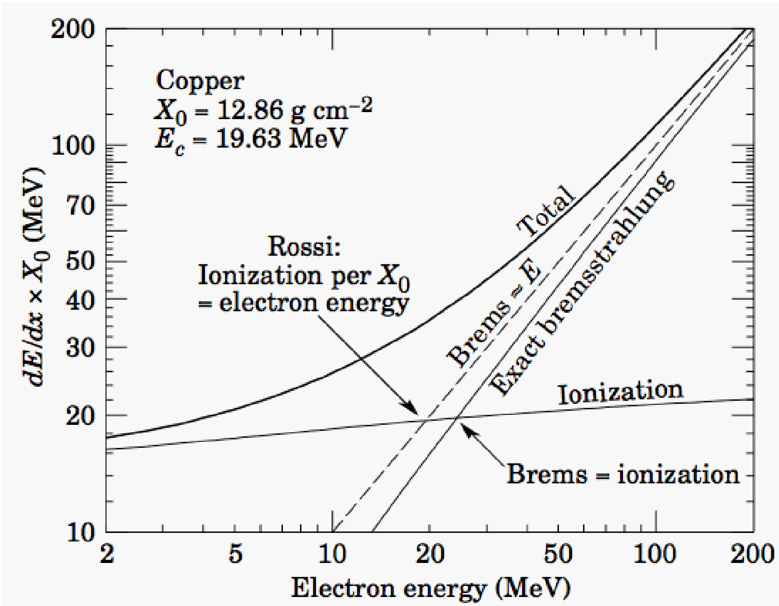

Critical Energy E_C is defined the energy at which dE/dx (Ionization)=dE/dx (Bremsstrahlung)

Muon in Copper: $E_C \approx$ 400 GeV

Electron in Copper: $E_C \approx$ 20 MeV

Electrons lose energy via ionization as other charged particles, however because of their small mass the Bremsstrahlung becomes the dominant process for energies ≥ 20 MeV

Particle Identification by Energy Loss

Energy loss depends on the $\beta\gamma$ of the particle and is ≈ independent from the mass of the particle. As a function of particle momentum $p = Mc\beta\gamma$ the energy loss depends on the mass of the particle.

By measuring the energy loss and the momentum of the particle, the mass of the particle can be measured: → Particle Identification !

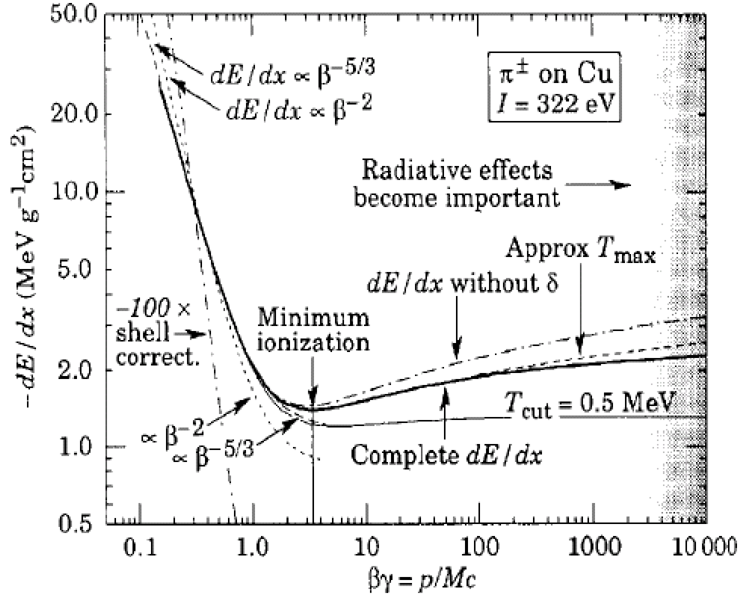

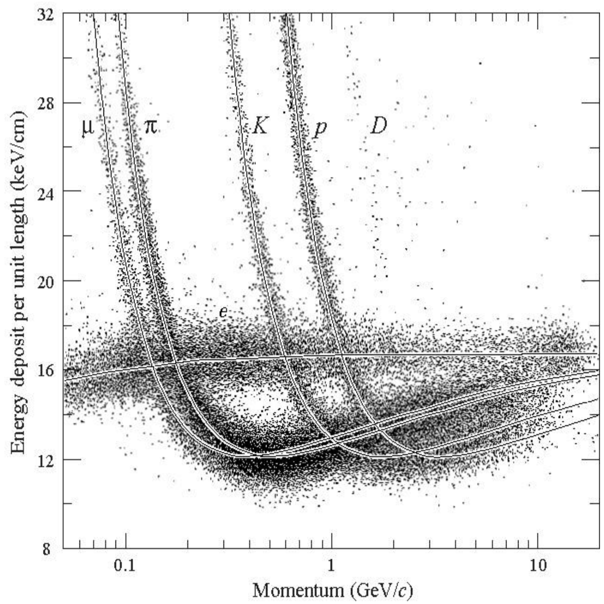

TPC in magnetic field

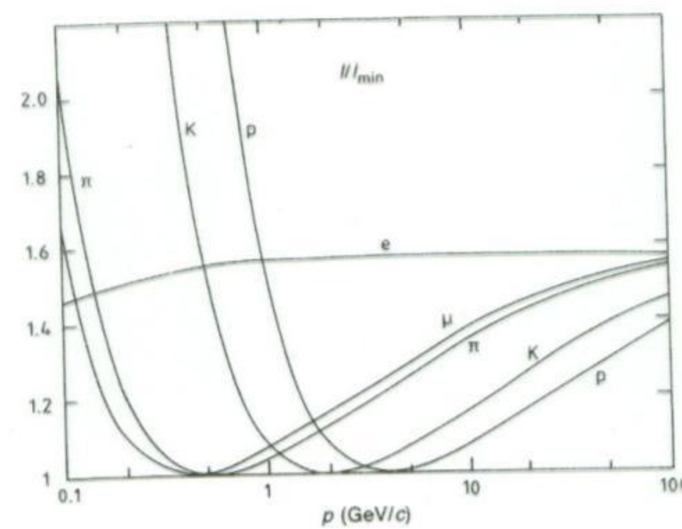

$$\frac{1}{\rho}\frac{dE}{dx} = -4\pi r_e^2 m_e c^2 Z_1^2 \frac{p^2 + M^2c^2}{p^2} N_A \frac{Z}{A}\left[\ln\frac{2m_ec^2F}{I}\frac{p^2}{M^2c^2} - \frac{p^2}{p^2 + M^2c^2}\right]$$

Ionization: the Bethe-Bloch formula

- Bethe-Block formula only gives the average energy loss, and do not take into account fluctuations from event to event.
- Large high energy tail – δ rays

δ-rays : electrons that have sufficient energy to ionize further atoms through subsequent interactions on their own.

Landau distribution:

$f(\Delta/X)$: Probability for energy loss Δ in a thickness X of matter.

Very asymmetric distribution: average and most probable energy loss must be distinguished !

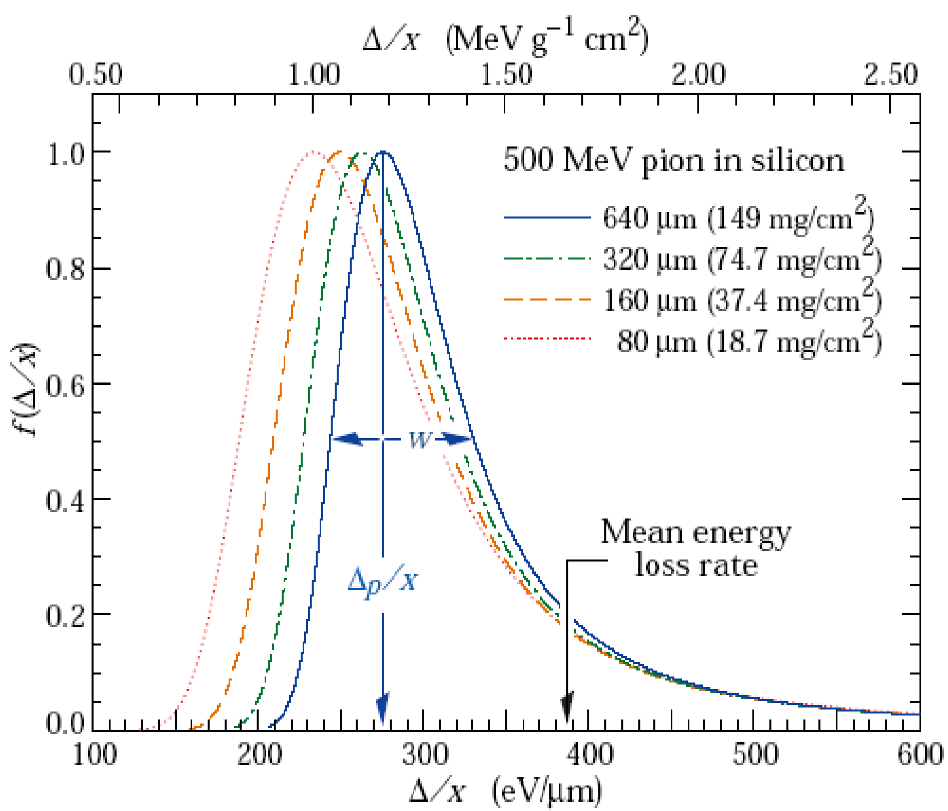

Multiple Scattering

A particle traversing material undergoes successive deflections due to multiple elastic scattering from nuclei.

The probability that the particle is defected by an angle θ after travelling a distance x in the material is well approximated (actually tails are larger than Gaussian tails) by a Gaussian distribution with sigma of:

$$\theta_{MCS} = \theta_{rms} = \frac{13.6\,MeV}{\beta c\, p} z \sqrt{\frac{x}{X_0}} \left[1 + 0.038 \ln\left(\frac{x}{X_0}\right)\right]$$

X_0 Radiation length of the material
z Charge of the particle
p Momentum of the particle

Radiation Length X_0 has 2 definitions:

◇ Mean distance over which high energy electron losses all but 1/e of its energy by Bremsstrahlung.

◇ 7/9ths of the mean free path for pair production by a high energy photon.

$$X_0 \approx \frac{716.4 g cm^{-2} A}{Z(Z+1)\ln(287/\sqrt{Z})}$$

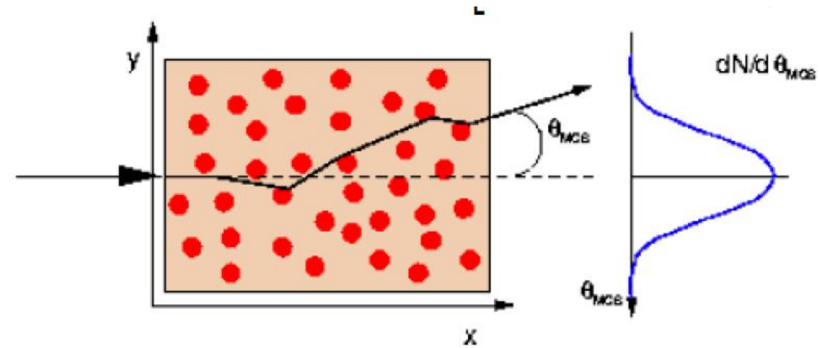

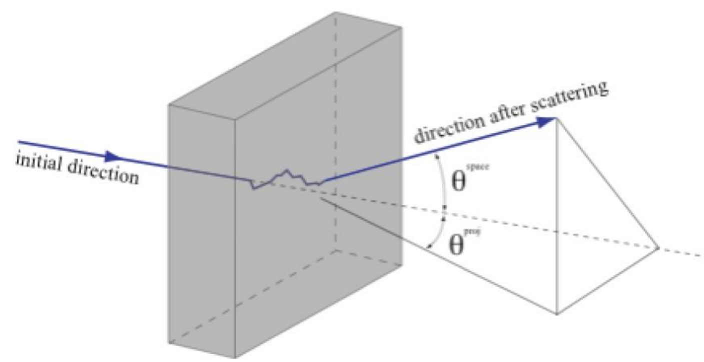

	X_0 (g cm^{-2})	X_0 (cm)
Air	37	30,000
Silicon	22	9.4
Lead	6.4	0.56

Gas Detectors: the avalanche multiplication

As the electric field increases to sufficient high value (~100kV/cm) more and more electrons gain kinetic energy in excess of the ionization energy so that they can ionize in turn other atoms (secondary ionzation) and so on.

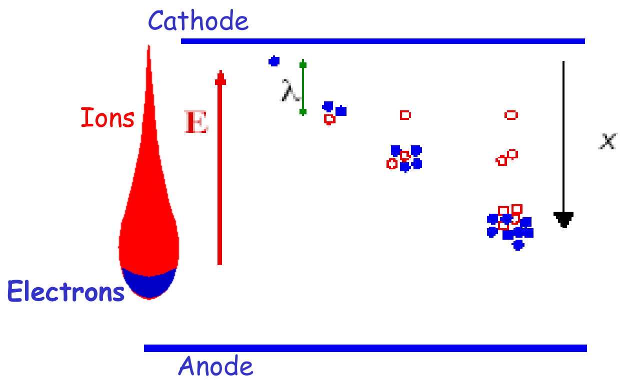

The mean free path λ is defined as the average distance that an electron must walk before another ionizing collision may occurs. On average every λ the number of ion pairs is doubled. $\alpha=1/\lambda$ is called Townsend coefficient:

$dN = N\,\alpha\,dx$

$N(x) = N_0 \exp(\alpha x)$ $N/N_0=A=$ Amplification or *Gas Gain*

The problem with an avalanche multiplication with an homogeneous electric field is that very high field on are needed and may easily cause breakdown
The solution is to obtain the avalanche multiplication in an inhomogeneous field:

$\alpha(E) \rightarrow N(x)/N_0 = A = \exp\left[\int \alpha(E(x'))dx'\right]$

Wire Chamber: Electron Avalanche

- **Basic design:** ionization chamber with HV sense wire

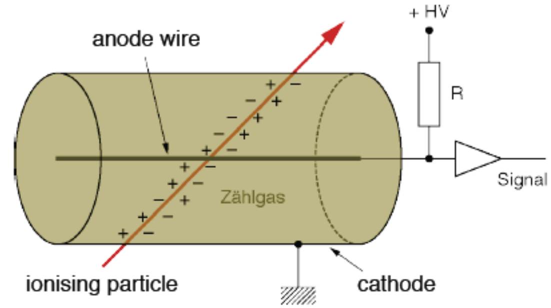

Typically a gas detector will have ~20 primary ions per cm created by a track: amplification needed in order to provide a measurable signal.

Consider a thin wire with radius a (10-25μm) at voltage V=0 in a tube of outer radius b (1-3cm) voltage V_0. The electric field inside the tube is given by:

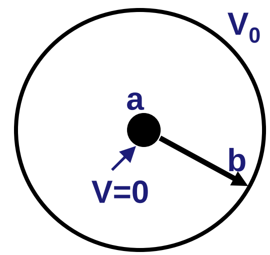

$$E = 2\lambda / r, \quad V_0 = 2\lambda \ln(b/a), \quad V(r) = V_0 \frac{\ln(r/a)}{\ln(b/a)}, \quad E(r) = \frac{V_0}{r \ln(b/a)}$$

Example: V_0=1000V, a=10μm, b=10mm,
E(a)=150kV/cm

Electric field is sufficient to accelerate electrons to energies which are sufficient to produce secondary ionization → electron avalanche → signal.
(tipical amplification: 10^3-10^5)

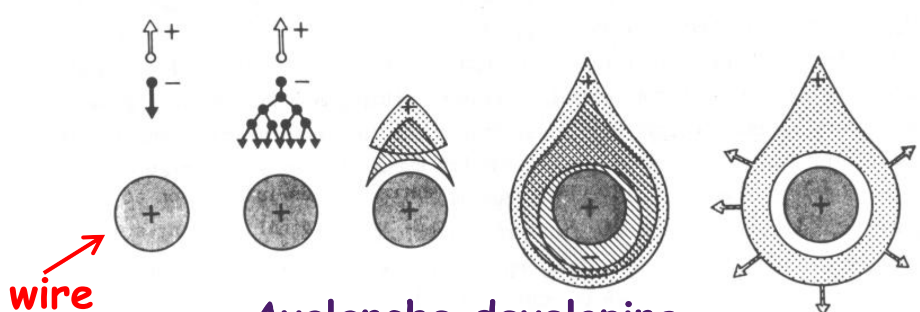

Avalanche developing

Wire Chamber: Signals from Electron Avalanches

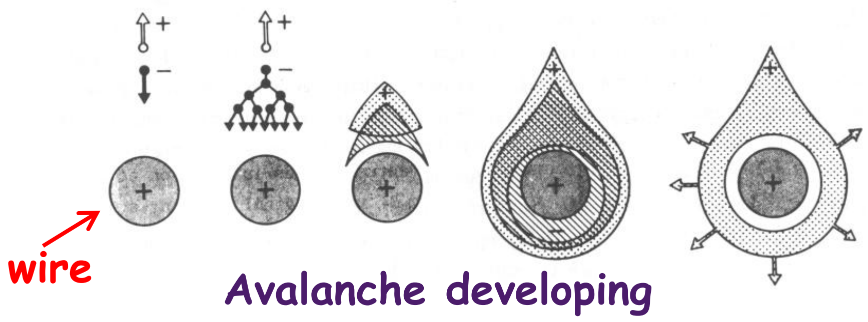

The electron avalanche happens very close to the wire. First multiplication only around R =2x wire radius. Electrons are moving to the wire surface very quickly (<<1ns). Ions are drifting slowly towards the tube wall (typically several 100μs).

The signal is characterized by a very fast 'spike' from the electrons and a long ion tail.

The total charge induced by the electrons amounts to 1-2% of the total induced charge.

Signal due to ions dominates, as they travel all the way to the cathode.

The signal is characterized by a very fast peak from the electrons and a long ion tail.

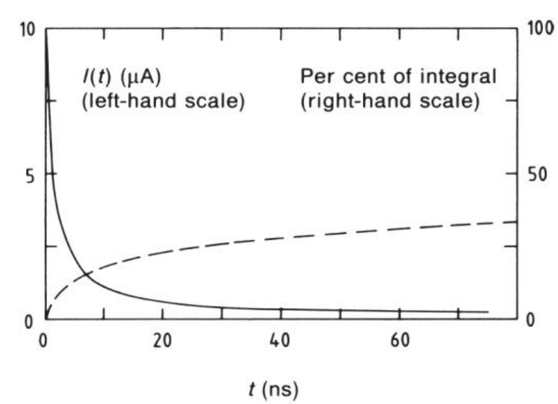

Amplification vs applied voltage

- Average energy lost in creating ion pair ~ 10-20 eV.
- Primary ionization: number of ionizing collisions per unit length for the incident particle. (Poisson distribution)
- Secondary ionization: the electric field is sufficient to accelerate electrons to energies which are sufficient to produce secondary ionization

For intermediate value of the electric field the number of electrons produced in the avalanche is proportional to the primary ionization (amplification $A \approx 10^3 - 10^4$; Landau distribution)

Increasing the electric field the amplification increases but the detector is not working anymore in a proportional regime:

$A \approx 10^4 - 10^5$ Semi proportional region due to space charge screening around the anode

$A > 10^6$ Saturation region: the number of ions collected are independent from the number of primary electrons.

$A > 10^7$ Streamer region: the avalanche develops along the particle track.

$A > 10^8$ Limited Geiger region: the avalanche is propagated by UV photons.

$A \approx 10^9$ Geiger region: the avalanche is produced along the entire wire.

• • • • Continuous discharge !

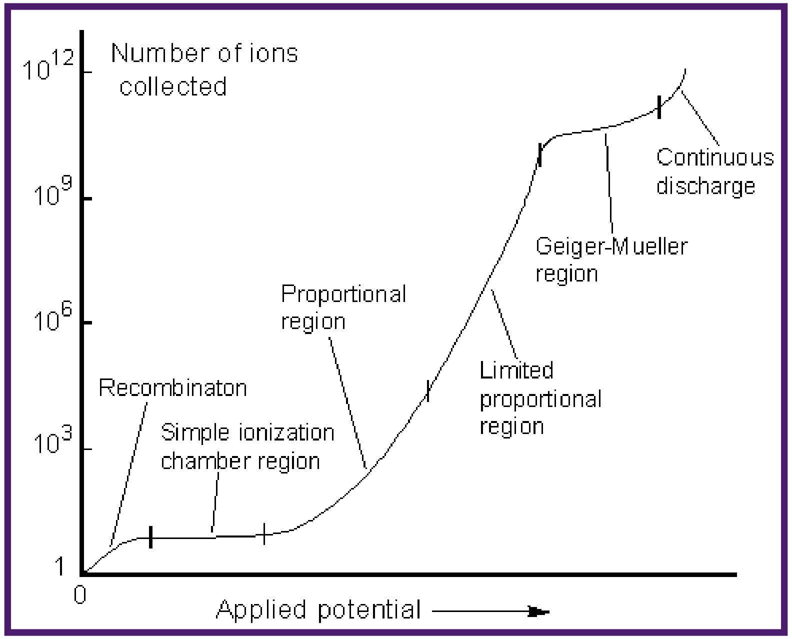

Multiwire Proportional Chambers

The MWPC was invented by Charpak at CERN 1992  Prize

Principle of proportional counter is extended to large areas. One plane of thin sense wires is placed between two parallel plates. Typical dimensions: wire distance 2-5mm, distance between cathode planes ~10mm.
Electrons ($v \approx 5 cm/\mu s$) are collected within ≈ 100ns.
The movement of the charges induces a signal on the wire AND on the cathode. By segmentation of the cathode plane and charge interpolation, resolutions of 50μm can be achieved.
Stack several wire planes up in different direction to get position location.

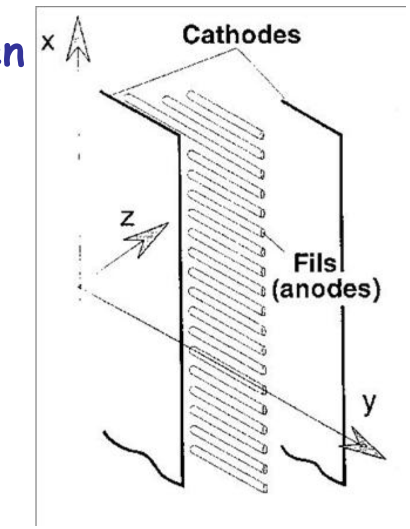

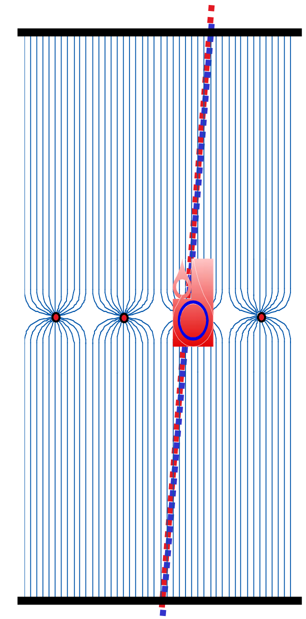

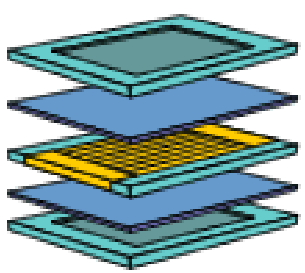

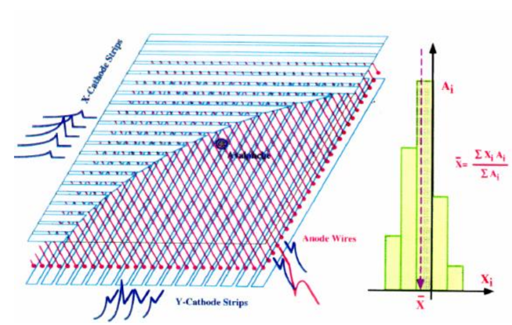

Lo Split Field Magnet Detector (CERN ISR 1972-1983)

40 large area MWPCs

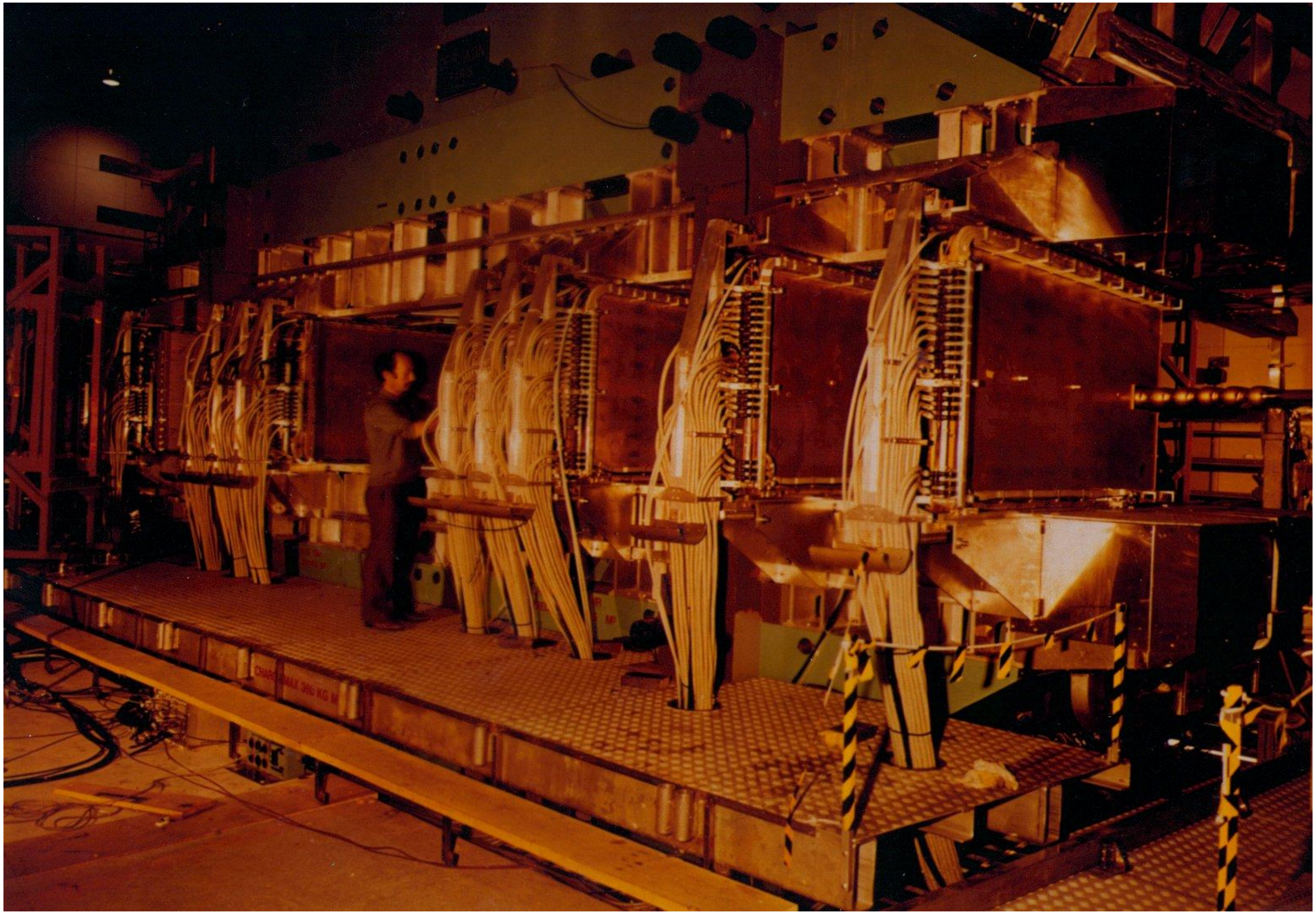

Drift Chamber (1971: H. Walenta)

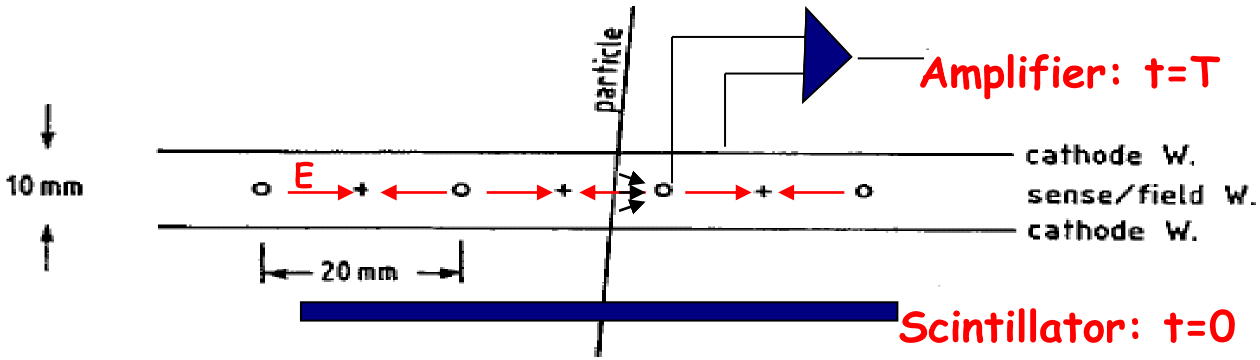

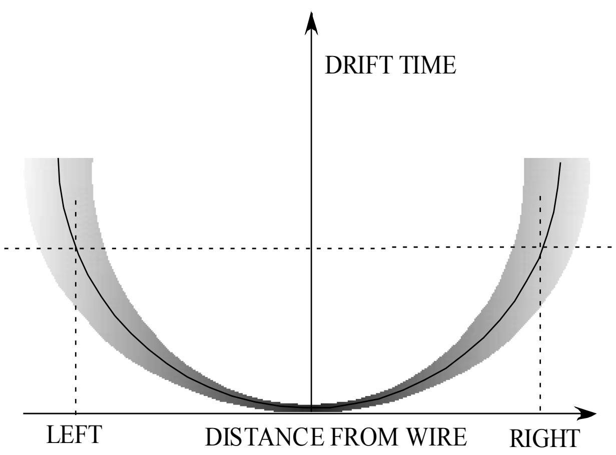

The electric field in an alternating sequence of sense and field wires at different potentials cause the electrons to drift toward the sense wire. The measurement of the drift time T between the passage of the particle and the arrival of the electrons at the sense wire is a measurement of the position of the particle (precision ~100μm)
The wire distance can be increased up to several centimeters (drift time ~μs; v≈5cm/μs) saving a lot of electronics channels with respect to the MWPC.
however:

- ❑ Left-Right ambiguity
- ❑ Not a linear relation between drift time and distance from the wire

Drift Chambers

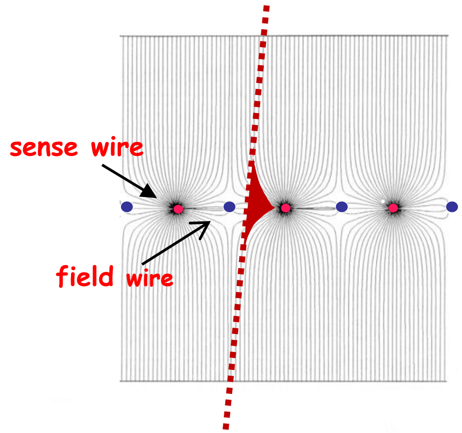

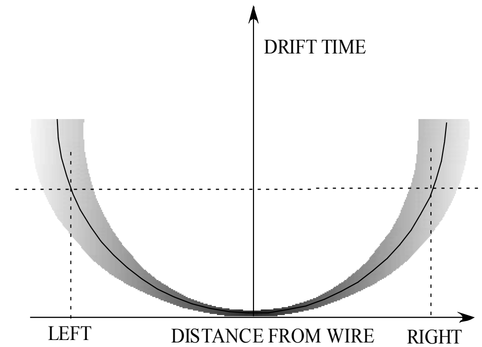

improved drift cell geometry with constant field

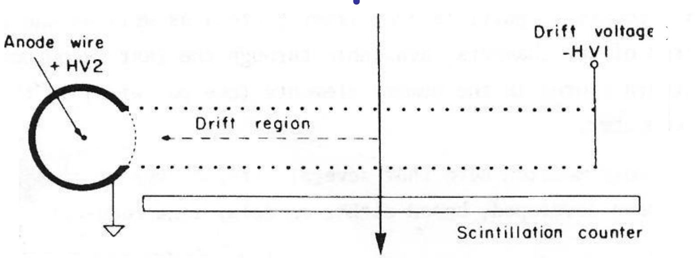

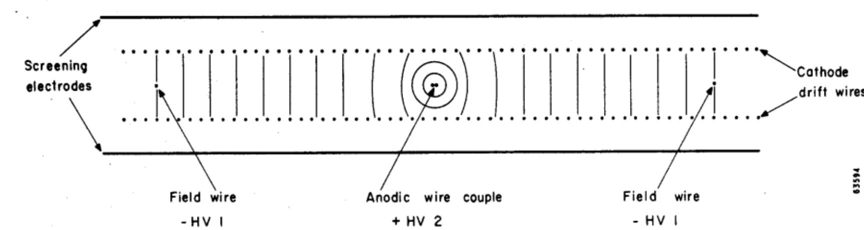

simplified drift geometry for construction of very large area chambers

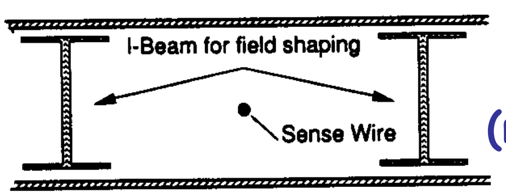

DT CMS
(muon chambers)

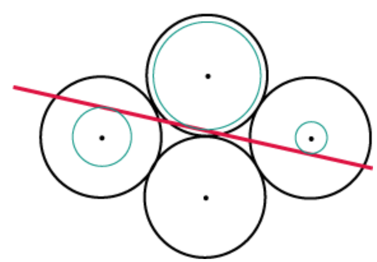

MDT ATLAS
(muon chambers)

Drift Chambers

CDF Central Tracking Chamber

660 drift cells tilted 45^0 with respect to the particle track to take into account ExB drift!

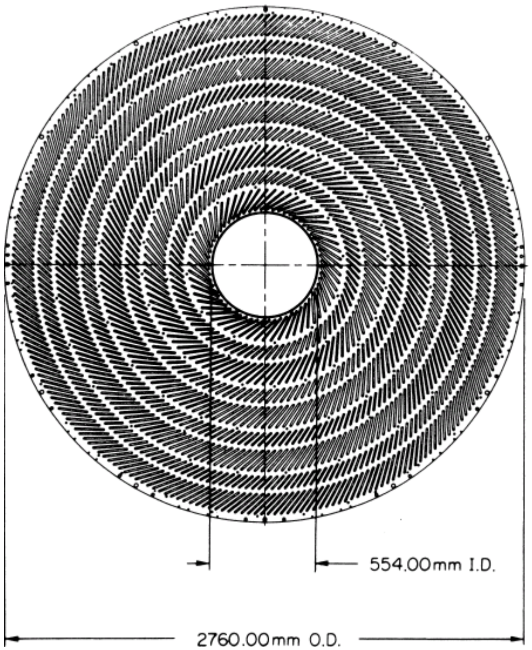

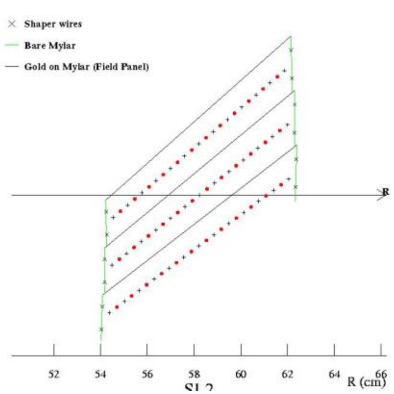

Drift Chambers

BABAR Central Tracking Chamber

- 2.8 m long
- Gas volume ~ 5.6 m^3
- 7100 anode sense wires
- ~50,000 wires in total

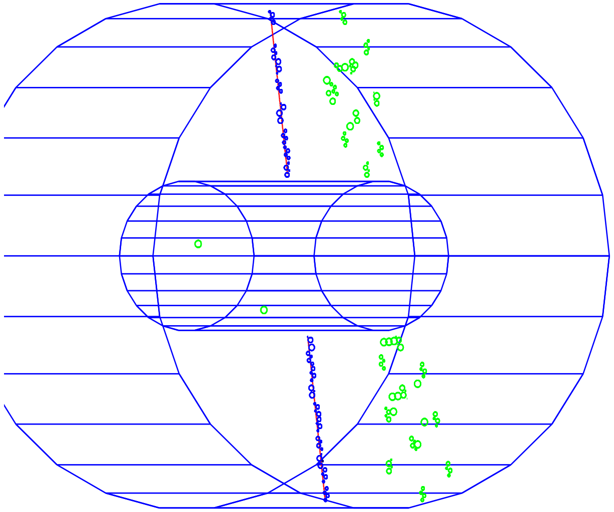

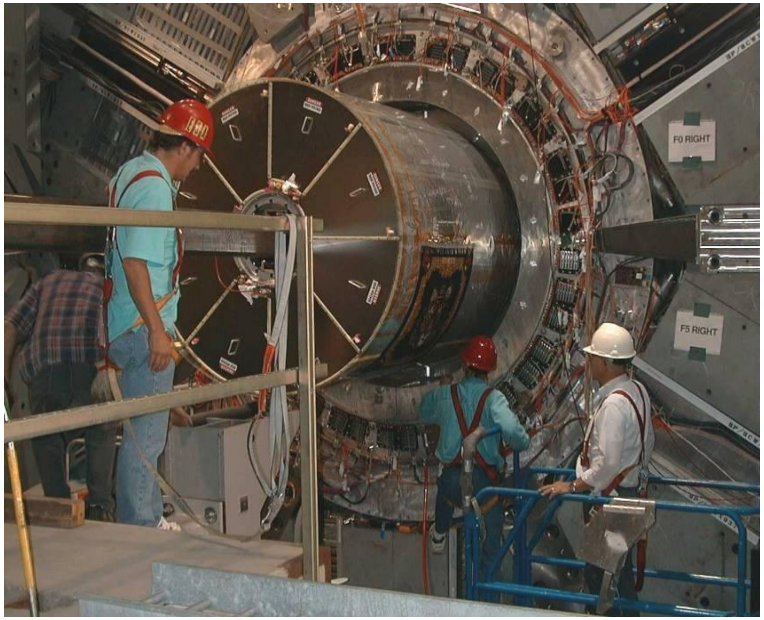

Time Projection Chamber (TPC)

1976: D. Nygren (LBL)

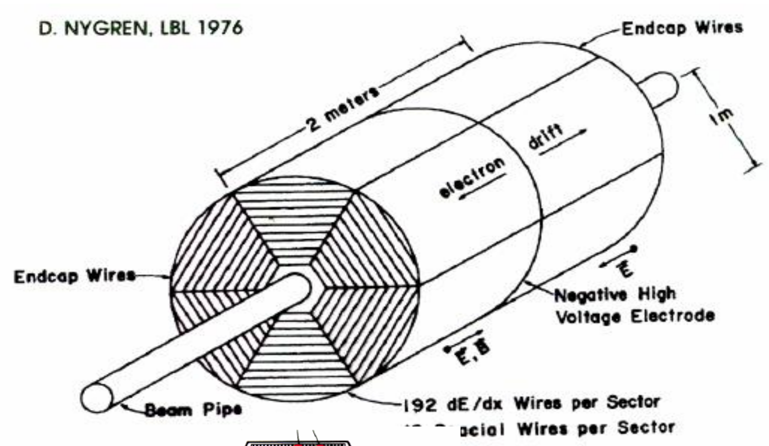

- E~100-300 V/cm. Drift times 10-100 μs
- B for momentum measurement
  (limit electron diffusion up to a factor 5)
- Wire chamber to detect projected tracks.
  Timing gives z measurement
- Long drift distances up to 2.5 m

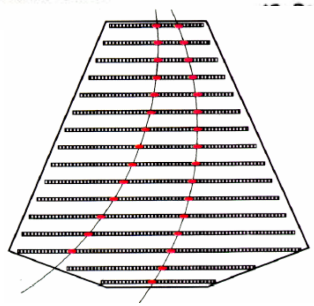

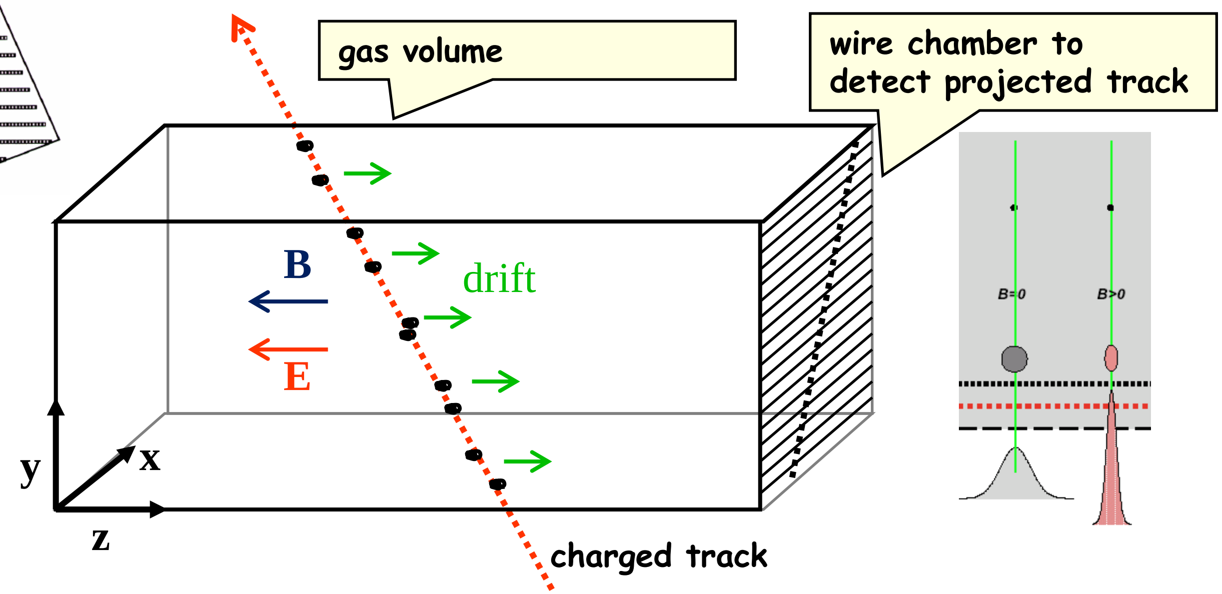

The ALEPH TPC

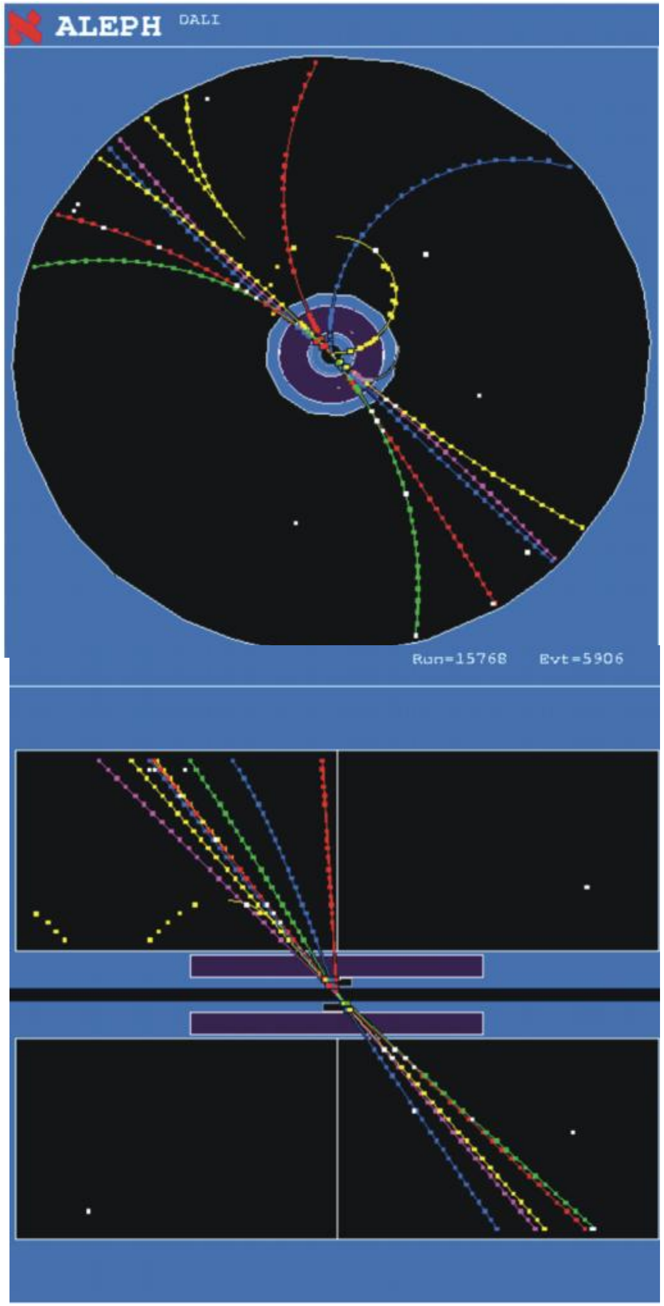

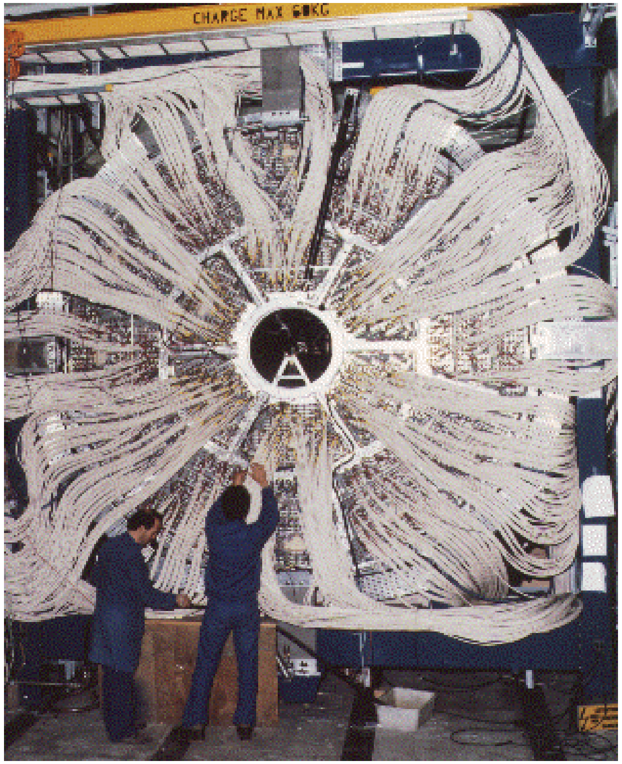

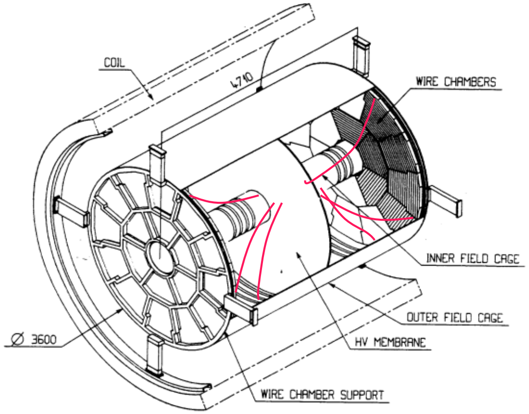

$\sigma_{R\phi} = 170\ \mu m$
$\sigma_z = 740\ \mu m$

very low multiple scattering in the gas volume of the detector
→ very good momentum resolution down to low momenta !

STAR TPC (BNL)

Event display of a Au-Au collision at CM energy of 130 GeV/n.

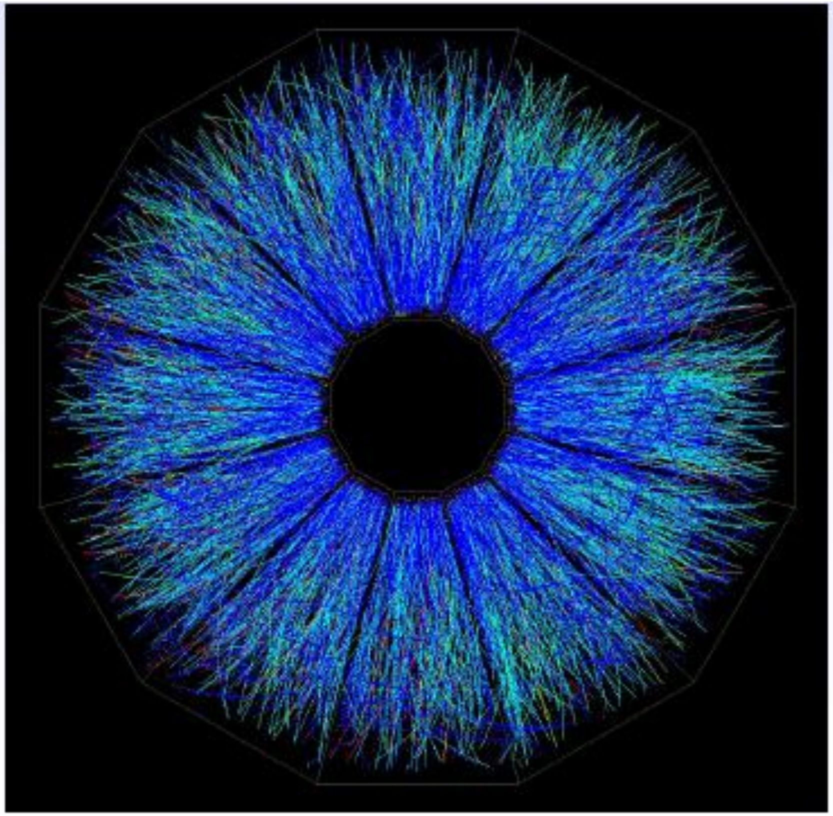

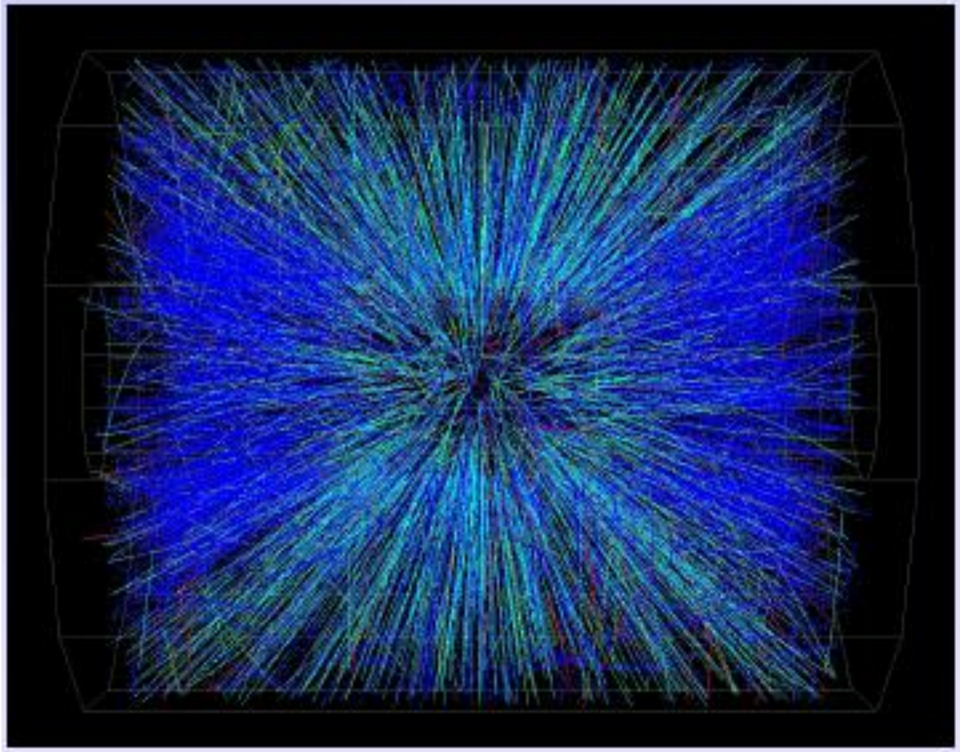

Micro Strip Gas Chamber

1988: Oed

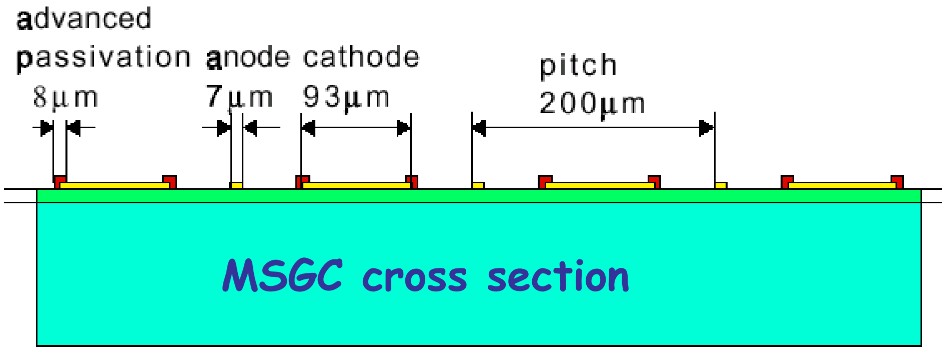

- advanced passivation: polyimide (2μm)
- metal: gold (0.6-0.8μm)
- undercoating: Pestov or S8900 glass (0.5-1μm)
- substrate: Desag glass (300 μm)

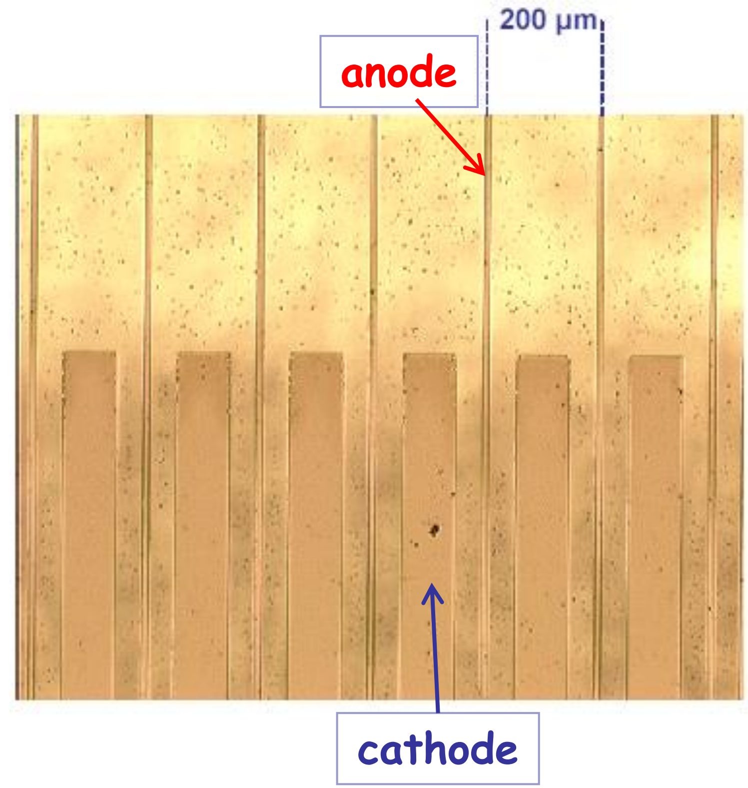

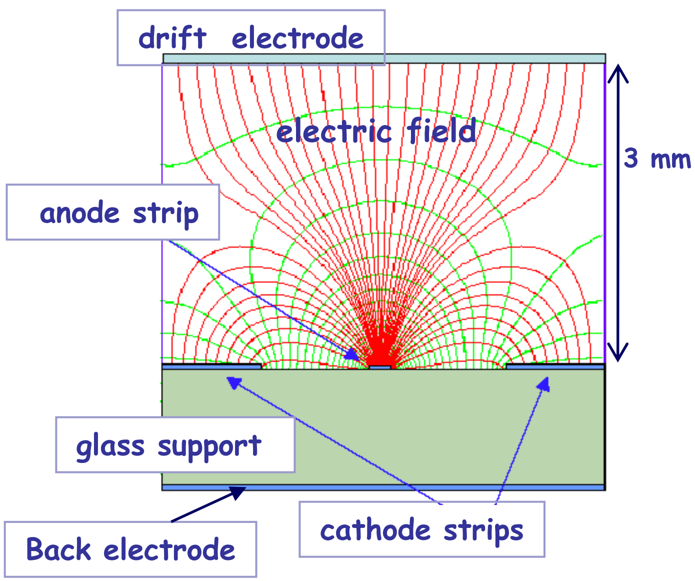

- Signals are much faster than in a MWPC: in 50 ns ~70% of the charge is collected !
- Resolution: ~40 μm

Gas Electron Multiplier (GEM)

Thin Kapton foil (50 mm) double side metal-coated (Cu 5 mm)
70 μm holes at 140 mm pitch

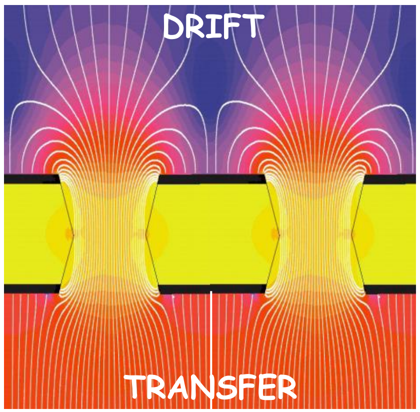

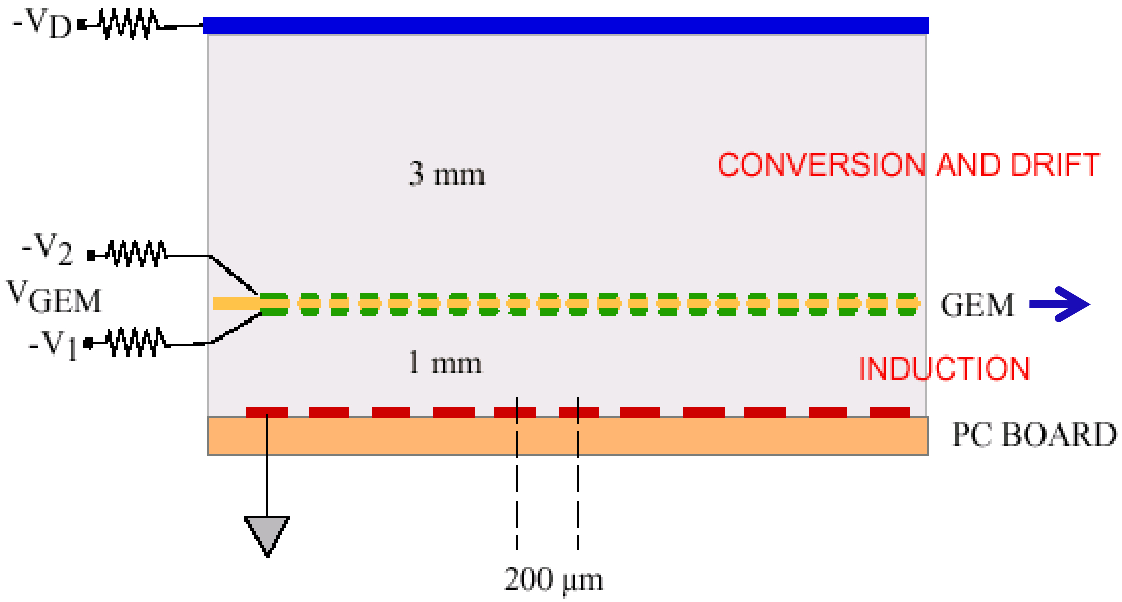

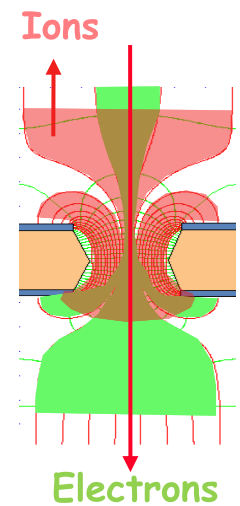

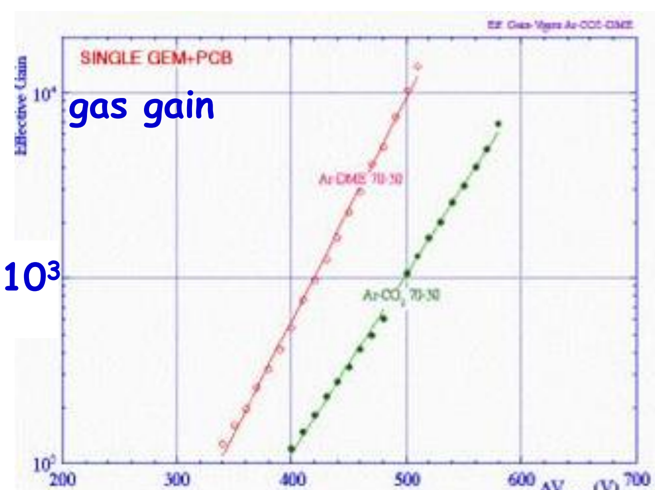

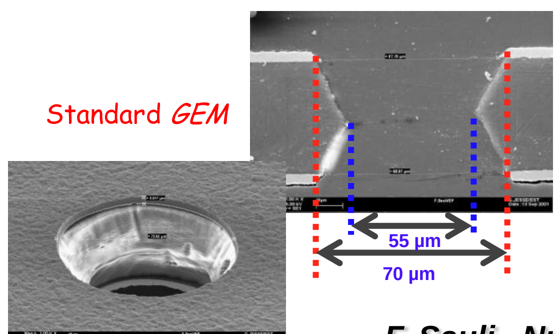

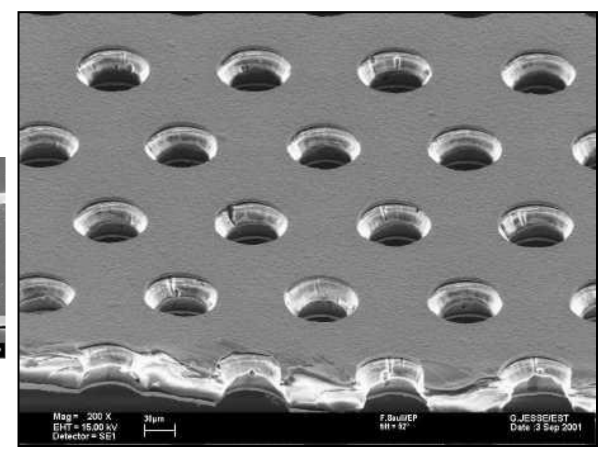

F. Sauli, Nucl. Instr. and Methods A386(1997)531

Gas Electron Multiplier (GEM)

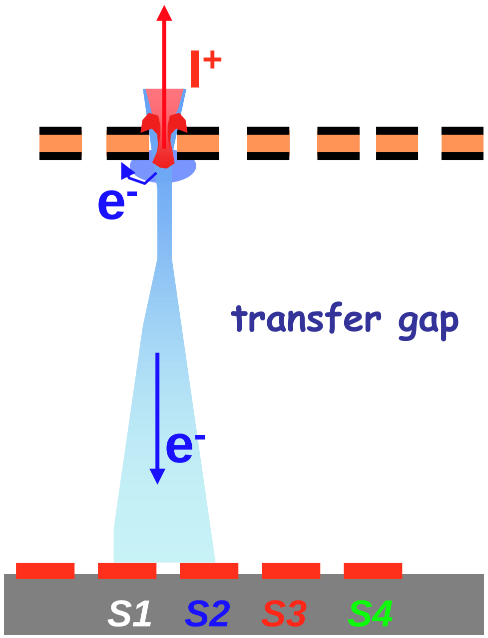

Only electrons are drifting in the transfer gap towards the readout electrodes:

⇒ no ion long tail

⇒ very fast signal

⇒ very good time resolution

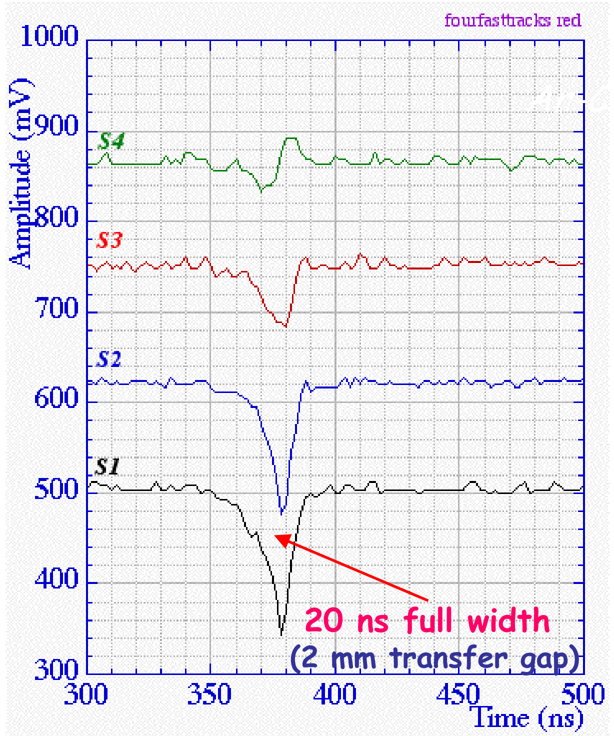

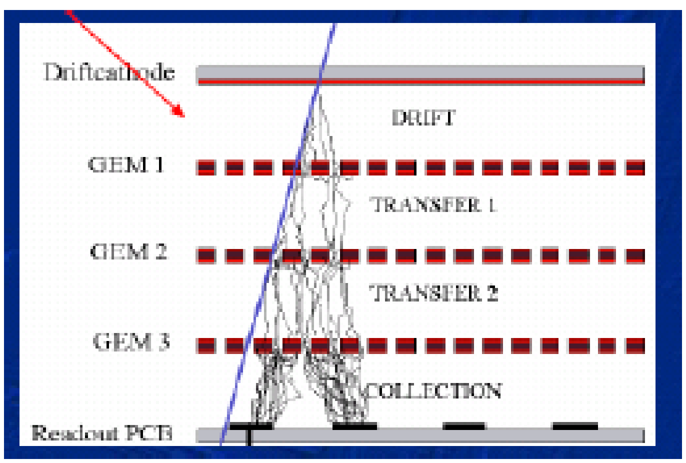

Triple GEM

Higher final gas gains can be obtained with a series of GEMs in cascade to reduce the gain/stage and therefore reducing the discharge probability

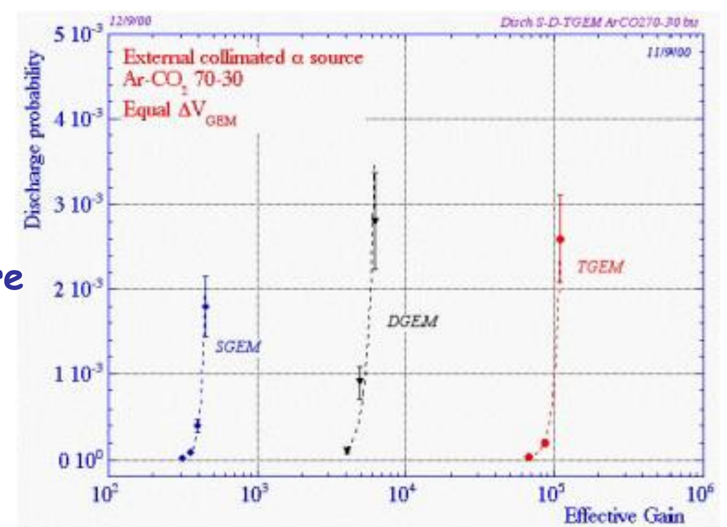

Other kinds of Micro Pattern Gas Detectors

Several different geometries of micro pattern gas detectors have proven to work efficiently at high rate: a couple of examples

MICROMEGAS

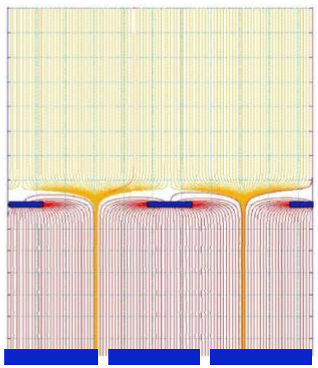

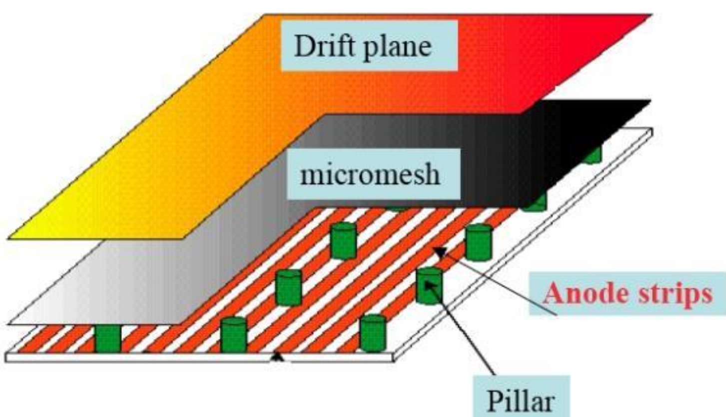

Y. Giomataris et al, Nucl. Instr. and Meth. A376(1996)239

MicroGap chamber (MGC)

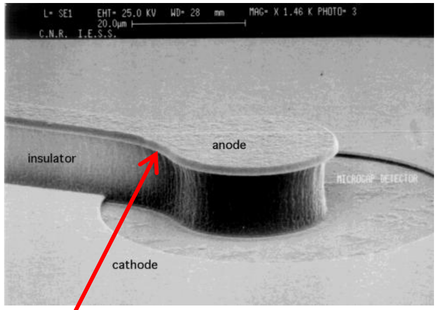

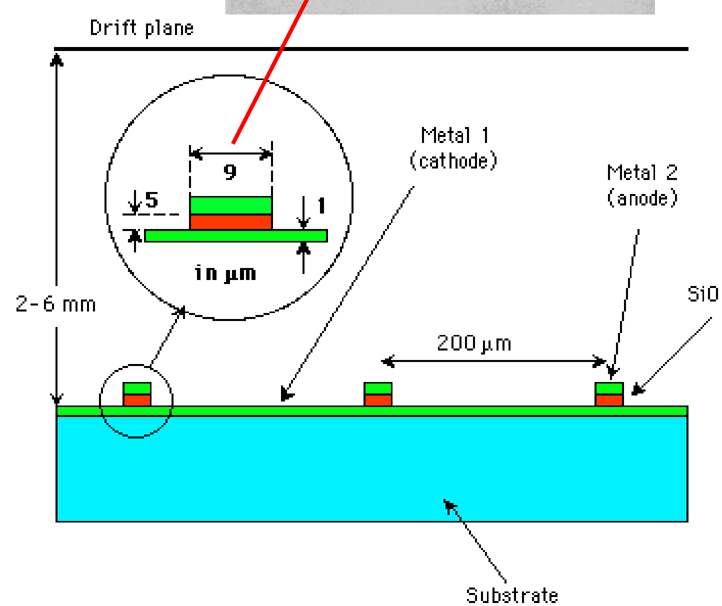

R. Bellazzini et al., Nucl. Instr. Meth. A335 (1993) 69

Solid State Detectors

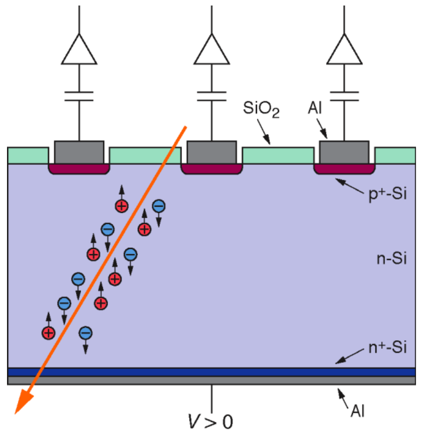

In solid state detectors the charges produced by the ionization due to the incoming particle are sufficient to provide a measurable signal.

- Solid state detectors have a high density
  ➔ large energy loss in a short distance:
  116 (78) keV = mean (most probable) energy loss
  for 300μm Silicon thickness
- Low ionisation energy (few eV per e-hole pair) compared to gas detectors (20-40 eV per e-ion pair)
  3.6 eV for silicon to create an e-hole pair
  $\Rightarrow$ 72 e-h/μm (most probable); 108 e-h/μm (mean)
  $\Rightarrow$ most probable charge 300μm Silicon thickness:
  $\approx$ 21600 e $\approx$ 3.5 fC
- Drift velocity much faster than in gas detectors:
  ➔ Very fast signals of only a few ns length !
- Diffusion effect is smaller than in gas detectors:
  ➔ achievable position resolution of less than 10 μm

Solid State Detectors

In an isolated atom of a gaseous detector the electrons have only discrete energy levels and when are liberated from the atoms by an ionizing particle they (and the ions) can freely move under an applied electric field. In solid state (crystal) material the atomic levels merge to energy bands. Inner shell electrons, in the lower energy bands, are closely bound to the individual atoms. However electrons in the conduction band and the holes in the lower valence band (bands that are still bound states of the crystal, but they belong to the entire crystal) can freely move around the crystal, if an electric field is applied.

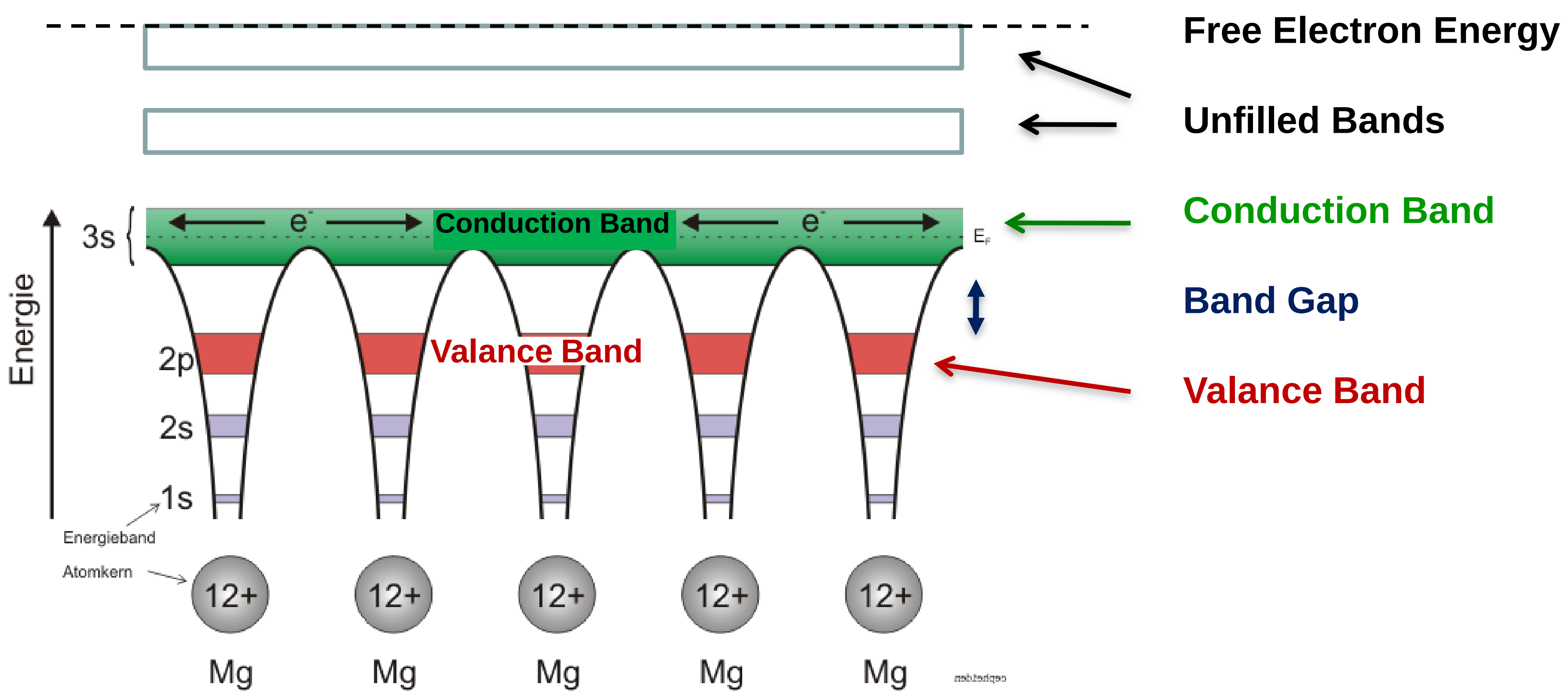

Solid State Detectors

Fermi distribution $f(E)$ describes the probability that an electronic state with energy E is occupied by an electron:

$$f(E) = \frac{1}{1 + e^{\frac{E - E_F}{kT}}}$$

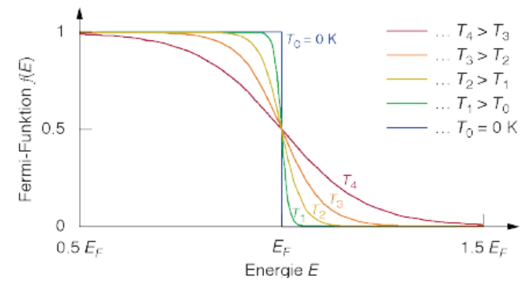

The Fermi level E_F is the energy at which the probability of occupation is 50%. For metals E_F is in the conduction band, for semiconductors and isolators E_F is in the band gap.
In metals the conduction and the valence band partially overlap, whereas in isolators and semiconductors these levels are separated by an energy gap. This energy gap E_g is called band gap. In isolators this gap is large.

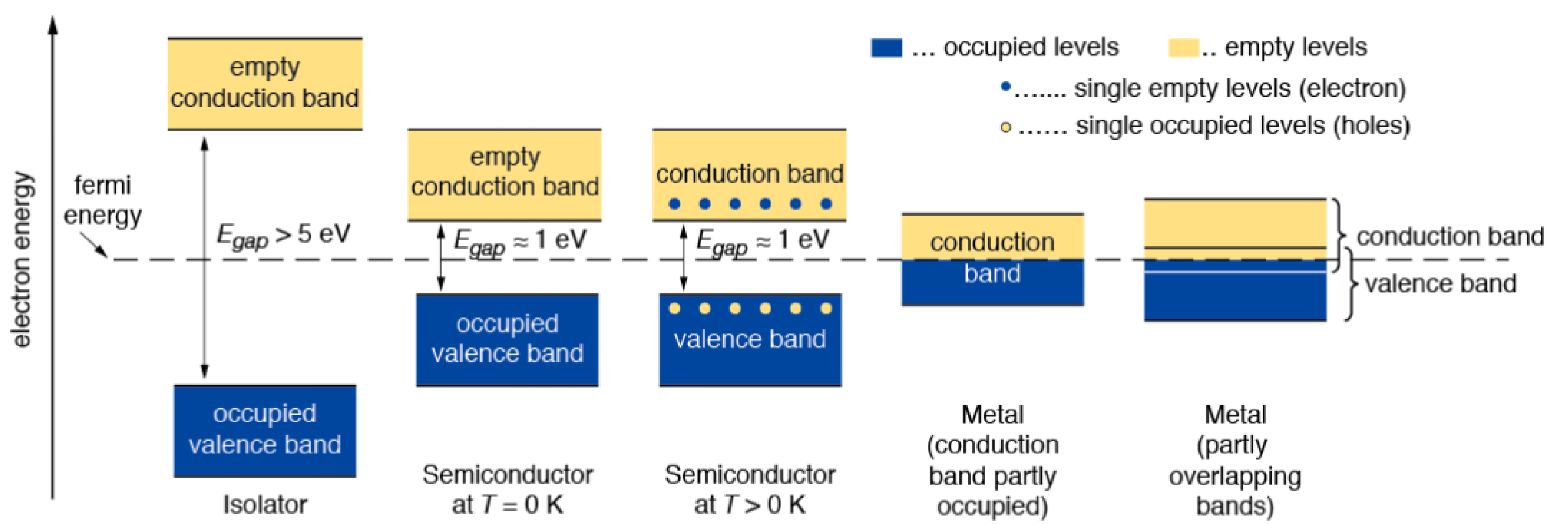

Solid State Detectors

- The energy gap E_g (band gap) of Diamond/Silicon/Germanium is 5.5,1.12,0.66 eV
- Due to the small band gap, electrons already occupy the conduction band gap in many semiconductors at room temperature.
- Electrons from the conduction band may recombine with holes
- The thermal excitation excites electrons into the conduction band leaving a hole in the valence band. Thermal equilibrium is reached at intrinsic carrier concentration:

$$n_i = n_e = n_h \propto T^{\frac{3}{2}} \cdot \exp\left(-\frac{E_g}{2kT}\right)$$

- Therefore the number of electrons in the conduction band, and thus also the conductivity of the semiconductor, increases with temperature.

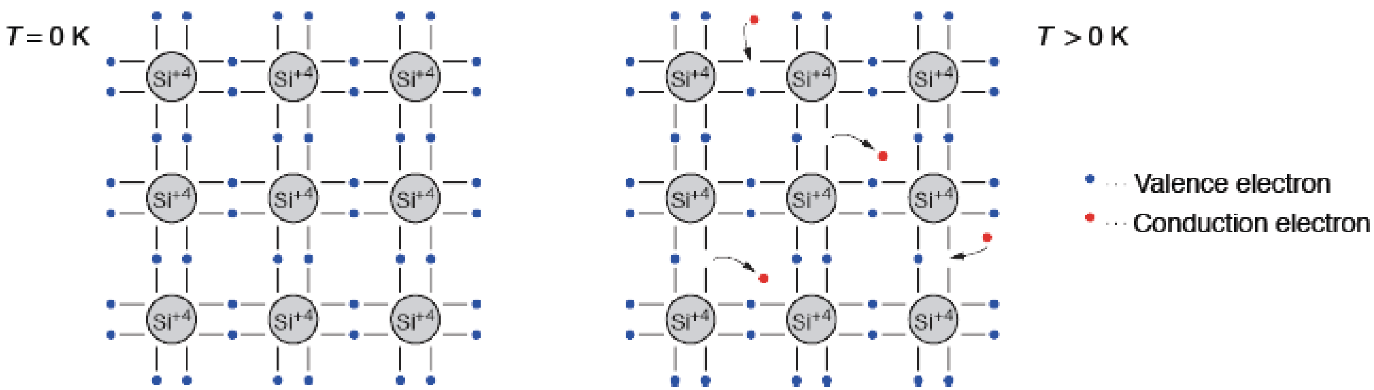

In silicon at room temperature the intrinsic carrier concentration is $1.45\cdot10^{10}$ cm^{-3}. With approximately 10^{22} Atoms/cm^3 about 1 in 10^{12} silicon atoms is ionised. This yields an intrinsic resistivity of: $\rho \approx 230$ kΩcm

Solid State Detectors

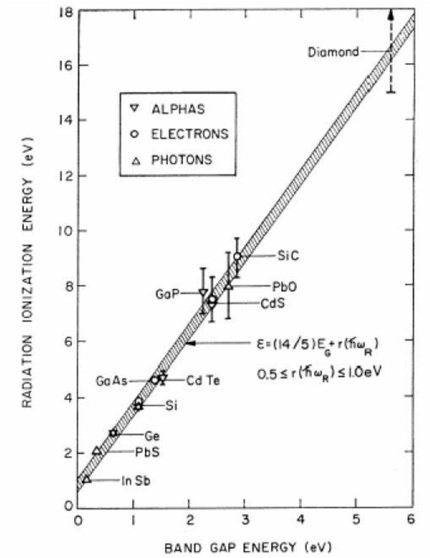

	Diamond /	Silicon /	Germanium
Band gap E_g [eV]	5.5	1.12	0.66
Energy $E_{e/h}$ for e-h pair [eV]	13	3.6	2.9
Density [g/cm^3]	3.51	2.33	5.32
e-mobility μ_e [cm^2/Vs]	1800	1450	3900
h-mobility μ_h [cm^2/Vs]	1200	450	1900
Intrinsic charge carrier:			
n_i [cm^{-3}] (T=300 K)	$\approx 10^{-27}$	$1.45\cdot 10^{10}$	$2.4\cdot 10^{13}$

In Diamond detectors there are very few charge carriers at room temperature (n_i[cm^{-3}] $\approx 10^{-27}$) due to large band gap while many e-h pairs are produced by an ionizing particle

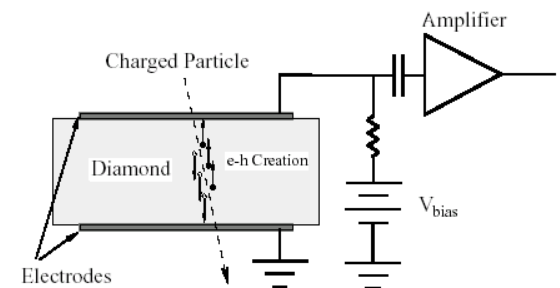

In a 300μm Silicon detector the number (mean) of e-h pairs produced by the passage of a charged particle at the minimum ionizing is given by:

$$n_{e/h} = dE/dx \cdot d \,/\, E_{e/h} = 3.87\cdot 10^{6} \text{eV/cm} \cdot 0.03\text{cm}/3.6\text{eV} \approx 3.2 \cdot 10^{4} \text{ e-h pairs}$$

In the same detector of an area A=1cm^2 the intrinsic charge carrier (T=300 K) is:

$$n_i \cdot d \cdot A = 1.45\cdot 10^{10}\text{cm}^{-3}\cdot 0.03\text{cm}\cdot 1\text{cm}^2 \approx 4.35 \cdot 10^{8} \text{ e-h pairs}$$

In silicon the thermal e-h pairs are four orders of magnitude larger than signal !!!

➔ remove the charge carrier !

n-Doping in Silicon

Doping with an element +5 atom with one valence electron more than silicon (e.g. P,As).
The 5th valence electrons is weakly bound. The doping atom is called donor.
The n-doped silicon becomes a n-type conductor (more electrons than holes)

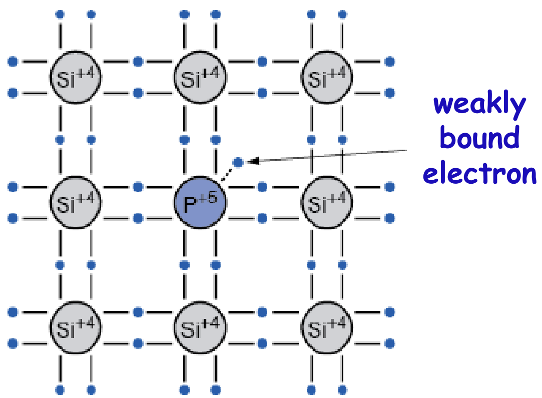

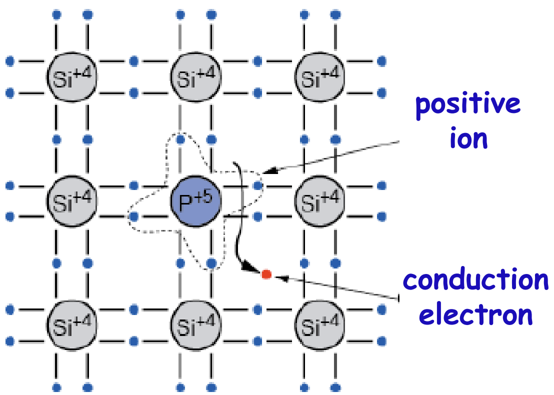

Typical doping concentrations for Si detectors are $\approx 10^{12}$ atoms/cm^3

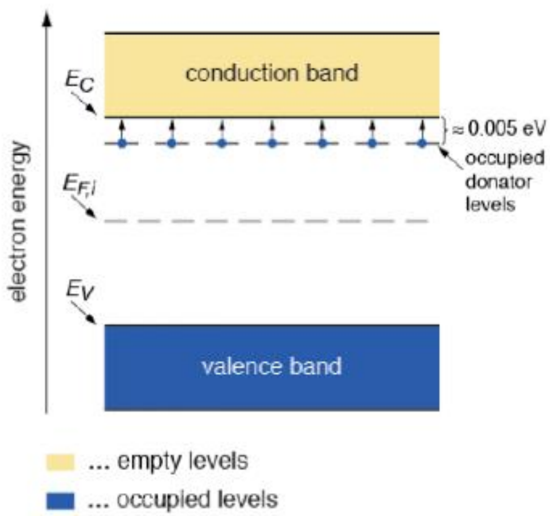

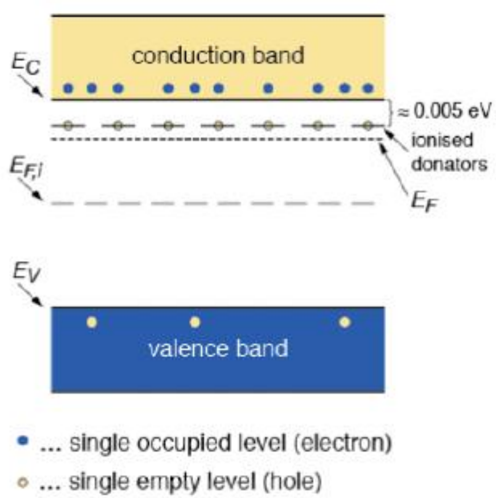

The energy level of the donor is just below the edge of the conduction band.
At room temperature most electrons are raised to the conduction band.
The Fermi level E_F moves up.

p-Doping in Silicon

Doping with an element +3 atom with one valence electron less than silicon (e.g. B,Ga).
One valence bond remains open and attracts electrons from the neighbor atoms.
The doping atom is called acceptor.
The p-doped silicon becomes a p-type conductor (more holes than electrons)

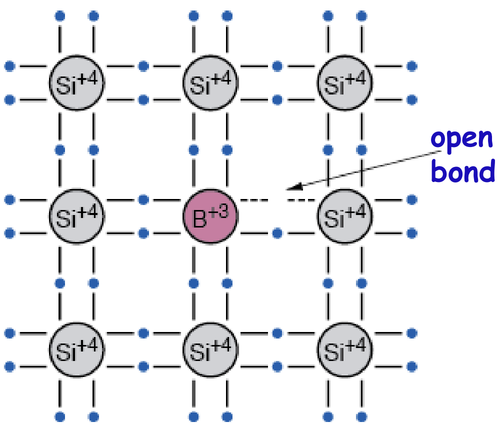

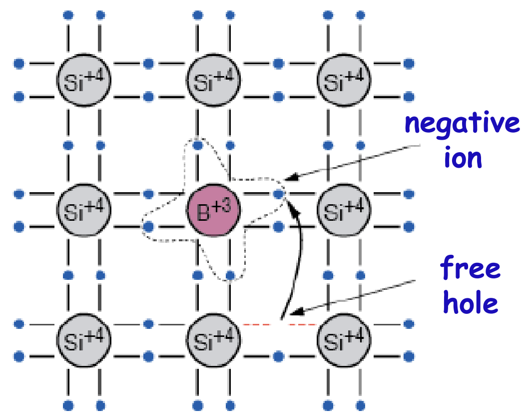

Typical doping concentrations for Si detectors are $\approx 10^{12}$ atoms/cm^3

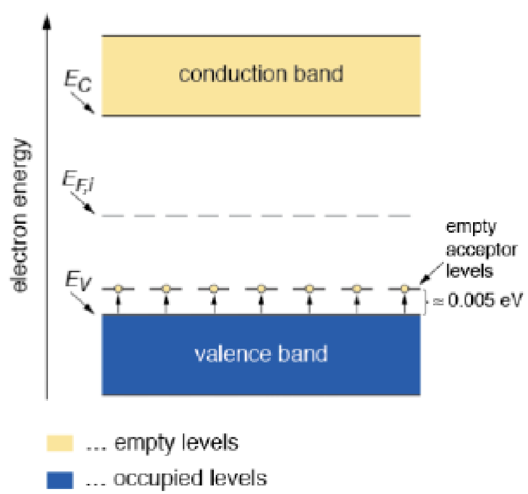

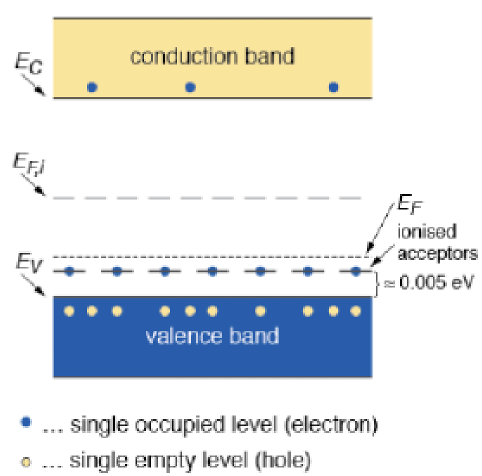

The energy level of the acceptor is just above the edge of the valence band.
At room temperature most levels are occupied by electrons leaving holes in the valence band.
The Fermi level E_F moves down.

Si-Diode as Si-Detector

At the p-n junction the difference in the fermi levels cause diffusion of charge carriers until thermal equilibrium is reached and the electric field thus created stops further diffusion. At this point the fermi level is equal.
A zone free of charge carriers, called depletion region, is thus established .

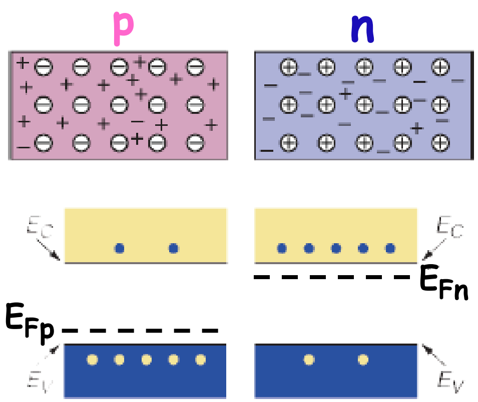

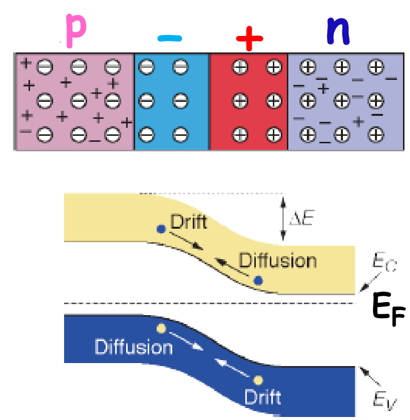

+ hole
− electron
⊖ acceptor
⊕ donator

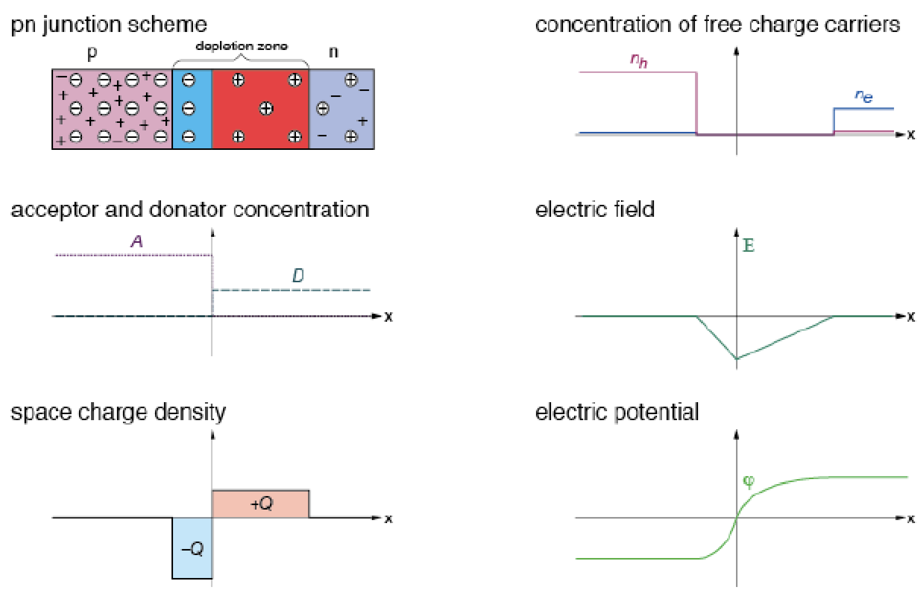

Si-Diode as Si-Detector

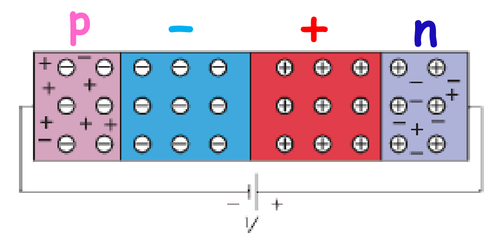

By applying an external voltage V, the depletion zone can be extended to the entire diode.

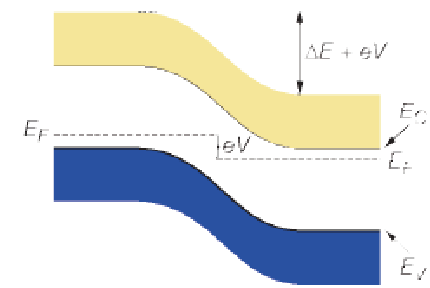

An incoming particle can then produce by ionization free charge carriers in the diode.
The charges carriers drift in the electric field and induce an electrical signal on the electrodes.

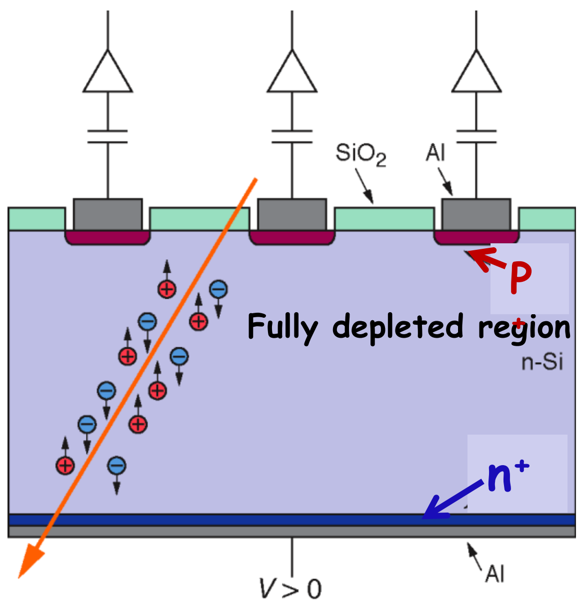

➔ That is the way a Silicon detector can work !

Detector Structures

DC coupled strip detector

AC coupled strip detector

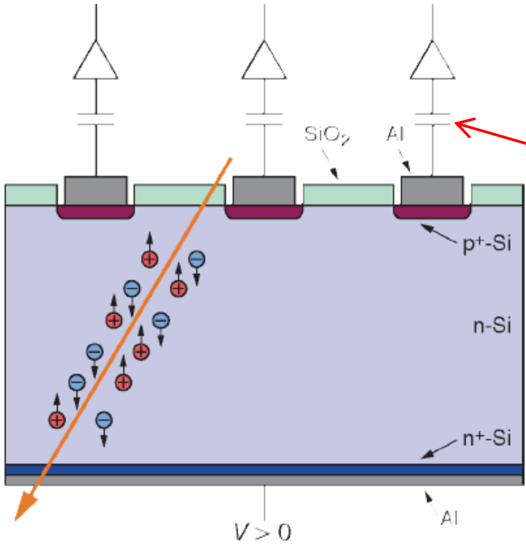

coupling capacitors

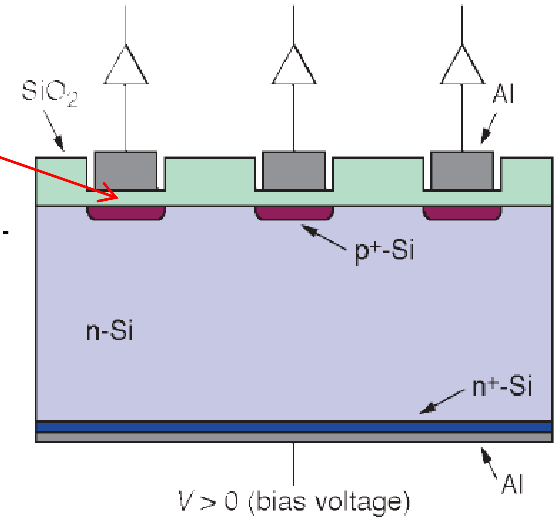

A typical n-type Si strip detector:

- ✓ about 30.000 e-h+ pairs in 300 µm detector thickness
- ✓ p+n junction: $N_a \approx 10^{15}$ cm^{-3}, $N_d \approx 1\text{–}5 \cdot 10^{12}$ cm^{-3}
- ✓ n-type bulk: ρ > 2 kΩcm
- ✓ operating voltage < 200 V.
- ✓ n+ layer on backplane to improve ohmic contact
- ✓ Aluminum metallization

Using p-type silicon and exchanging p+ and n+ would give a perfectly working p-type detector.

- ➢ Deposition of SiO2 with a thickness of 100–200 nm between p+ and aluminum strip
- ➢ AC coupling blocks leakage current from the amplifier.
- ➢ Problems are shorts through the dielectric (pinholes). Usually avoided by a second layer of Si3N4.
- ➢ Need to isolate strips from each other to collect charge from each strip:
  several methods for high impedence bias voltage connection (≈ 1MΩ resistor): polysilicon resistor, punch through bias, FOXFET bias.

Detector Structures

Top view of a strip detector with polysilicon resistors:

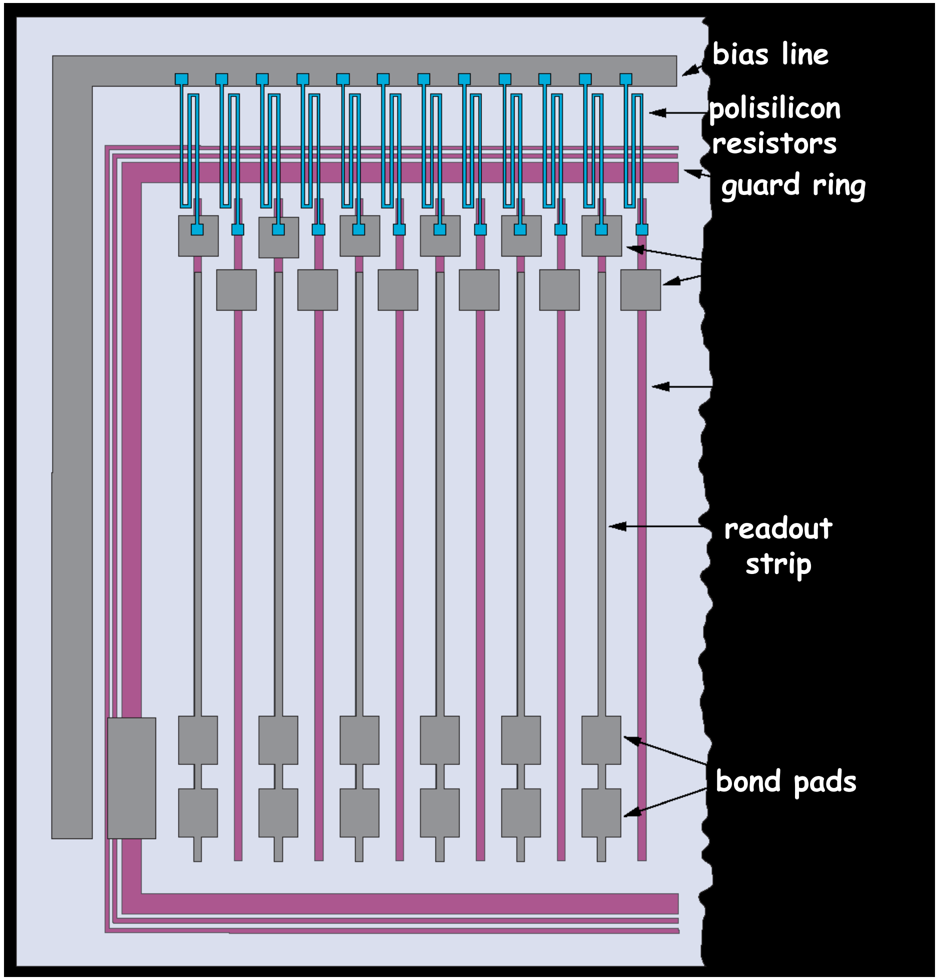

CMS-Microstrip-Detector: Close view of area with polysilicon resistors, probe pads, strip ends.

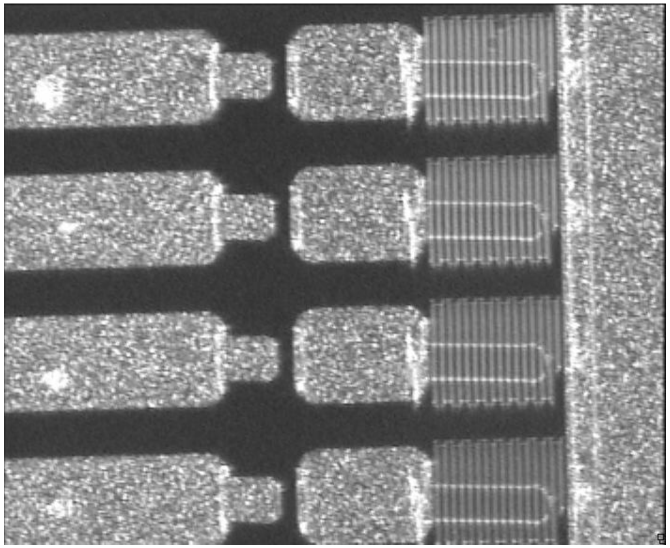

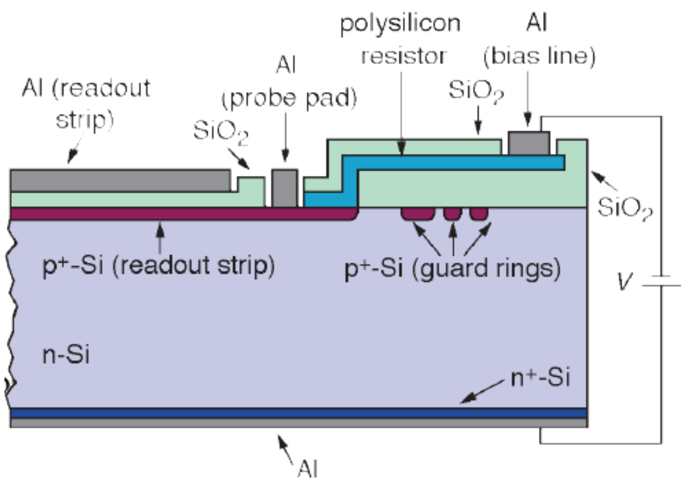

Biasing and AC coupling

Bias resistor and AC Coupling

extra slide not shown

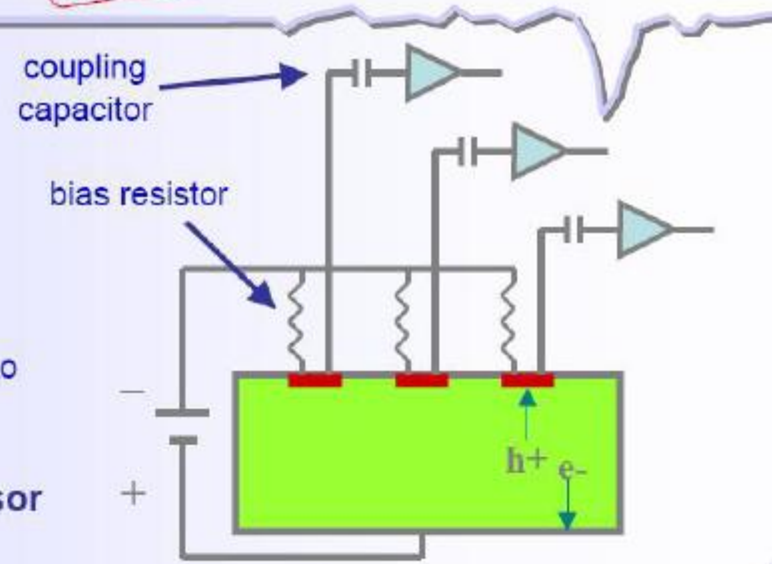

Bias resistor

- Need to isolate strips from each other to collect/measure charge on each strip
  - ⇒ high impedance bias connection (≈ 1MΩ resistor)

Coupling capacitor

- Couple input amplifier through a capacitor (AC coupling) to avoid large DC input from leakage current

Integration of capacitors and resistors on sensor

- Bias resistors via deposition of doped polysilicon
- Capacitors via metal readout lines over the implants but separated by an insulating dielectric layer (SiO_2, Si_3N_4).

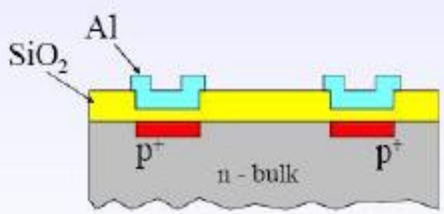

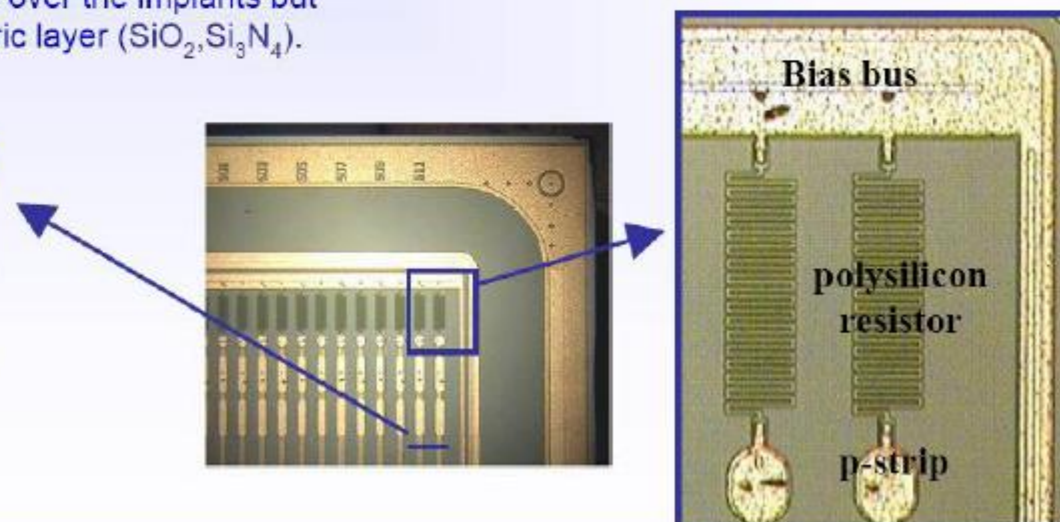

⇒ nice integration

⇒ more masks, processing steps

⇒ pin holes

CERN Academic Training Programme 2004/2005

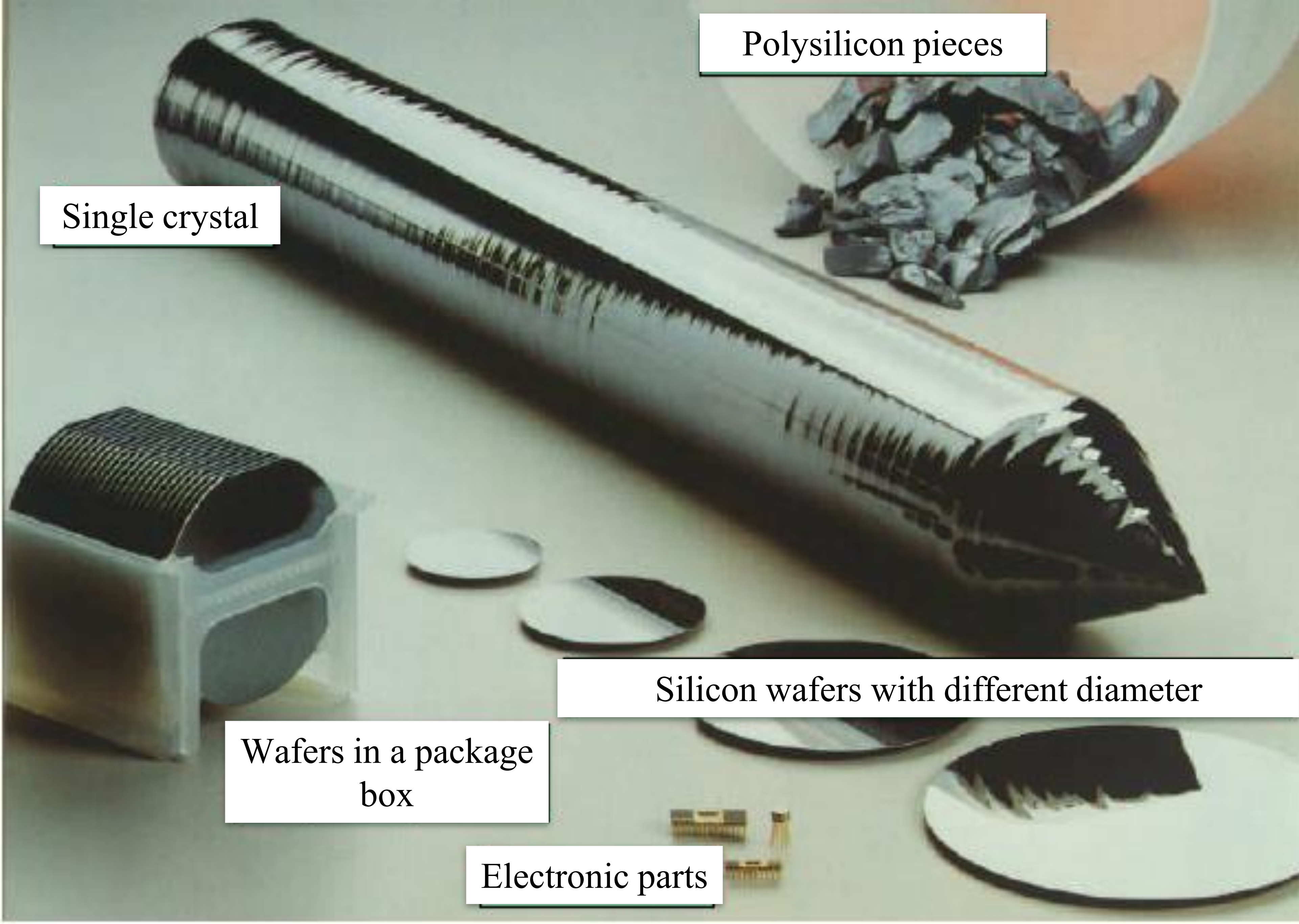
Polysilicon pieces
Single crystal
Silicon wafers with different diameter
Wafers in a package box
Electronic parts

A CMS silicon strip detector built with a 6” wafer

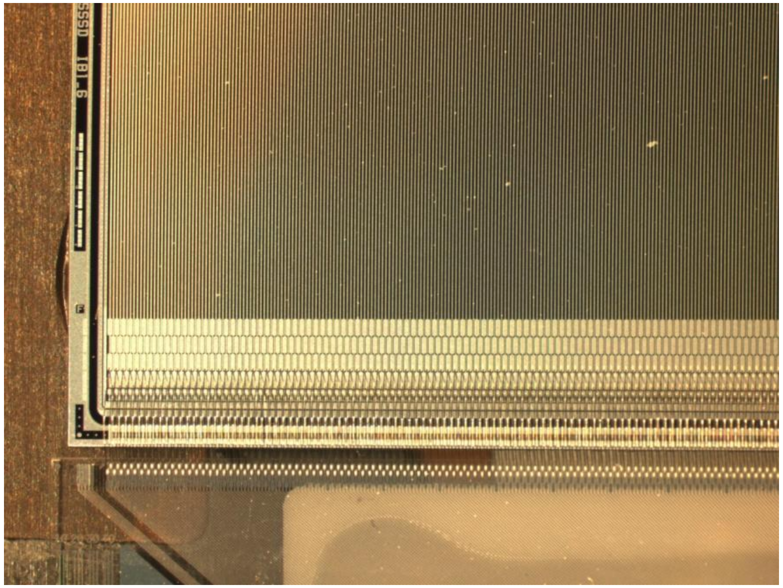

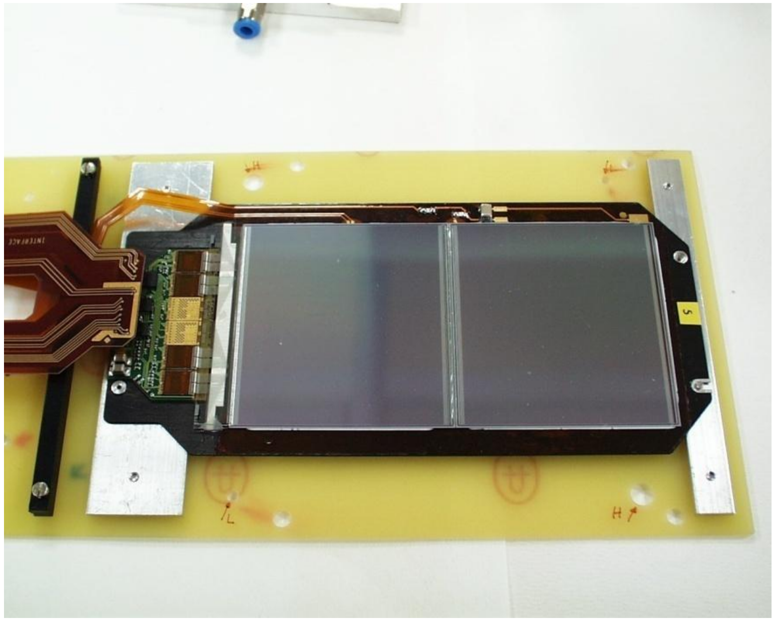

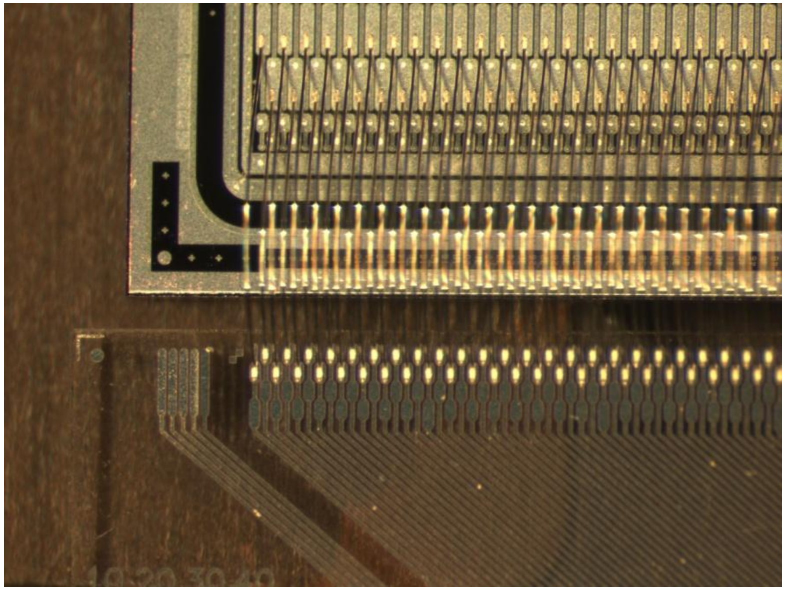

Double Sided Strip Detectors

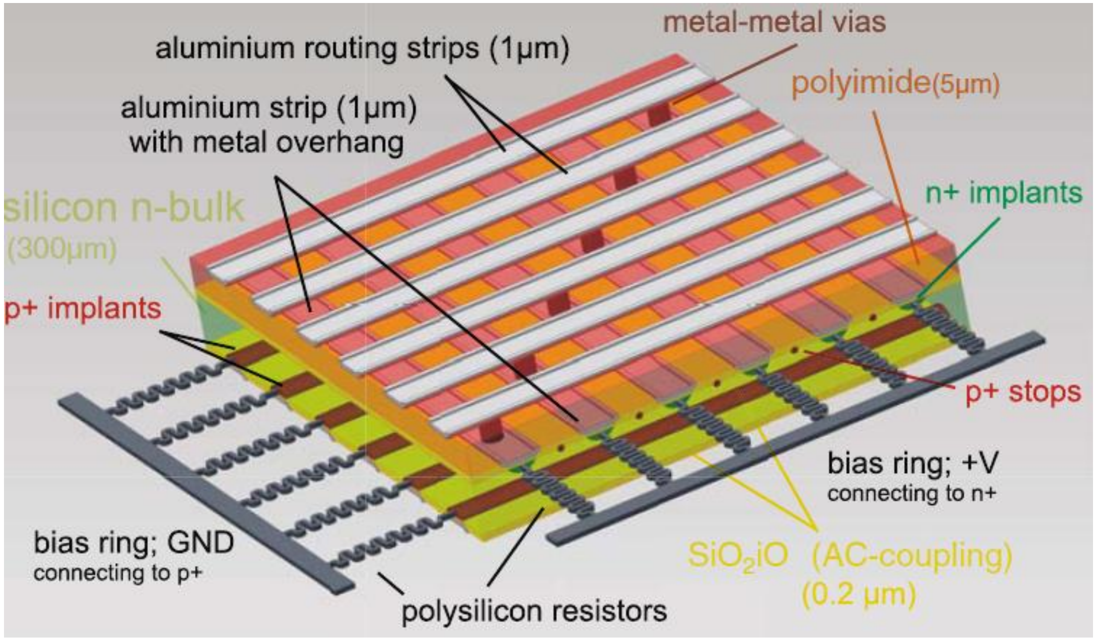

- Single sided strip detector measures only one coordinate. To measure second coordinate requires second detector layer.
- Double sided strip detector minimizes material measuring two coordinates in one detector layer.
- In n-type detector the n+ backside becomes segmented e.g. strips orthogonal to p+ strips.
- Drawback: Production, handling, tests are more complicated and hence double sided detector are expensive.

Double Sided Strip Detectors

Problem with n+ segmentation:

Static, positive oxide charges in the Si-SiO2 interface.

➔ These positive charges attract electrons. The electrons form an accumulation layer underneath the oxide.

➔ n+ strips are no longer isolated from each other (resistance ≈ kΩ).

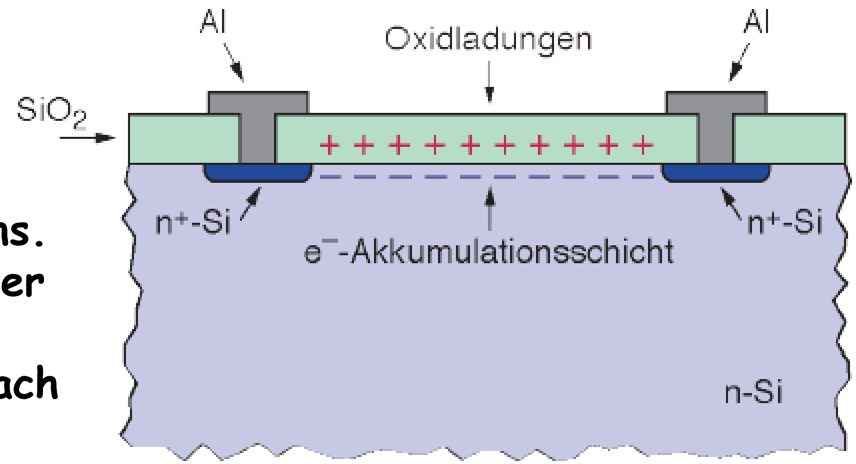

Solution: interrupt accumulation layer using

p⁺-stops or **field plates**

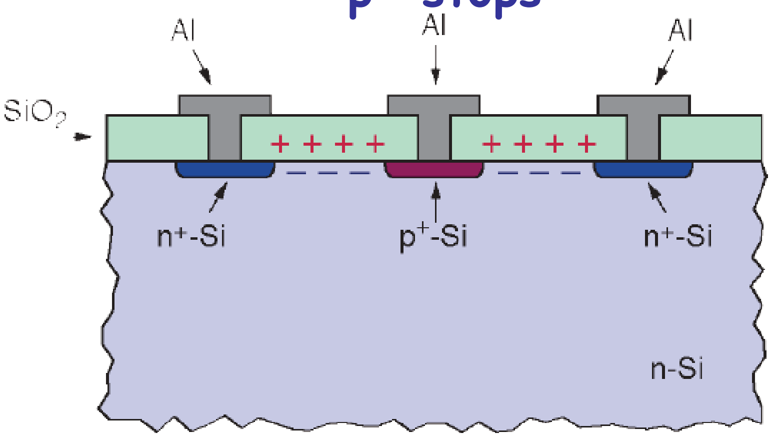

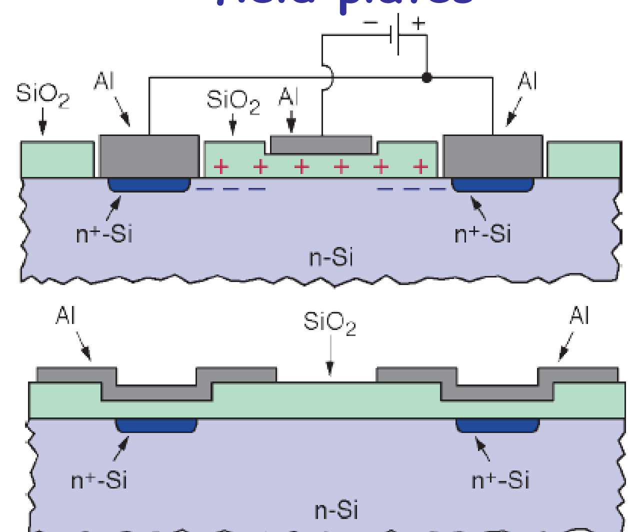

Interstrip resistance reach again GΩ.

The aluminum readout lines act as field plates

Double Sided Strip Detectors

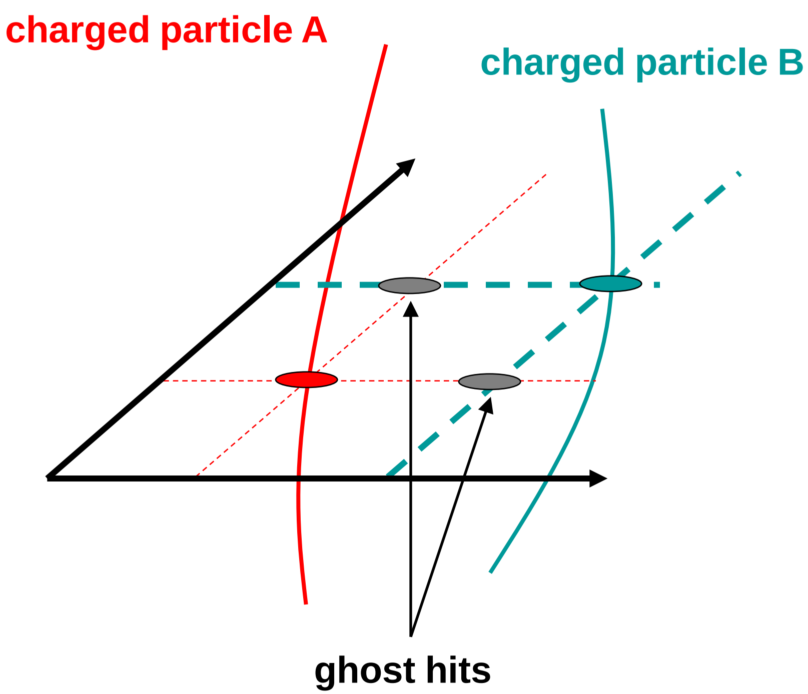

Double sided strip sensors measure the 2 dimensional position of a particle track. However, if more than one particle hits the strip detector the measured position is no longer unambiguous. “Ghost”-hits appear!

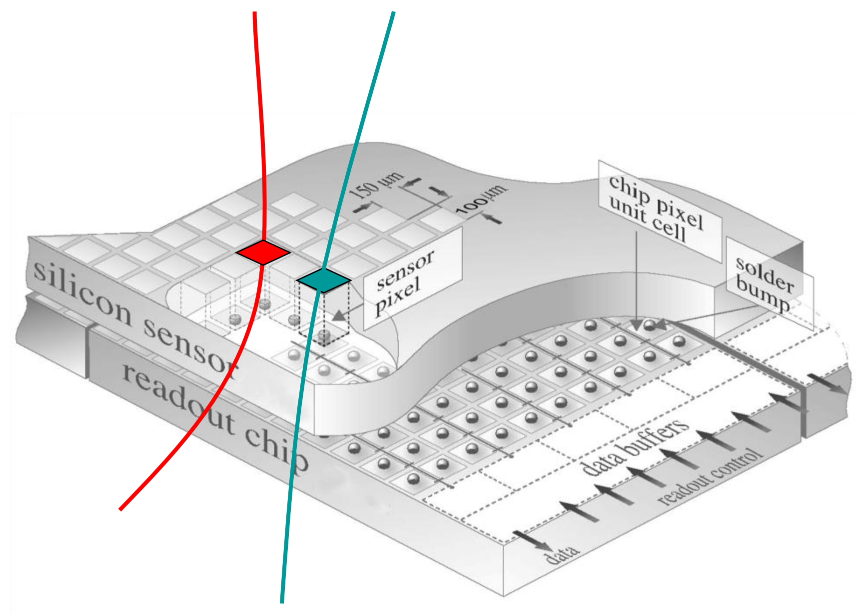

Pixel detectors produce 2-dimensional position measurements without ambiguity also in case of two particles crossing the detector!

Pixel Detectors

- ❑ Typical pixel size 50 x 200 μm^2; 100 x 100 μm^2:
  - ➢ Small pixel area ➔ low detector capacitance (≈1 fF/Pixel) ➔ large signal-to-noise ratio (e.g. 150:1).
  - ➢ Small pixel volume ➔ low leakage current (≈1 pA/Pixel)
- ❑ Large number of readout channels:
  - ➢ Large number of electrical connections
  - ➢ Large power consumption of electronics

Problem:

Coupling of readout electronics to the detector

Solution:

Bump bonding

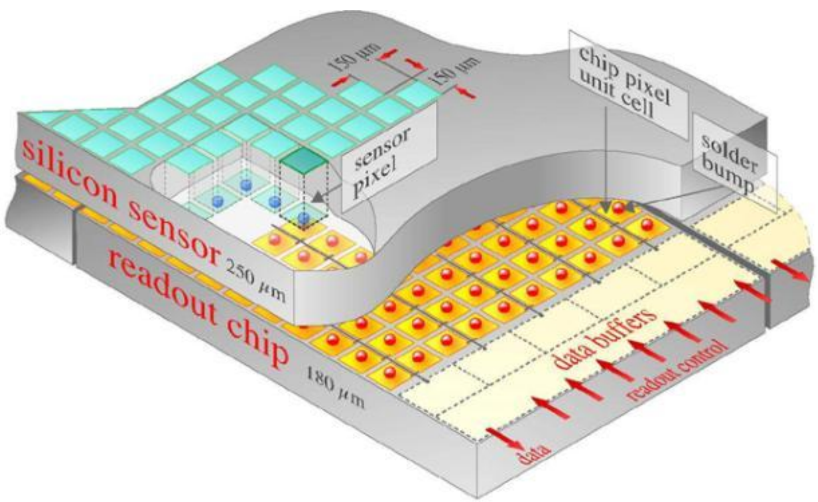

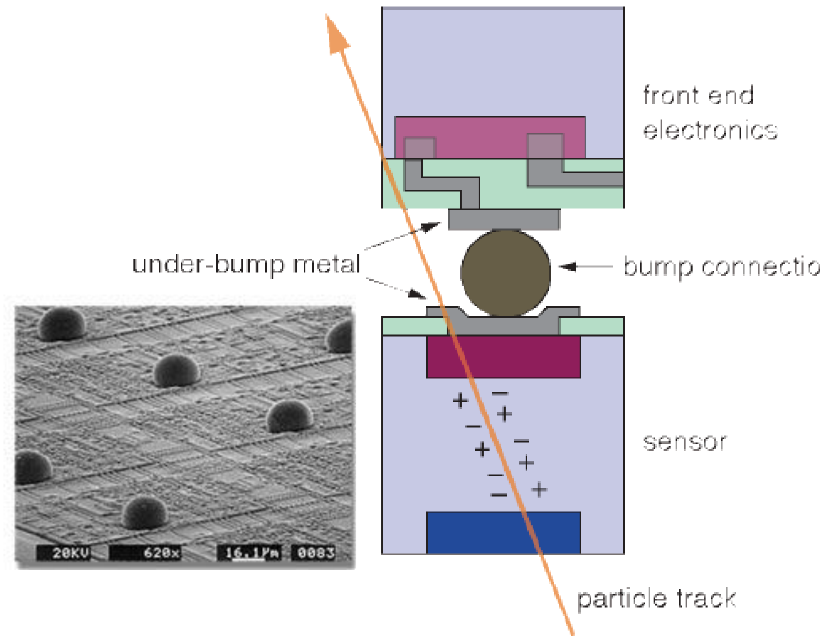

Pixel Detector Module Breakdown

PP0 connection

Flex Hybrid

Bump bonds

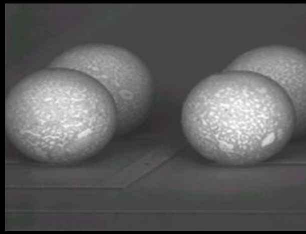

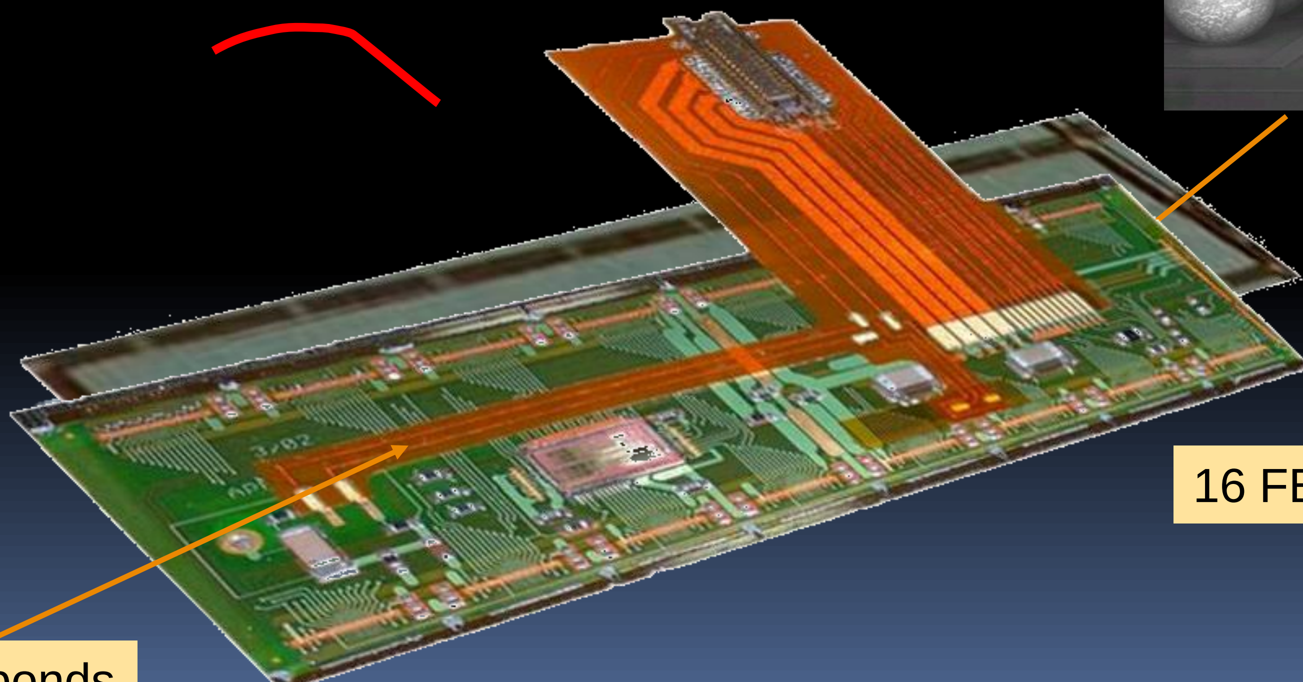

Sensor tile

16 FE chips

Wire bonds

Silicon Drift Detector (like gas TPC !)

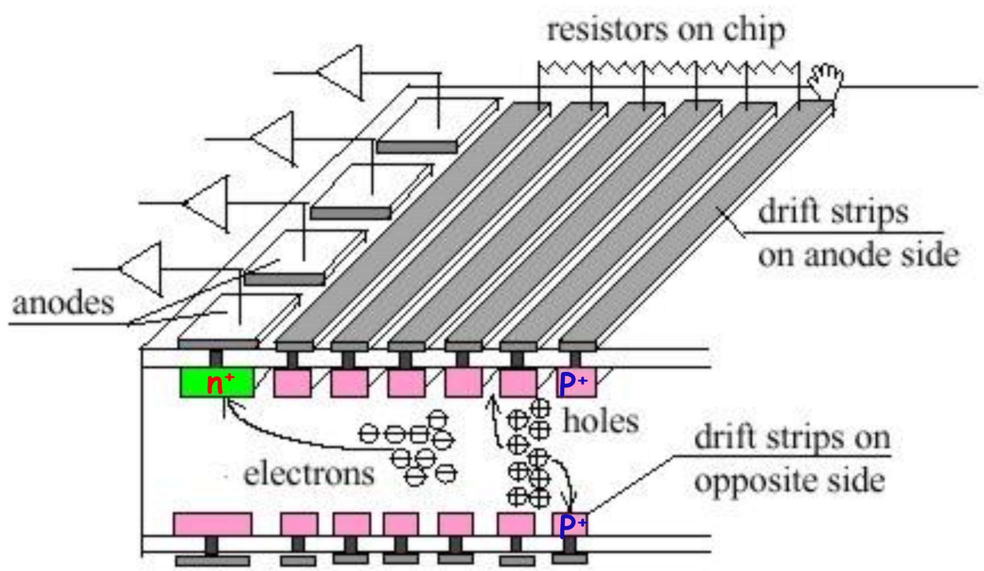

In silicon drift detectors the p+ strips and the backplane p+ implantation are used to fully deplete the bulk.

A drift field transports the generated electrodes to the readout electrodes (n+).

One coordinate is measured by signals on strips, the second by the drift time.

Radiation environment at the LHC

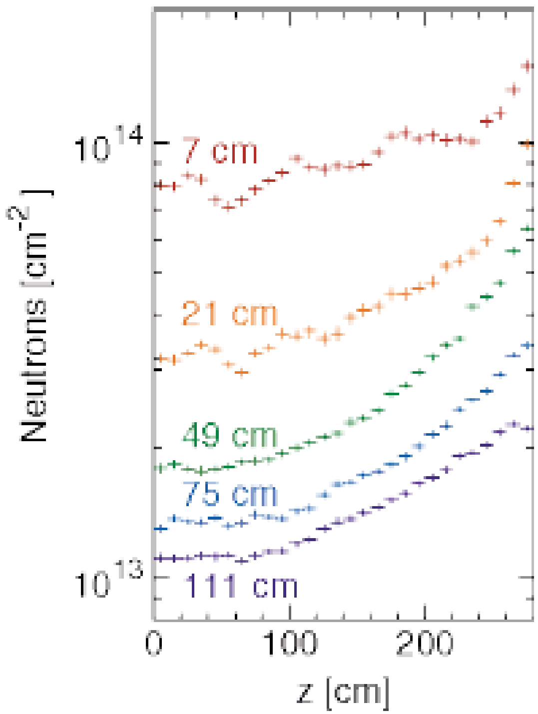

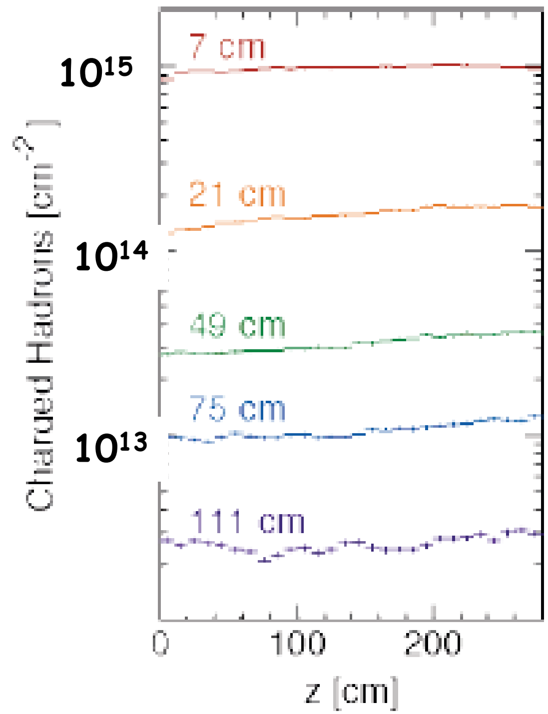

Expected particle fluences for the silicon detector inner layers in CMS integrated over 10 years as a function of the distance from the vertex point and for various radii.

Left: neutrons

Right: charged hadrons

Radiation damage

Particles (radiation) interact with atoms of the detector material and may cause permanent changes (defects) in the detector bulk.

- **One distinguishes two types of radiation damage:**
  - damage inside the detector bulk (bulk damage): dislocated atoms from their position in the lattice caused by massive particles.
    - ➔ Bulk damage is primarily produced by neutrons, protons and pions.
  - damage introduced in the surface layers (surface damage) is due to the charges generated in the amorphous oxide
    - ➔ Surface damage is primarily produced by photons and charged particles.
- **Defects may change with time:**
  - one distinguishes between primary defects and secondary defects
  - the secondary defects appear with time caused by moving primary defects
- **Comulative effects:**
  - increased leakage current
  - silicon bulk type inversion (n-type to p-type)
  - increased depletion voltage
  - increased capacitance
- **Sensor can stop working :**
  - noise too high
  - depletion voltage too high
  - loss of inter-strip isolation

Typical limits of Si Detectors are at 10^{14}-10^{15} Hadrons/cm^2

Radiation damage

- Defects in the semiconductor lattice create energy levels in the band gap between valence and conduction band. Depending on the position of these energy levels the following effects will occur:
  - Modification of the effective doping concentration
    ➔ shift of the value of the depletion voltage.
  - Trapping of charge carriers
    ➔ reduced lifetime of charge carriers
  - Easier thermal excitement of e- and h+
    ➔ increase of the leakage current

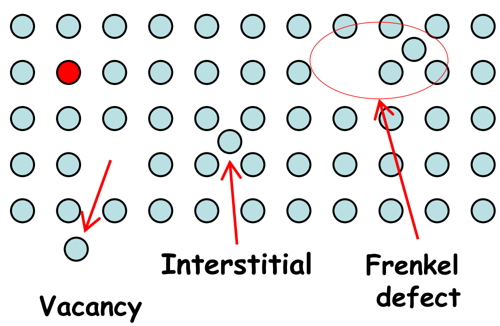

A displaced silicon atom produces an empty space n the lattice (Vacancy) and in another place an atom in an inter lattice space (Interstitial, I). A vacancy-interstitial pair is called a Frenkel-defect.

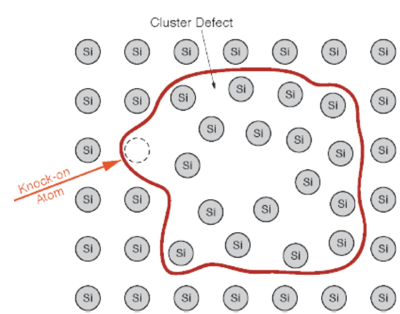

In hard impacts the primary knock-on atom displaces additional atoms. These defects are called cluster defects. The size of a cluster defect is approximately 5 nm and consists of about 100 dislocated atoms.

Radiation damage

Increase of leakage current as function of irradiation fluence (different materials)

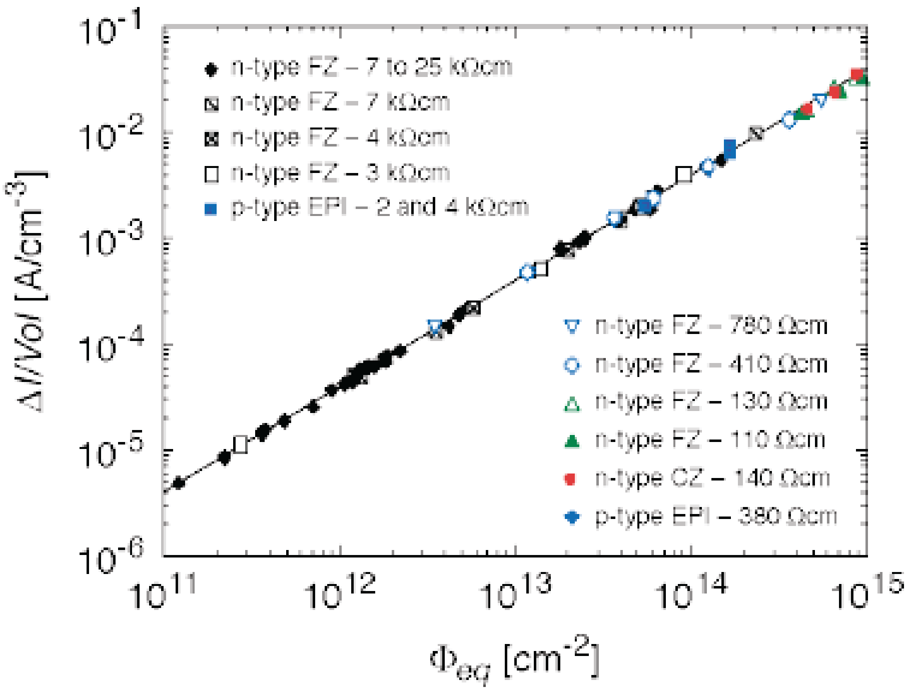

M. Moll, *Radiation Damage in Silicon Particle Detectors*, PhD-Thesis (1999)

In ten years of LHC operation the currents of the innermost layers increase by 3 orders of magnitude!

- $\Delta I = \alpha \Phi_{eq} V$

α damage constant $\cong 3\text{x}10^{-17}$ A/cm

Radiation damage

Full depletion voltage and effective doping concentration of an originally n type silicon detector as a function of the fluence Φeq:

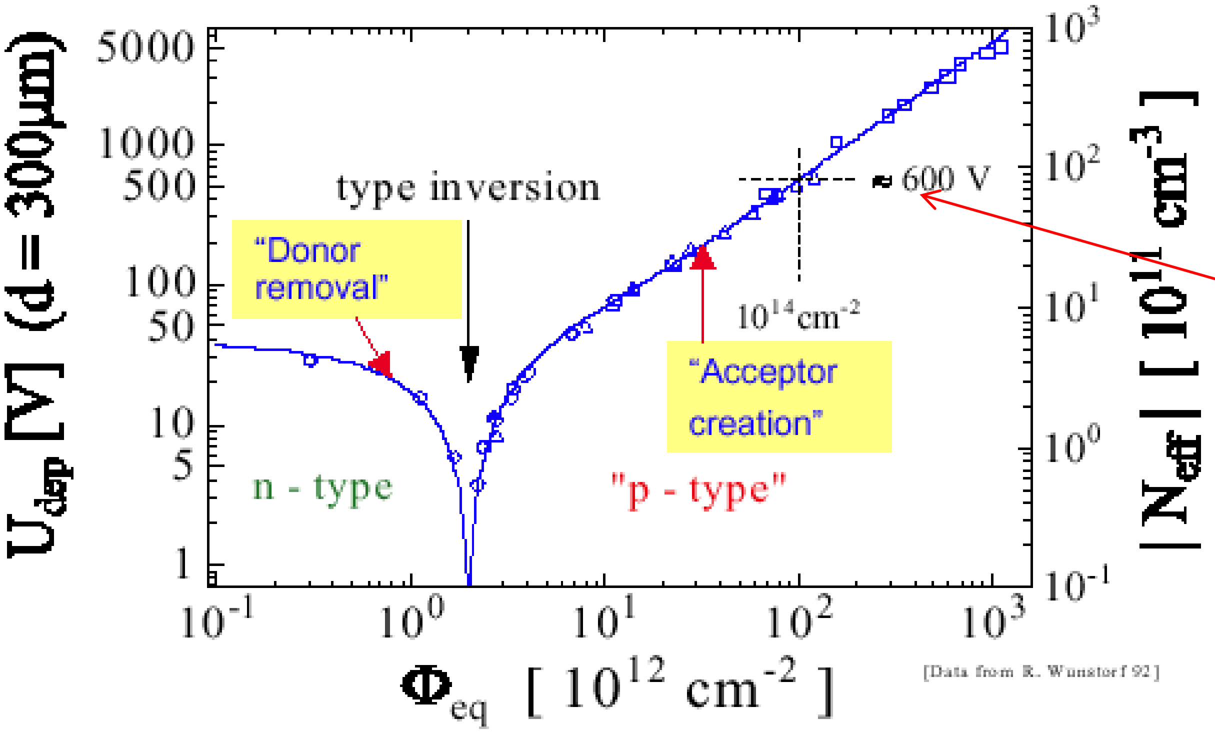

voltage may becomes too high to fully deplete:

Type inversion ! an n-tyle Si detector becomes a p-type Si detector !

Radiation damage

In n type sensors with p+ implants the depletion zone grows from the p+ implants to the backplane n+ implant.
After type inversion the p+ bulk is now depleted from the backside (polarity of bias voltage remains the same)

Unirradiated detector:

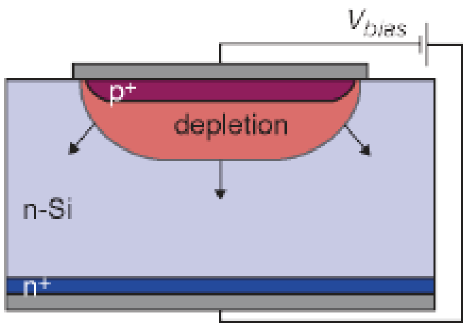

Detector after type inversion:

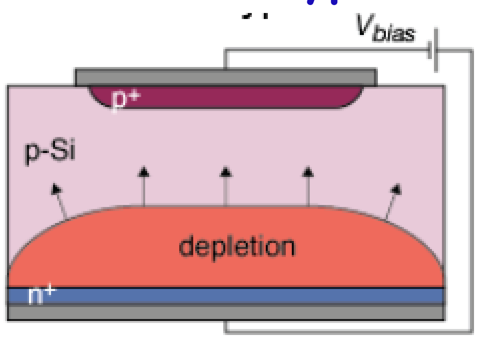

n-type detectors before type inversion can be operated below full depletion

after type inversion, the depletion zone has to reach the strips.

(a possible solution is to use n+p or n+n detectors)

Surface defects in the oxide

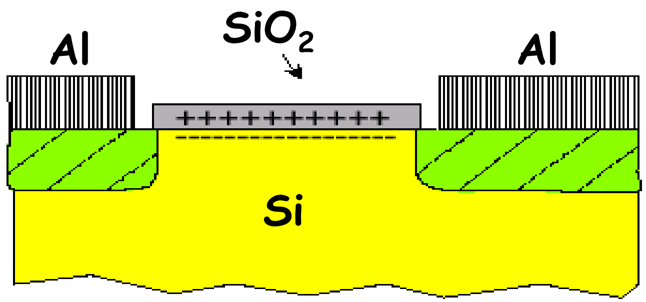

- ❑ **Ionizing radiation creates charges in the oxide**
  (in the amorphous oxide dislocation of atoms is not relevant)

- ❑ **The mobility of electrons in SiO2 is much larger than the mobility of holes**
  - ➔ electrons diffuse out of the oxide, holes remain semi permanent fixed
  - ➔ the oxide becomes positively charged due to these fixed oxide charges.

➢ **Consequences for the detector:**
- ✓ reduced electrical separation between implants
- ✓ increase of interstrip capacitance
- ✓ increase of detector noise
- ✓ worsening of position resolution
- ✓ increase of surface leakage current
- ✓ reduced break down voltage